PREDICTION OF PILOT-INDUCED OSCILLATIONS (PIO) DUE TO ACTUATOR RATE LIMITING USING THE OPEN-LOOP ONSET POINT (OLOP) CRITERION

THESIS

Gregory P. Gilbreath, Captain, USAF
AFIT/GAE/ENY/01M-02

DEPARTMENT OF THE AIR FORCE
AIR UNIVERSITY

AIR FORCE INSTITUTE OF TECHNOLOGY

Wright-Patterson Air Force Base, Ohio

The views expressed in this thesis are those of the author and do not reflect the official policy or position of the United States Air Force, Department of Defense, or the U.S. Government.

AFIT/GAE/ENY/01M-02

PREDICTION OF PILOT-INDUCED OSCILLATIONS (PIO) DUE TO ACTUATOR RATE LIMITING USING THE OPEN-LOOP ONSET POINT (OLOP) CRITERION

THESIS

Presented to the Faculty

Department of Aeronautics and Astronautics

Graduate School of Engineering and Management

Air Force Institute of Technology

Air University

Air Education and Training Command

In Partial Fulfillment of the Requirements for the

Degree of Master of Science in Aeronautical Engineering

Gregory P. Gilbreath, B.S.

Captain, USAF

March 2001

AFIT/GAE/ENY/01M-02

PREDICTION OF PILOT-INDUCED OSCILLATIONS (PIO) DUE TO ACTUATOR RATE LIMITING USING THE OPEN-LOOP ONSET POINT (OLOP) CRITERION

Gregory P. Gilbreath, B.S.
Captain, USAF

Approved:

(original signed)	
Dr. Bradley S. Liebst (Chairman)	Date
(original signed)	
Lt Col Thomas A. Buter, Ph.D. (Member)	Date
(original signed)	
Lt Col David R. Jacques, Ph.D. (Member)	Date

Acknowledgements

I would like to extend my thanks to several individuals whose contributions made this effort possible. To my advisors Dr. Brad Liebst, Air Force Institute of Technology, and Lt Col Tom Buter, USAF Test Pilot School, who provided me with advice and guidance throughout this project. To Mr. Dave Leggett, Air Force Research Laboratory, who brought this topic to our attention and offered suggestions on how we might conduct a flight test. To Mr. Andy Markofski, and all the employees of Veridian Engineering, whose intimate knowledge of the VISTA Simulation System made the flight test portion an efficient and rewarding experience. Also, to Mr. Dave Mitchell, Hoh Aeronautics Inc., who provided hours of invaluable consultation, data analysis, and advice.

I would specifically like to thank the members of the HAVE OLOP test team who made the flight test a reality. Maj Dave Evans (TPS Staff Monitor), Capt Mike Meyer, Capt Shaun Hick, Capt Scott Ormsby, Capt Luciano Ippoliti (Italian AF), and Lt Marco Latela (Italian AF). Most importantly, I thank my wife for her support, enthusiasm, and the sacrifices she has made over the last 2½ years while I have been a student. Thanks to my children, for providing me with smiling, cheerful faces after those long days at work. This journey would have been much more difficult without the support of a loving family. Lastly, I thank God for carrying me through yet another chapter in my Air Force career.

Greg Gilbreath

Table of Contents

List of Figures

Figure Page

Figure Page

Figure Page

List of Tables

Table Page

List of Abbreviations, Symbols, and Acronyms

Abbreviation/Symbol	Definition	Unit
α	Angle-of-Attack	deg
δ, δ_e	Elevator Output	deg
δ_c	Elevator Input Command	deg
δ_{co}	Elevator Input Command Amplitude	deg
δ_{RLE}	Rate Limiter Element Input Command	deg
Φ_c	Crossover Angle	deg
$\Delta\phi, \phi$	Phase Angle	deg
θ	Pitch Angle	deg
θ_{cmd}	Commanded Pitch Tracking Angle	deg
τ	LOES Delay Factor	sec
ω	Frequency	rad/sec
ω_{sp}	Short Period Frequency	rad/sec
ν_{onset}	Closed-Loop Onset Frequency	rad/sec
ω_{onset}	Local Onset Frequency	rad/sec
ζ_{sp}	Short Period Damping Factor	--
2D, 2P, 2DU	HAVE LIMITS TMP Configurations	--
Dis	Discrete HUD Tracking Task	--
deg	Degrees	--
$F(\phi, \delta_{co})$	Sum of squares of left hand sides of eqs. 17 & 18	--
G_{ac}	Aircraft Dynamics Transfer Function	--
G_c	Control Law Transfer Function	--
in	Inches	--
j	Complex Number	--
K	Output/Input Magnitude Ratio	--

K_a	Angle-of-Attack Feedback Gain	--
K_g	Pilot Gain	--
K_p	Neal-Smith Pilot Model Gain	--
K_q	LOES Gain/Pitch Rate Feedback Gain	--
L1, L2	Linear System Models	--
N_c	Closed-Loop Describing Function	--
N_o	Open-Loop Describing Function	--
$N(jw)$	Describing Function	--
$N_{sin}(jw,w_{onset})$	Quasi-Linear Sinusoidal Input Describing Function	--
P	Pilot Input Command	in
P_o	Pilot Input Command Amplitude	in
q	Pitch Rate	deg/sec
q_c	Pitch Rate Command	deg/sec
q_{co}	Pitch Rate Command Amplitude	deg/sec
R	Rate Limit	deg/sec
rad	Radians	--
s	Laplacian Operator	rad/sec
sec	Seconds	--
T	Period	sec
T_{q2}	LOES Zero Determinant	sec
T_{p1}, T_{p2}	Neal-Smith Lead/Lag Time Constants	sec
t	Time	sec
U_{OLOP}	Open-Loop System Input	deg
Y_{OLOP}	Open-Loop System Output	deg
x_i	Sinusoidal Input Signal	deg
x_o	Triangle Output Signal	deg
AFFTC	Air Force Flight Test Center	--
AFIT	Air Force Institute of Technology	--
AFRL	Air Force Research Laboratories	--

AIAA	American Institute of Aeronautics and Astronautics	--
CAP	Control Anticipation Parameter	--
DLR	German Aerospace Center	--
FFA	Aeronautical Research Institute of Sweden	--
HAFA	Highly Augmented Fighter Aircraft	--
HQDT	Handling Qualities During Tracking	--
HUD	Heads-Up Display	--
LARL	Large Aircraft Rate Limit Program	--
LOES	Lower Order Equivalent System	--
MIL-STD	Military Standard	--
NASA	National Aeronautics and Space Administration	--
OLOP	Open-Loop Onset Point	--
PIO	Pilot-Induced Oscillation	--
PIOR	Pilot-Induced Oscillation Rating	--
RLE	Rate Limiting Element	--
RLPF	Rate Limiter Pre-Filter	--
SOS	Sum-of-Sines Tracking Task	--
SR	Stick Ratio	--
SWRL	Software Rate Limiter	--
TIFS	Total In-Flight Simulator	--
TMP	Test Management Project	--
TPS	Test Pilot School	--
USAF	United States Air Force	--
VISTA	Variable Stability In-flight Simulator Test Aircraft	--
WPAFB	Wright-Patterson Air Force Base	--

Abstract

Actuator rate limiting has been a causal or contributing factor for Pilot Induced Oscillations (PIO) experienced on highly augmented fighter aircraft. As part of the joint Air Force Institute of Technology/Test Pilot School (AFIT/TPS) program, a critical examination of the Open-Loop Onset Point (OLOP) criterion, developed by DLR German Aerospace, was conducted to see if it could accurately predict PIO due to actuator rate limiting and to evaluate its potential as a design tool.

The OLOP criterion was applied to three previous flight test programs involving rate limiting to study its applicability as a design tool. A Modified Neal-Smith pilot model was used in the analysis in addition to the gain pilot models suggested by DLR. Findings from this analysis led to the HAVE OLOP flight test project which was flown using the NF-16D Variable Stability In-flight Simulator Test Aircraft (VISTA). HAVE OLOP evaluated the OLOP criterion's ability to predict PIO on four different longitudinal configurations with rate limiting elements inside the feedback loop .

OLOP was found to over-predict PIO in some cases when using maximum stick amplitude as DLR suggests. When using actual stick amplitudes, correlation between OLOP predictions and PIO ratings was quite good. A new metric called stick ratio was developed to help explore the full range of stick amplitudes when using OLOP.

OLOP could be a useful design tool, but because of the strong influence of stick amplitude, engineering judgement will have to be exercised. Recommendations on its use as a design tool are presented.

PREDICTION OF PILOT-INDUCED OSCILLATIONS (PIO)

DUE TO ACTUATOR RATE LIMITING USING THE

OPEN-LOOP ONSET POINT (OLOP) CRITERION

I. Introduction

General

The pilot-induced oscillation (PIO) problem has been present in aviation throughout the history of manned flight. PIOs have caused numerous accidents with results ranging from minor damage to total loss of the aircraft and pilot [16]. There are several interpretations of what exactly a PIO is and how it is triggered. MIL-STD-1797A defines PIO as "sustained or uncontrollable oscillations resulting from efforts of the pilot to control the aircraft" [3]. PIOs often occur during high gain events requiring tight control by the pilot; such as takeoff, landing, aerial refueling, and formation flying. As the name implies, it is necessary to have the pilot in the closed-loop system of the aircraft for a PIO to occur. However, it should be emphasized that there is no blame placed on the pilot for the resulting oscillations.

Predicting PIO is difficult to do with any certainty and becomes even more difficult with the evolving complexity in newer aircraft designs. With the advent of high gain, digital fly-by-wire flight control systems, the potential for PIO has increased [6].

This has been vividly demonstrated by three recent events involving the YF-22 [4], the JAS-39 [18], and the Boeing 777 [5].

The purpose of this investigation and flight test was to determine if the Open-Loop Onset Point (OLOP) criterion could accurately predict pilot-induced oscillations (PIO) caused by rate limiting. Although not a new problem, PIOs caused by rate limiting are still not fully understood and have been cited as the cause of some of our more modern aircraft accidents [16]. The validation of a new criterion may provide the basis for updated standards and future revisions of MIL-STD-1797A.

Background

It is largely understood how PIOs due to linear effects are caused. Mr. Ralph Smith studied and developed much of the classical PIO theory [27]. He categorized PIOs into two broad types: 1) Type I PIO occurs when the pilot switches from tracking pitch attitude to pilot-felt normal acceleration, 2) Type II PIO is initiated by a sudden change in the flight control system or non-tracking abrupt maneuvers (high g maneuvering, activation/deactivation of a stability augmentation system (SAS), trim malfunction, etc.) which is not likely during the landing phase.

A more recent study has offered another PIO classification [16]: 1) Category I PIOs are essentially linear pilot-vehicle system oscillations, 2) Category II PIOs are quasi-linear pilot-vehicle system oscillations with series rate or position limiting, and 3) Category III PIOs are essentially non-linear pilot-vehicle system oscillations with

transitions. Note that Category II PIOs are basically Category I PIOs with dominant lag introducing nonlinearities.

The focus of this study will be on the Category II case because almost all of the severe PIO time histories of operational and test aircraft show surface position and/or rate limiting in the fully developed PIO [16]. It should be noted that the analyses of these events seldom identified rate limiting as the primary cause of these PIOs and that simple saturation of an actuator does not automatically cause a severe PIO [25]. Indeed, rate limiting was sometimes a result of the PIO. However, recent flight tests examining the effects of rate limiting [15][25], and the JAS-39 accident report [18] have identified rate limiting as a primary cause for PIOs.

The rate limiting effect is twofold. First, it adds additional phase lag in series with the pilot, increasing the delay between pilot input and aircraft response. This effect not only degrades the aircraft dynamics, possibly resulting in a PIO or an unstable closed-loop system, but it tends to make the pilot try and compensate with faster responses, often worsening the situation. Second, rate limiting effectively reduces the gain, which the pilot interprets as a lack of control response. This effect lures the pilot into making larger command inputs, again worsening an already bad situation. These two concepts are illustrated for a highly saturated case in Figure 1-1. The time histories represent a typical first order lag model for an elevator actuator of the form $20/(s+20)$ with a sinusoidal input command of 15 degrees magnitude, and a maximum rate limit of 40 deg/sec.

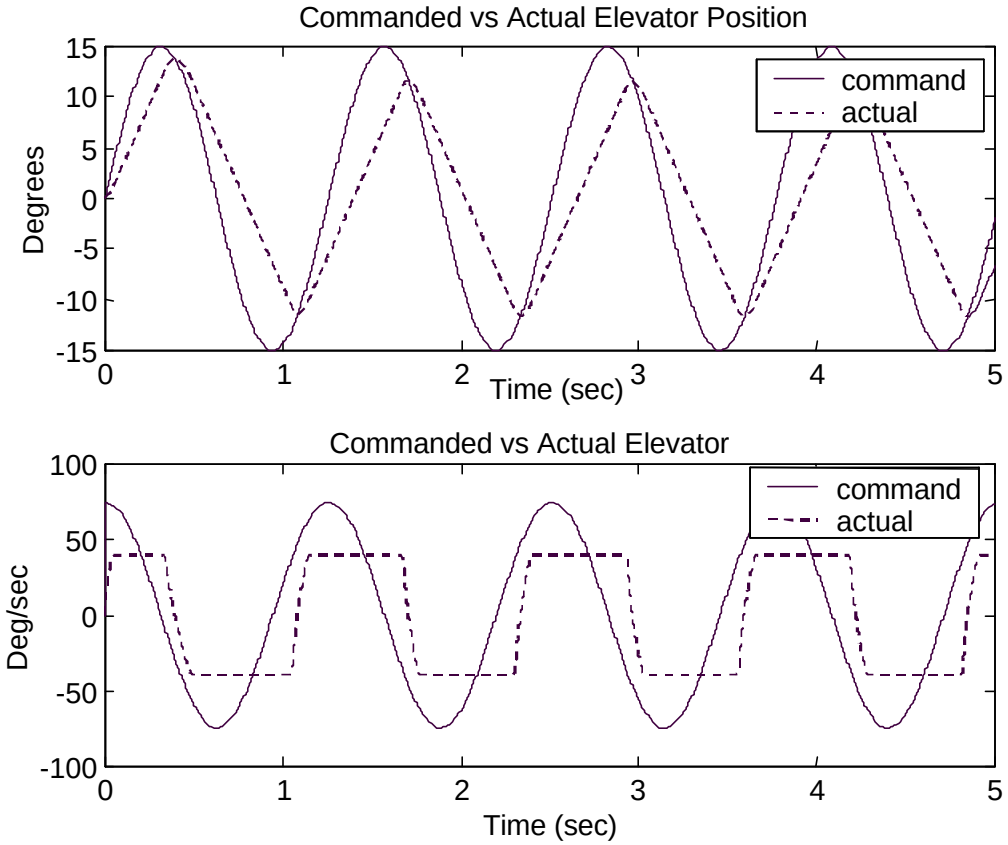

Figure 1-1. Example Time History of Rate Limiting

These affects can mislead the pilot into thinking that they are not in a PIO, but rather that the aircraft is somehow malfunctioning. The rate limiting effects perhaps can be most vividly shown by the YF-22 accident [4]. Although the report identified several triggers that initiated the PIO, flight data showed a "severe PIO with rate limiting, impossible for the pilot to recover from unless he removed himself from the loop." The test pilot remarked after the flight that he did not realize he was in a PIO but felt as if the aircraft was somehow malfunctioning. Rate limiting as a cause of PIO is not just limited to high performance fighters. The Boeing 777 encountered a longitudinal PIO due to elevator rate limiting upon landing during one of its early test flights [5]. The PIO lasted

for approximately three full cycles and the chief pilot remarked that "we were completely out of phase with it (elevator)".

Clearly, the need for a method to accurately predict Category II PIOs is needed. Unfortunately, according to David J. Moorhouse, the chief investigative engineer for the YF-22 accident, "its typical to not check for PIO during the design phase, particularly if the aircraft is designed to have good Level I handling qualities" [4]. This can result in expensive "after the fact" fixes for problems that are discovered during flight test, or worse, loss of the aircraft.

DLR (Deutsches Zentrum für Luft-und Raumfahrt), German Aerospace, has proposed a new method for examining stability problems of rate saturated (synonymous with an actuator nearly always at its rate limit) closed-loop systems called the Open-Loop Onset Point (OLOP) Criterion [6]. This method was developed using describing function techniques and stability regions on the Nichols chart on a number of existing rate saturated aircraft systems. In addition, DLR claims that OLOP can predict PIOs for a rate limiting element in either the feedback loop or forward loop. This study will attempt to validate its claim as a suitable design tool to predict Category II PIOs of aircraft with rate limiting elements. First, by analyzing data generated by previous flight tests examining rate limiting and then by developing and flying a limited flight test profile. Recommendations on its use as a design tool will be developed.

Objectives

The specific objectives of this study are as follows:

1) Apply the OLOP criterion to existing data from previous flight test programs involving rate limiting to examine its applicability as a design tool.

2) Conduct a limited flight test evaluating the ability of the OLOP criterion to predict PIO caused by rate limiting further exploring the concepts developed in objective 1.

3) Make recommendations on the application of OLOP as a design tool and obtain additional flight test data for others to use for further PIO research.

Approach

The following steps were taken to accomplish the objectives of this study.

1) The OLOP criterion was applied to data from three flight test programs that examined handling qualities effects due to rate limiting. The programs were HAVE LIMITS [15], HAVE FILTER [1], and the Large Aircraft Rate Limit (LARL) program [26]. The criterion was applied as suggested by DLR using the simple gain pilot model and the maximum stick amplitude. Additionally, the criterion was applied using the Modified Neal–Smith pilot model for comparison. A new metric, *stick ratio*, was developed to aid in the application of OLOP using the full spectrum of stick amplitudes. Strengths and weaknesses of the criterion were uncovered giving insight into its potential

as a design tool and paving the way for a limited flight test further examining the criterion's viability.

2) Four longitudinal flight control system configurations were developed for flight test on the USAF NF-16D Variable Stability In-Flight Simulator (VISTA) to further test OLOP's ability to predict PIO. One involved an unstable bare airframe while the other three contained stable bare airframes with undesirable characteristics. Each configuration contained stabilizing feedbacks feeding into a stabilator with rate limits varying from 10 to 60 deg/sec. PIO ratings were obtained after conducting "up-and-away" tracking tasks. These ratings were then compared to the OLOP predictions for these configurations for evaluation.

3) Recommendations were developed on how OLOP could be applied as a design tool based on the findings of this research.

Scope

The scope of this study was limited to the following:

1) Only PIOs in the longitudinal axis of the flight control system were studied.

2) Only "up-and-away" HUD generated tracking tasks were used to obtain the necessary data. Additional flight time and sorties would have permited and extension to other tasks such as offset landings.

3) Due to budget and time constraints the flight test portion was limited to only 12 sorties and 15.4 hours.

The USAF Test Pilot School (TPS) sponsored this investigation. The analytical study was accomplished at the Air Force Institute of Technology (AFIT), Wright-Patterson AFB, Ohio. The flight test was a conducted at the USAF TPS, Edwards AFB, California. The flight test was performed on the USAF NF-16D VISTA aircraft, which was maintained and operated by Veridian Engineering at Edwards AFB.

II. Theoretical Development

This chapter will discuss the theoretical development of the OLOP criterion and its implementation. First, a discussion on the derivation of the rate limiting describing function will be presented. Then the concepts behind the OLOP criterion will be discussed followed by the specific steps that need to be taken to use OLOP for PIO analysis.

Sinusoidal Input/Triangle Output Describing Function

Several time histories from actual PIO incidents showed that a sinusoidal input generally approximated the actuator command [16]. For the highly saturated case, as illustrated in Figure 1-1, the output can be approximated by a triangle function. Since saturation is a simple nonlinearity, it can be represented by a quasi-linear system using the describing function and the remnant [14]. The output can be represented in terms of its Fourier components:

$$x(t) = \sum_{n=-\infty}^{\infty} \hat{x}_n e^{jnwt} \tag{1}$$

with Fourier coefficients

$$\hat{x}_n = \frac{1}{T} \int_{t_o}^{t_o+T} x(t) e^{-jnwt} dt \tag{2}$$

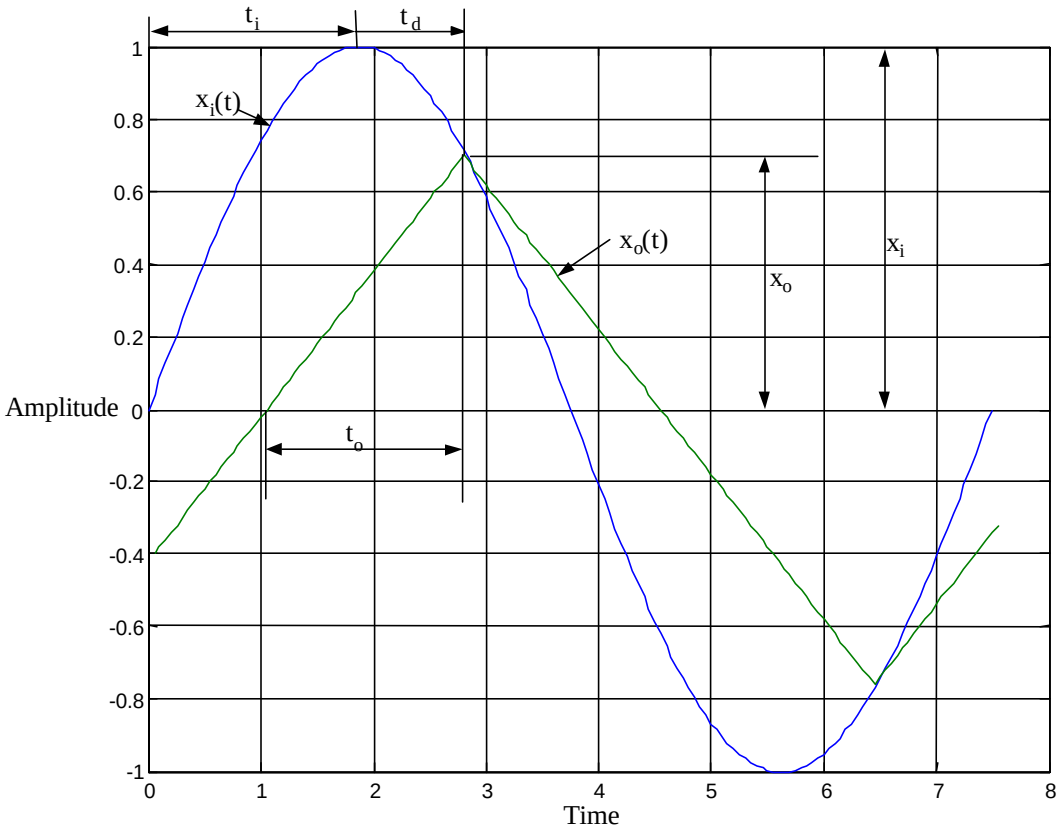

Figure 2-1. Rate Limiting Time Response for a Sinusoidal Input

The describing function is defined as the magnitude ratio of the fundamental component (first term of the Fourier series) of the output to the input. The remnant consists of all the higher harmonics (remaining terms of the Fourier series) and can be neglected if the linear system exhibits low-pass character. In general, higher order systems effectively suppress the high frequency harmonics such that using the fundamental alone usually results in a good approximation. A detailed look at the sinusoidal input/triangle output relationship is shown in Figure 2-1 with the variables detailed in the following derivation [16].

The sinusoidal input can be defined by the following equation:

$$x_i(t) = x_i \sin(\omega t) \tag{3}$$

and the input rate is therefore:

$$\dot{x}_i(t) = x_i \omega \cos(\omega t) \tag{4}$$

The maximum input rate occurs when $\cos(\omega t)=1$. The frequency can be written in terms of the period as $\omega=2\pi/T$, where $T=4t_i$. Note also that in the steady state $t_i=t_o$. Utilizing the expressions for ω and T results in the following expression for the maximum input rate:

$$\dot{x}_{i\max} = \frac{\pi}{2}\frac{x_i}{t_i} \tag{5}$$

The constant output rate is simply the slope of the triangle wave and is equivalent to the actuator rate limit R. It can be expressed by the following equation:

$$R = \dot{x}_o = \pm\frac{x_o}{t_o} \tag{6}$$

The output/input magnitude ratio, $K=x_o/x_i$, can be found by taking the ratio of the constant output rate to maximum input rate and solving for x_o/x_i.

$$K = \frac{x_o}{x_i} = \frac{\pi}{2}\frac{\dot{x}_o}{\dot{x}_{i\max}} \tag{7}$$

In terms of R and ω equation 7 becomes:

$$K = \frac{\pi}{2}\frac{R}{x_i \omega} \tag{8}$$

The K parameter is then used to calculate the magnitude of the describing function $N(j\omega)$. The Fourier fundamental for a triangle wave with magnitude x_o is $8x_o/\pi^2$ [17]. Thus the ratio of the Fourier fundamental to the input magnitude, i.e. the definition of the describing function, becomes:

$$\left|N(j\omega)\right| = \frac{8x_o}{\pi^2}\Big/ x_i = \frac{8}{\pi^2}K \tag{9}$$

Furthermore, we will define the following onset frequency $\omega_{onset}=R/x_i$; which is used throughout the OLOP literature and is the frequency where actuator saturation first occurs. It is derived by simply equating the maximum input rate to the rate limit of the output. This leads to the following equation for the describing function magnitude:

$$\left|N(j\omega)\right| = \frac{4}{\pi}\frac{\omega_{onset}}{\omega} \tag{10}$$

The phase delay can be determined by examining the time difference, t_d, between the two signals in Figure 2-1. Noting that at the point where the two curves meet, $t=t_i+t_d$, and that the magnitude of the input signal is equal to the maximum value of the output, one can write:

$$x_i \sin[\omega(t_i + t_d)] = x_o \tag{11}$$

After expanding the sin term in equation 11, substituting K for the magnitude ratio, and noting that $\omega t_i = \pi/2$, results in the following equation for the phase shift:

$$\Delta\phi = -\cos^{-1}(K) \tag{12}$$

Where $\Delta\phi = \omega t_d$ is the phase angle between the output and input signals.

The complete quasi-linear describing function for a sinusoidal input can be written in the following form in terms of ω and ω_{onset}:

$$N_{\sin}(j\omega, \omega_{onset}) = \frac{4}{\pi}\frac{\omega_{onset}}{\omega} e^{-j\cos^{-1}\left(\frac{\pi}{2}\frac{\omega_{onset}}{\omega}\right)} \tag{13}$$

The Bode plot of this describing function with $\omega_{onset} = 1$ *rad/sec* is shown in Figure 2-2. For $\omega \leq \omega_{onset}$, the rate limiting element is not engaged thus there is no amplitude attenuation or phase delay. A cubic spline interpolation was used to fill the gap between the 'no saturation' and 'fully developed' regions (see 'dfunction' m-file in Appendix B). Equation 13 is only valid for the frequency range $\omega \geq 1.862\omega_{onset}$ (see Reference [7] for proof), ensuring that the input rate is always greater than or equal to the rate limit thus satisfying the fully developed saturation case. Note the decrease in amplitude and the strong increase in phase delay in the transition region leading to fully developed saturation. Also, for greater rate limit values, R, and with the input magnitude held constant, ω_{onset} increases in frequency. This correlates physically to the situation where for higher and higher rate limits the pilot will have to demand higher rates in order to saturate the system.

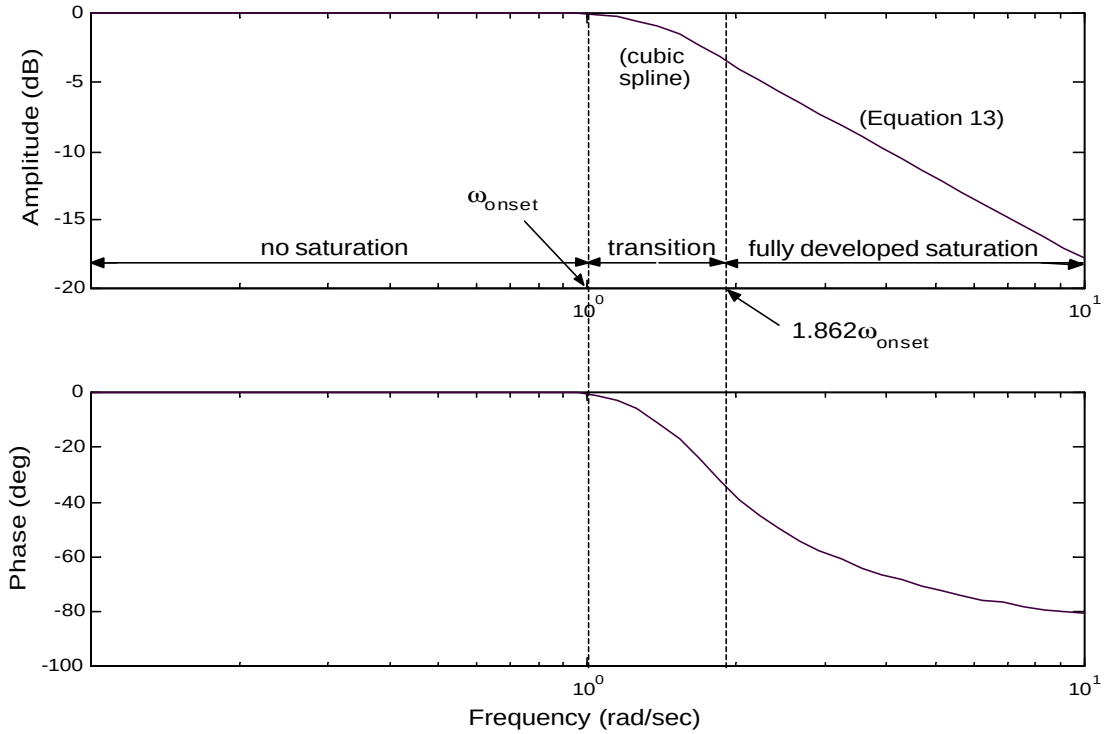

Figure 2-2. Rate Limiter Describing Function Bode Plot

The rate limiting element is similar to a standard linear frequency response function in that for a given frequency it generates a complex number with its relative phase and magnitude. The difference is that it is not only dependent on frequency but input magnitude as well, thus it is given the descriptive nomenclature of *quasi-linear*.

The Open-loop Onset Point (OLOP)

The following is an overview of the method developed by DLR (Deutsches Zentrum für Luft-und Raumfahrt), German Aerospace, using the describing function

derived in the previous section, to aid in the prediction of Category II PIOs. The findings and examples come from various sources cited throughout the chapter.

Closed-Loop Example.

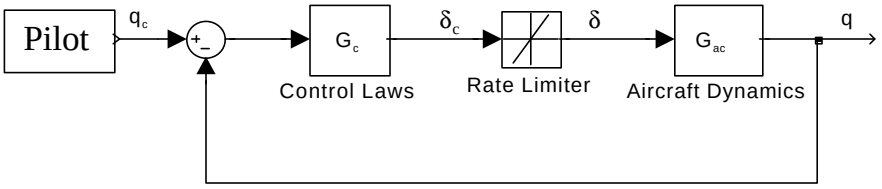

Figure 2-3. Typical Highly Augmented Aircraft with Rate Limiting

An examination of closed-loop stability of a rate saturated system using the describing function can now be performed. A sample model of a highly augmented aircraft with a rate limiter inside the feedback loop and pilot input q_c (details of the various blocks are contained in Reference [6]) is shown in Figure 2-3. The OLOP point is defined as the frequency response value of the open-loop system at the closed-loop onset frequency, ν_{onset}. This frequency is the point at which actuator saturation first occurs. It is similar to the onset frequency defined in the derivation of the describing function and is determined by solving the following equation, where q_{co} is the pilot input amplitude:

$$q_{c_o} \cdot \left| \frac{\delta_c}{q_c}(j\nu_{onset}) \right| = \frac{R}{\nu_{onset}} \tag{14}$$

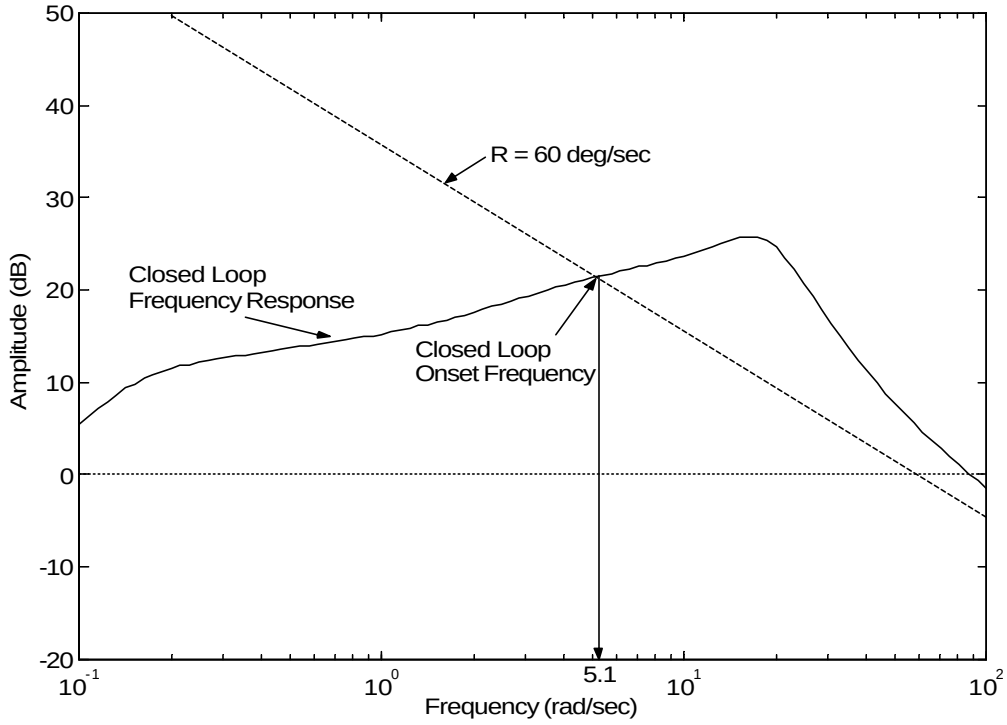

Figure 2-4. Determination of the Closed-Loop Onset Frequency

Solving this equation for ν_{onset} requires determining the intersection of the frequency response amplitude (from the input of the closed-loop system, q_c, to the input of the rate limiter, d_c) and a straight line with slope –20 dB/decade that crosses the 0-dB line at the rate limit, R. (Note: The magnitude of the ratio of frequency response amplitudes is multiplied by the input amplitude, q_{co}, to obtain the true frequency response amplitude.) With a rate limit of R = 60 deg/sec, and at maximum input amplitude, the graphical solution is shown in Figure 2-4, resulting in an onset frequency of approximately 5.1 rad/sec.

The describing function for the entire closed-loop system can be thought of in two parts. Below the onset frequency the system simply acts as a linear model. Above this frequency, the overall describing function must be calculated for the entire closed-loop system. Because the rate limiting element is inside the feedback loop of the closed-loop system, and is a function of both frequency and input amplitude, the traditional method for calculating the closed-loop linear frequency response is not valid. Referring again to Figure 2-3, the system input signal can be represented in the complex time domain by the following equation:

$$q_c(t) = q_{co} e^{jwt} \tag{15}$$

Additionally, the input signal into the rate limiting element can be written as follows:

$$\delta_c(t) = \delta_{co} e^{(jwt+f)} \tag{16}$$

Where f represents the additional phase lag contributed by the linear and describing function elements in the closed-loop system. For a given input amplitude, q_{co}, and frequency, w, one can solve for the remaining variables δ_{co} and f in terms of the amplitude and phase contributions of all the elements in the system. This can be accomplished by first replacing the rate limiter element in Figure 2-3 with the describing function, $N(\delta_{co}, w)$, derived earlier. Then the real and imaginary parts of the complex time domain system can be equated separately at the summing junction resulting in two highly non-linear equations for δ_{co} and f (equations 17 & 18). Here, G_{ac} and G_c represent the linear transfer function blocks and N the describing function block.

$$\frac{\delta_{co}}{|G_c(\omega)|}\cos[\phi - \angle G_c(\omega)] + \delta_{co}|G_{ac}(\omega)||N(\delta_{co},\omega)|\cos[\phi + \angle G_{ac}(\omega) + \angle N(\delta_{co},\omega)] - q_{co} = 0 \qquad (17)$$

$$\frac{\delta_{co}}{|G_c(\omega)|}\sin[\phi - \angle G_c(\omega)] + \delta_{co}|G_{ac}(\omega)||N(\delta_{co},\omega)|\sin[\phi + \angle G_{ac}(\omega) + \angle N(\delta_{co},\omega)] = 0 \qquad (18)$$

These equations were solved for the two unknowns, δ_{co} and ϕ, using an unconstrained nonlinear optimization algorithm in MATLAB® (see M-file in Appendix B) for a constant q_{co} over a frequency range of .1 to 100 rad/sec. Once the equations were solved, the overall closed-loop describing function, N_c, was determined in terms of phase and magnitude using standard linear system techniques. A similar detailed iterative method was derived and verified with the results of nonlinear simulations by Holger Duda, author of the OLOP criterion [7]. Once the closed-loop describing function, N_c, was determined, the open-loop describing function, N_o, was needed in order to compare it to the linear response on a Nichols chart. N_o was determined from the equivalent systems shown in Figure 2-5 and equation 19:

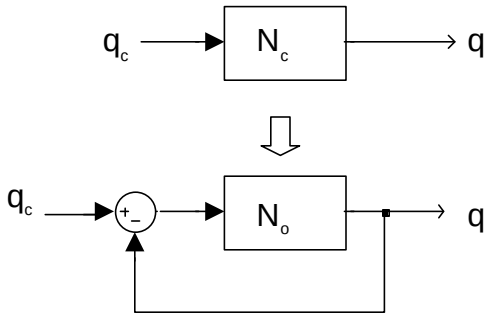

Figure 2-5. Equivalent Open-Loop Describing Fuction

$$N_c = \frac{N_o}{1 + N_o} \qquad \Leftrightarrow \qquad N_o = \frac{N_c}{1 - N_c} \qquad (19)$$

This open-loop describing function, N_o, contained the nonlinear effects due to loop closure. A Nichols chart of the open-loop linear frequency response (without the effects of saturation) and the describing function response is provided in Figure 2-6. Notice the dramatic phase jump at the onset frequency point. This is also referred to as *jump resonance* and has been noted in non-linear theory since the 1950s [14].

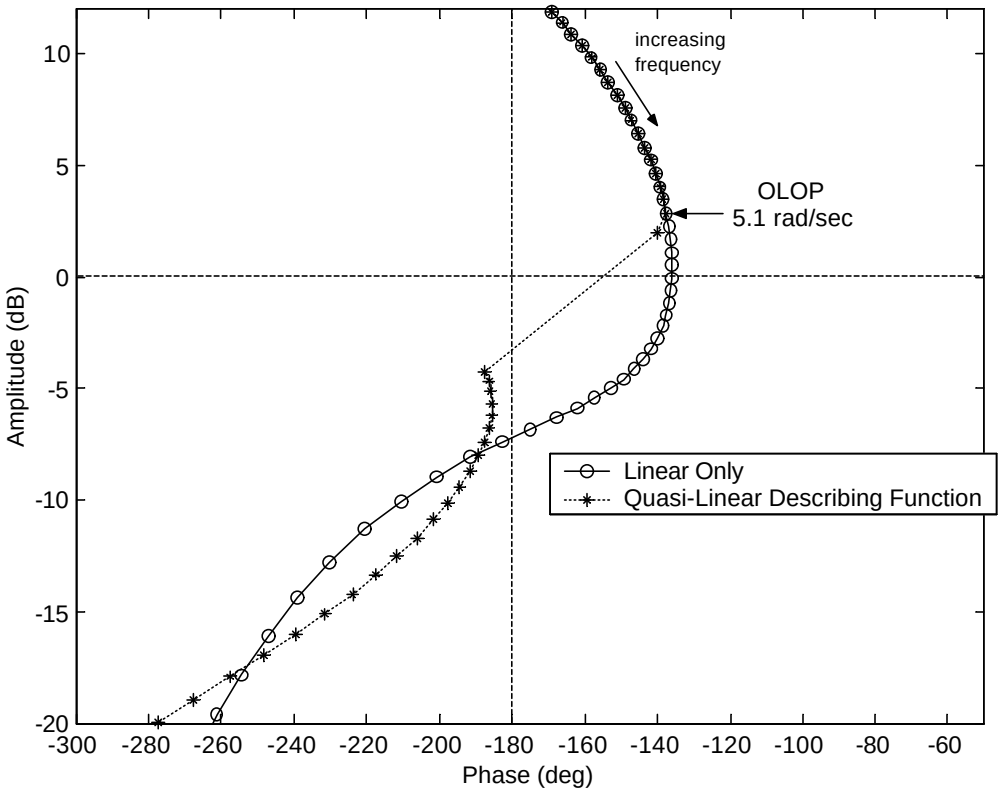

Figure 2-6. Open-Loop Frequency Response and Describing Function q/q$_c$

The jump resonance phenomena is visually illustrated in Figure 2-7. The four graphs depict a three dimensional surface plot of the function, $F(f, d_{co})$, (given by the sum of the squares of the left hand sides of equations 17 and 18) solved in the non-linear optimization algorithm. The solution to the function can be determined by noting where the surface touches the horizontal plane (i.e. where the function equals zero), and then reading the values for f and d_{co}.

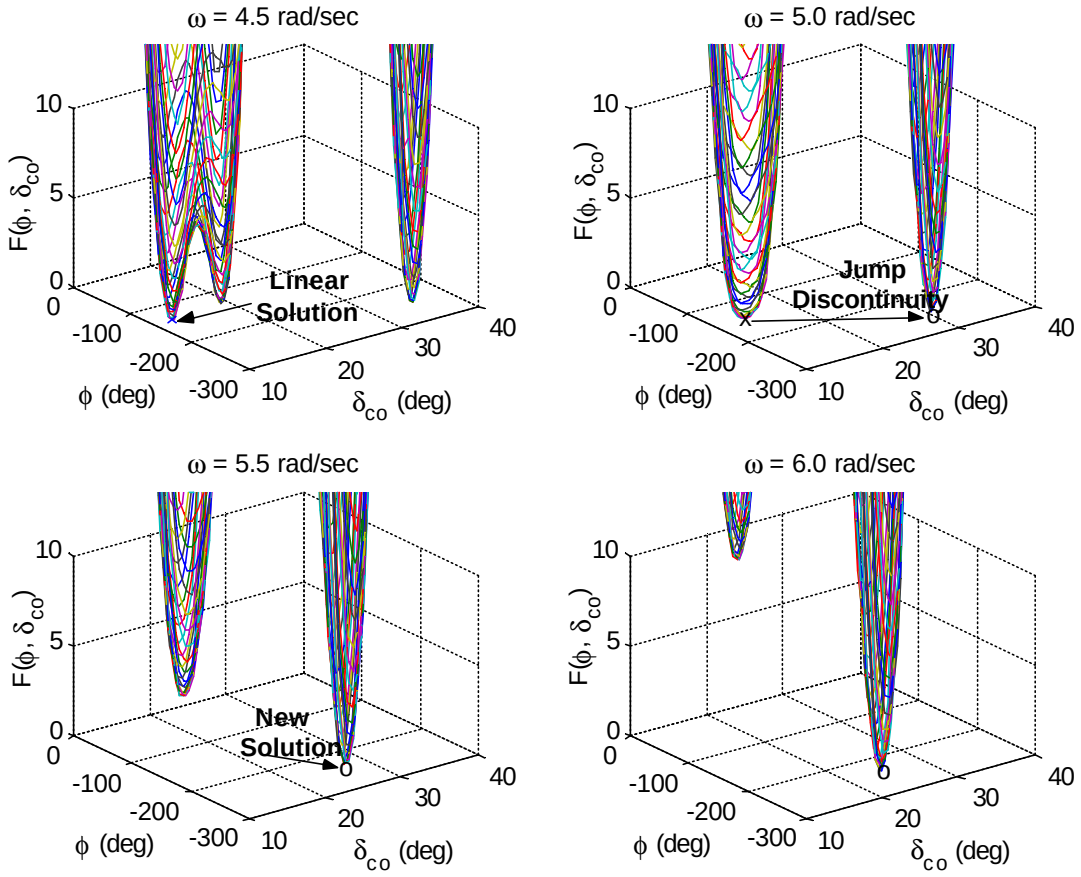

Figure 2-7. Jump Phenomena Illustration

The first chart shows that for a frequency value of 4.5 rad/sec, well below the onset frequency of 5.1 rad/sec, the mathematical solution agrees with the linear solution. This correlates with the Nichols chart where, as expected, prior to the onset frequency, the quasi-linear and linear plots are concurrent. Or in other words, the rate limiting element has no effect on the system. For a frequency of 5.0 rad/sec, closer to the onset frequency, a second 'spike' has extended and is close to touching the horizontal plane as shown in the next chart. As the frequency continues to increase the left hand 'spike' begins to detach itself from the horizontal plane leaving the new right hand 'spike' as the only valid solution. Thus the values for d_{co} and f must make a 'jump' in order to satisfy the mathematical solution when the frequency is in the vicinity of v_{onset}.

Upon reaching the onset frequency, this jump in phase has the effect of pushing the frequency response past the critical point (180°, 0 dB) in the Nichols chart suggesting the possibility of an unstable closed-loop system when rate limiting is in effect. This can be evaluated using a nonlinear simulation of the system from Figure 2-3 and is shown in Figure 2-8. A stable system response to a sinusoidal input of maximum amplitude and frequency ω = 5 rad/sec is apparent in the first two graphs. When the frequency is increased to ω = 5.3 rad/sec, just slightly beyond the onset frequency, the rate limiter is activated causing closed-loop instability after approximately three seconds as shown in the second two graphs. This instability occurs even though the demanded elevator rate is only slightly more than the maximum rate allowed by the elevator.

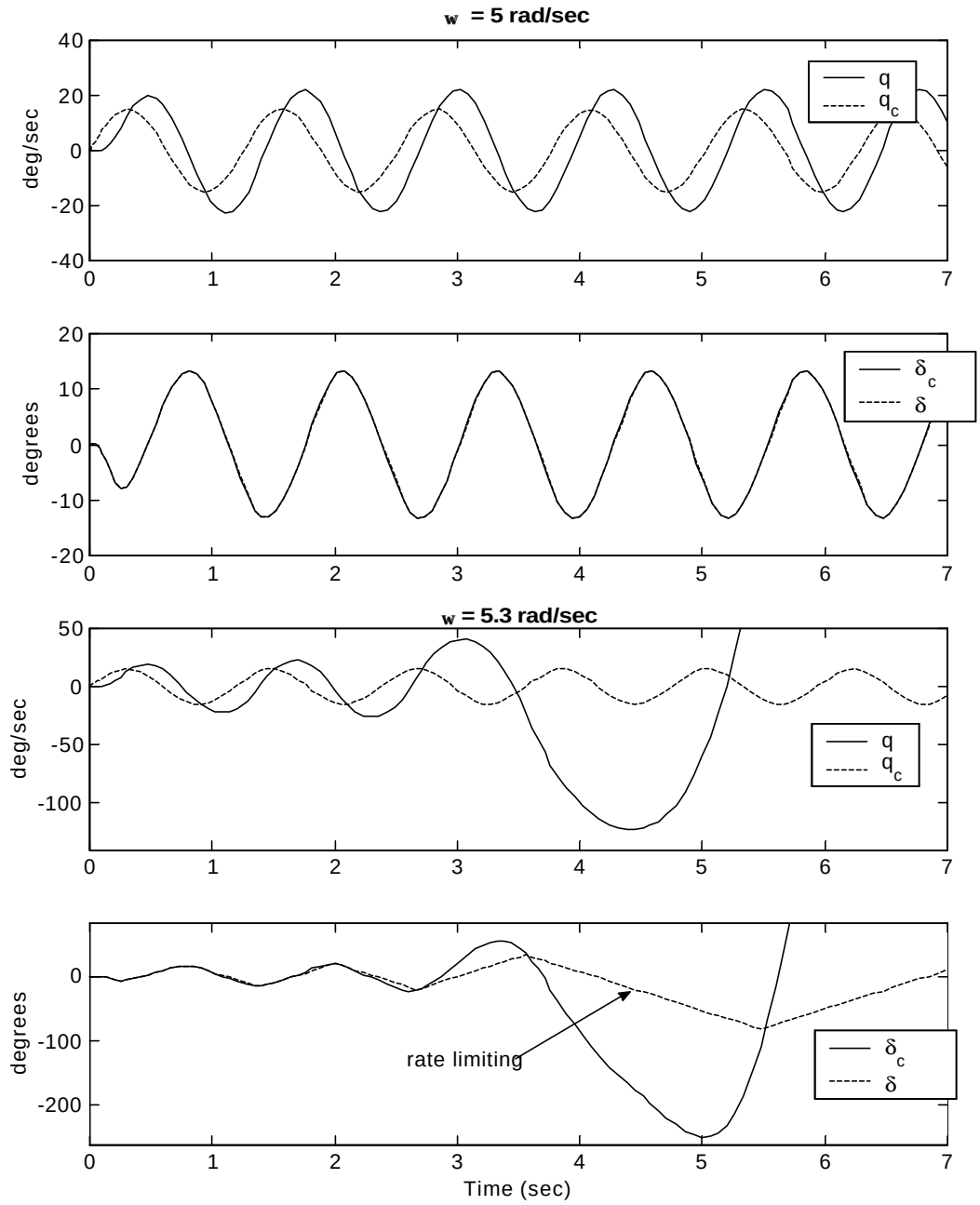

Figure 2-8. Time Domain Analysis

It should be noted that in this example the system went unstable without including the effects of the pilot's feedback response. This is not always the case. A second example was done evaluating the YF-12 in Reference [6] and it showed that without the pilot loop closed the system did not jump close to the critical area in the Nichols chart. However, this does not guarantee pilot-plus-aircraft system stability because a PIO is often characterized by a stable aircraft, but with a misadaptation by the pilot to the sudden change in aircraft dynamics at the onset of rate limiting.

The OLOP Criterion.

The describing function technique and the OLOP parameter were used on a number of aircraft systems with rate limiters both in the forward path and feedback path. It has been shown that the OLOP location in the Nichols chart and the jump resonance in the frequency domain are correlated to the instabilities of the closed-loop systems observed in the time domain simulations [7]. A proposed stability boundary for the location of the OLOP is shown in Figure 2-9 with the lines of closed-loop amplitude labeled.

This is an updated boundary from the original OLOP work, which was derived from some new simulator experiment results conducted by DLR and FFA, The Aeronautical Research Institute of Sweden [8]. The arrows show the general direction of the phase jump at onset. If the OLOP is located above the stability boundary the phase delay caused by the onset of the rate limiter leads to an increase in closed-loop amplitude as demonstrated in the Nichols chart. This causes stronger rate saturation and further increases phase delay leading to possible closed-loop instability and the potential for a

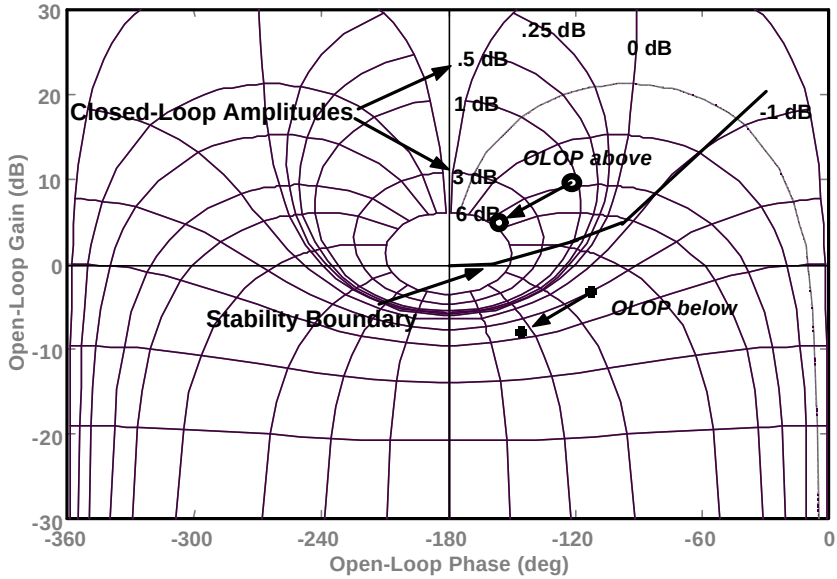

Figure 2-9. Proposed OLOP Stability Boundary

Category II PIO. The OLOP in the closed-loop example from the previous section is clearly above the stability boundary.

If the OLOP is located below the stability boundary, the onset of the rate limiter still causes additional phase delay but the change in closed-loop amplitude is less dramatic. Thus the potential for misadaptation by the pilot and a subsequent PIO is less likely.

Application to Combined Pilot-Aircraft Systems.

To study the application of OLOP on combined pilot-plus-aircraft systems the required open-loop frequency response is obtained by opening the loop at the position of the rate limiter and evaluating the system with the limiter removed, thus eliminating the need for calculating the describing function. A generalized feedback block diagram that

can be applied to both possible positions of the rate limiter is shown in Figure 2-10. For limiters in the forward path (these are placed to protect the system from high input rates by the pilot), linear system L1 contains the pilot model and any feel system dynamics, while linear system L2 contains the complete aircraft dynamics to include the actuator and any inner loop feedback control laws. For limiters in the feedback path (these represent the physical rate limits of the actuator), linear system L1 contains the pilot model *and* feedback dynamics, while linear system L2 includes the actuator and bare airframe dynamics.

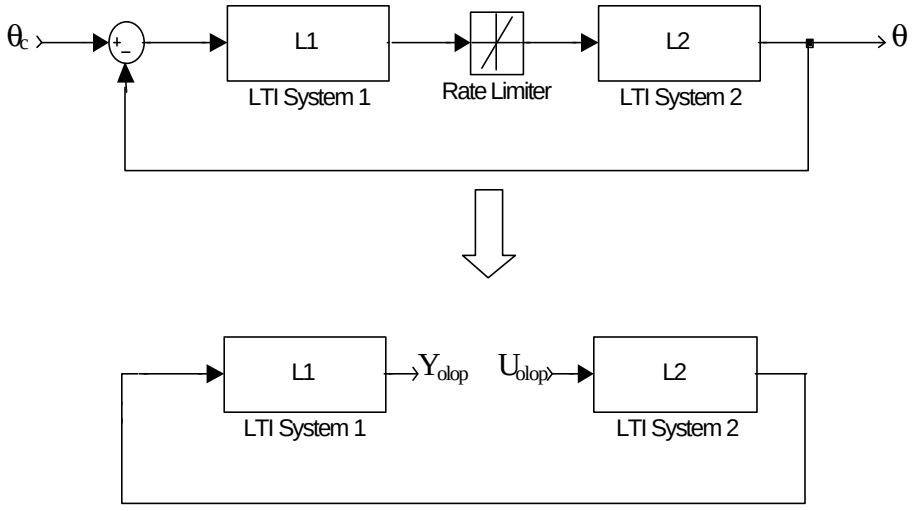

Figure 2-10. Determination of Open-loop Frequency Response for OLOP

The output of the rate limiter is defined as the input of the open-loop system, U_{olop}. The input to the rate limiter is then defined as the output of the open-loop system, Y_{olop}.

In the development of OLOP it was suggested that the pilot be modeled as a pure gain because previous research has shown that a pilot acts as a simple gain during a fully developed PIO (synchronous precognitive behavior) [20]. This gain has to be adjusted based on the linear crossover phase angle (Φ_c) of the open-loop pilot-plus-aircraft system. Initially, DLR suggested a crossover angle spectrum of –110 deg (low pilot gain) to –160 deg (high pilot gain) to evaluate pilot gain sensitivity. Further correspondence with DLR suggests using a range of –90 deg to –130 deg for longitudinal motion and –110 deg to –160 deg for lateral motion [11]. An investigation into utilizing other pilot models for the linear frequency response will be discussed in the next chapter.

Steps to Determine OLOP.

As mentioned previously, the describing function technique is not required in the determination of OLOP. The following steps should be taken to examine a pilot-plus-aircraft system using OLOP:

1) Define a simple gain pilot model as discussed above.

2) Determine the closed-loop onset frequency, ν_{onset}, by solving equation 14 using maximum stick amplitude.

3) Calculate the required open-loop frequency response (Figure 2-10).

4) Determine where the OLOP parameter is on the Nichols chart in relation to the stability boundary (Figure 2-9).

III. Analysis of HAVE LIMITS

This chapter presents the methodology and results from applying the OLOP criterion to flight test data from the HAVE LIMITS Test Management Project (TMP). First, a brief description of HAVE LIMITS is presented. Then OLOP is applied using the recommended simple gain pilot model and also using the Modified Neal-Smith pilot model for comparison. OLOP predictions are compared to the flight test results. Finally, a new metric, *stick ratio*, is introduced.

HAVE LIMITS Overview

The HAVE LIMITS TMP was conducted on 11-22 April 1997 at the Air Force Flight Test Center, Edwards AFB, California, as part of the curriculum for the United States Air Force Test Pilot School (TPS) [2][15]. The purpose of the TMP was to gather in-flight data on longitudinal PIO tendencies due to elevator rate limiting and to evaluate pitch attitude tracking tasks. The flight test was conducted on the NT-33A variable stability aircraft maintained by the Calspan Corporation of Buffalo, New York. Three test pilot students were the evaluation pilots for the project. All three pilots had primarily fighter backgrounds with some limited time in a variety of trainers and transports. A Calspan safety pilot flew on all of the test missions. A total of nine test missions were flown.

The TMP examined three different longitudinal configurations each with various rate limits. The rate limits used were 10, 20, 30, 40, 50, 60, and 157 deg/sec. The highest rate limit was the actual rate limit of the NT-33A elevator and was considered to

be effectively unlimited. The various Low Order Equivalent System (LOES) short period approximation parameters for the three configurations are presented in Table 3-1. Configuration 2D was based on a configuration used in a Neal-Smith experiment where it was evaluated as a Level 1 airplane [23]. Adding a simple 2/s+2 filter to the forward path of the 2D configuration developed configuration 2P. This configuration was evaluated as Level 2 with possible PIO due to the added lag in the system. Configuration 2DU was developed to examine rate limiting effects on a highly augmented aircraft with an unstable plant. The NT-33A variable stability system destabilized the basic NT-33A characteristics to create a plant with an unstable short period with a time to double of approximately 3.5 seconds. Then digital pitch rate and angle-of-attack feedback loops were used to stabilize the aircraft so that it had similar characteristics to 2D when the loops were closed and rate limiting was not present.

Table 3-1. NT-33A Longitudinal Aircraft Dynamics

LOES Short Period Model Form: $\frac{q}{d_e}(s) = K_q \frac{w_{sp}^2 (T_{q2} s + 1) e^{-ts}}{(s^2 + 2z_{sp} w_{sp} s + w_{sp}^2)}$			
Configuration	**2D**	**2P**	**2DU**
$\omega_{sp\ (rad/sec)}$	4.820	4.820	4.863
ζ_{sp}	.732	.732	.651
$T_{\theta 2}$	.844	.844	.844
K_q	3.368	3.368	3.959
τ	.114	.114	.120

The evaluation pilots were instructed to track a Heads Up Display (HUD) generated command bar as closely as possible during a tracking task. HAVE LIMITS utilized two tracking tasks for the evaluation. The first was a combination of ramp and discrete step inputs in both the pitch and roll axes developed by Calspan. The second

was developed by Hoh Aeronautics Inc. and is a sum-of-sines task [21]. Both tasks are shown in Figure 3-1 as pitch command versus time. The pilots were asked to rate each configuration based on aircraft handling qualities during the task. The Cooper-Harper and PIO rating scales used are included in Appendix A.

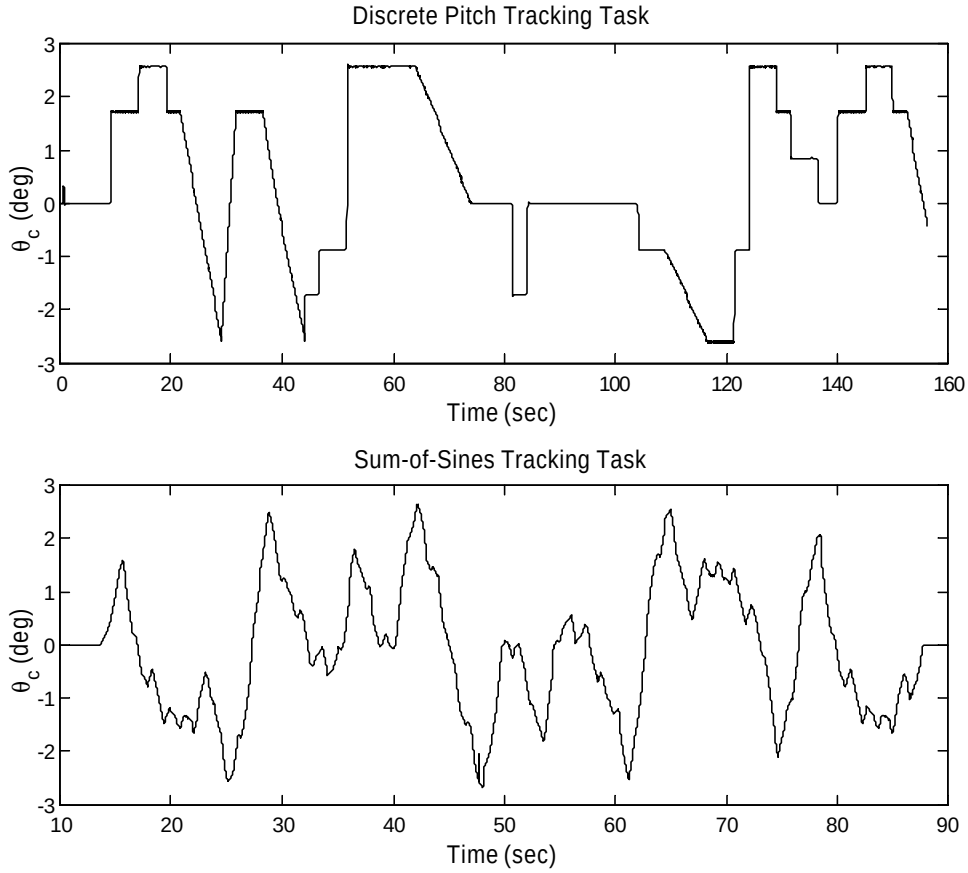

Figure 3-1. Evaluation Tasks

The details of each mission and the various pilot ratings are contained in Reference [2]. After the TMP the test team concluded that the sum-of-sines task required higher gains and made the evaluation of handling qualities quite difficult but was still

suitable for PIO evaluation. The discrete task, on the other hand, was more operationally relevant and was suitable for both handling qualities and PIO evaluation. For the purpose of comparing the OLOP results to the flight test, PIO ratings from both tasks were used.

The following sections outline the steps taken to apply the OLOP criterion to the HAVE LIMITS flight test data.

Aircraft Model

The Simulink® model used for the OLOP analysis is shown in Figure 3-2. It was used by Calspan during the HAVE LIMITS TMP and was shown to be an accurate model of the NT-33A [24].

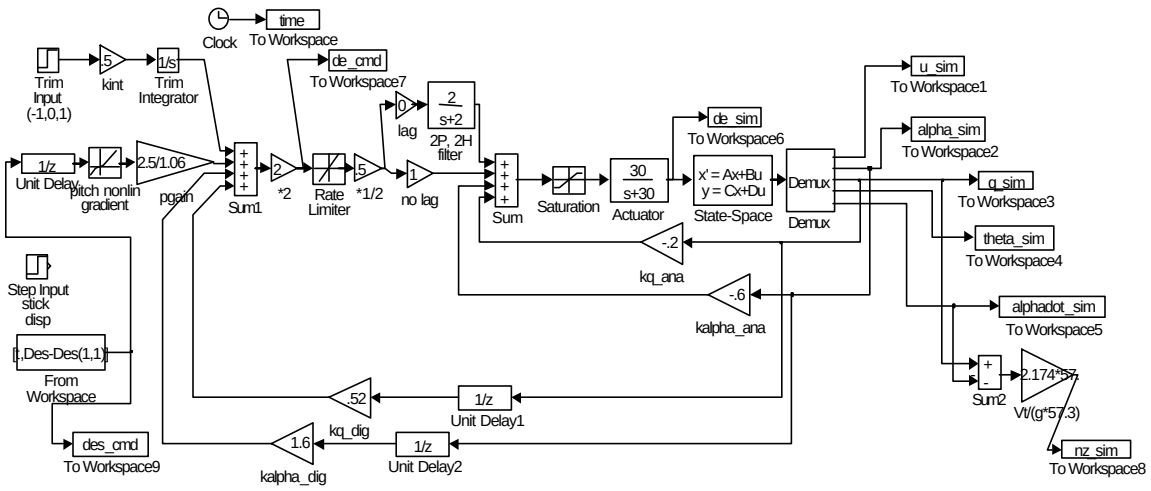

Figure 3-2. HAVE LIMITS Aircraft Model

All three HAVE LIMITS configurations can be derived from this block diagram by varying the feedback gains and the pre-filter status. The inner analog gains and outer digital gains to achieve the required configurations are listed in Table 3-2. To change from 2D to 2P the gain in front of the lag filter in the forward path is set to one and the direct path gain is set to zero. The rate limiting element was inserted into the forward path to represent the effects of rate limitations on the aircraft's elevator actuator. The effectiveness of the NT-33A's elevator was considered very high so a factor of two was placed in front of the rate limiting element and a factor of ½ behind it. This artificially induced rates into the rate limiting element that would not have been there were the gains not present. This had the effect of causing the pilot to demand twice the amount of surface rate than would have been necessary had the gains not been there.

Table 3-2. HAVE LIMITS Configuration Parameters

Gains/Filter	**Configuration**		
	2D	**2P**	**2DU**
K_q (analog)	.32	.32	-.2
K_α (analog)	1.0	1.0	-.6
K_q (digital)	0	0	.52
K_α (digital)	0	0	1.6
Filter on/off	off	on	off

For the linear analysis of the aircraft model, the rate limit and saturation blocks were neglected. The pitch-stick nonlinear gradient block is shown in Figure 3-3. For the linear analysis this block was replaced with a simple gain of 2.5 corresponding to the inner slope with a stick deflection range of ± 1 inch. Although the full range of movement for the stick was –2 to +3.6 inches, the majority of the HAVE LIMITS flight

test data showed that stick inputs rarely exceeded ± 1 inch throughout the tracking task profiles, so the 2.5 gain was deemed a good approximation for the linear analysis.

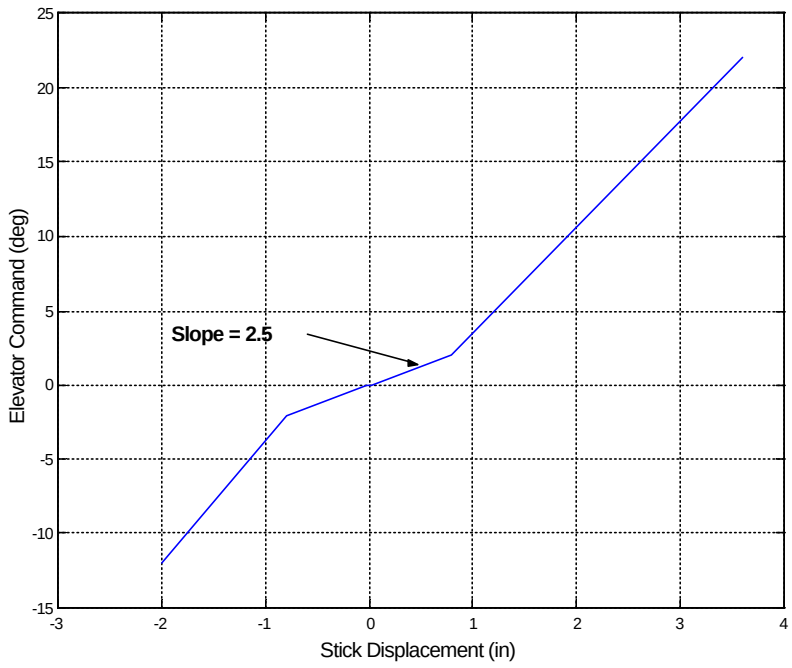

Figure 3-3. NT-33A Pitch-Stick Nonlinear Gradient

Pilot Model Development

Simple Gain Model

As mentioned in Chapter 2, the first step in the application of OLOP is defining a simple gain pilot model. The authors of the OLOP criterion argue that this pilot model should be used because a pilot acts as a pure gain when in a fully developed PIO. McRuer and others also agree that a pure gain pilot model is appropriate in the presence of sustained oscillations referring to this as *synchronous precognitive* behavior [16]. That

is, up to about 3 Hz, a pilot can duplicate a sinusoidal input with little or no phase lag. The question then becomes what gain does one assign to the pilot? Obviously all pilots are different so there is no one magic value. The OLOP method recommends using a range of pilot gains based on the linear crossover phase angle in the open-loop pilot-plus-aircraft system Bode plots. The crossover angle is defined as the phase angle value at the frequency where the amplitude curve crosses 0 dB. The gain value should be adjusted such that the crossover angle, Φ_c, falls into the following ranges [11]:

Longitudinal Motion:	$-130 \leq \Phi_c \leq -90$ deg
Lateral Motion:	$-160 \leq \Phi_c \leq -110$ deg

The lower magnitude (-90°) of the ranges will be referred to as low gain pilots and the upper (-130°) as high gain pilots for this longitudinal analysis. Using this range of gains for the OLOP analysis proves somewhat useful when comparing PIO prediction versus gain sensitivity as will be shown later in the chapter. Duda [9] showed that in an analysis of a particular highly augmented flight test configuration, with the rate limiter in the forward path, only high gain pilots resulted in an OLOP above the PIO boundary. This suggests that a simple gain reduction would alleviate the possibility of a Category II PIO for limiters in the forward path.

The pilot gains, K_g, obtained for the HAVE LIMITS configuration versus crossover angle, Φ_c, are listed in Table 3-3. The longitudinal range of phase crossover angles was used since the HAVE LIMITS TMP investigated elevator rate limiting only. The three values represent low, medium, and high gain pilots respectively.

Table 3-3. Pilot Gain Model for HAVE LIMITS

2D and 2DU		2P	
Φ_c	K_g	Φ_c	K_g
-90°	-.35	-90°	-.05
-110°	-.42	-110°	-.37
-130°	-.56	-130°	-.51

Another question arose regarding the viability of the pilot gain model. Recall that the pure gain model was a good approximation for a *fully* developed oscillation or PIO. It may not, however, be a valid model for the onset period prior to full PIO development. Most likely, prior to onset, the airplane was acting in a linear fashion and the pilot was well adapted to the linear dynamics. If there was a sudden change in aircraft dynamics, such as that due to the onset of a rate limiter, then the pilot dynamics would tend to remain, at least momentarily, as those that were in effect prior to the change. This pilot characteristic is referred to as *post-transition retention* [16]. The retention phase can last from one or two pilot reaction times to several seconds. It is believed that during this time of sudden change in aircraft behavior, a pilot may not properly adapt to the new dynamics and possibly trigger a PIO or aircraft departure.

Since the OLOP in the Nichols chart is based on when the rate limiter first activates, representing the start of the transition period to the new aircraft dynamics, perhaps a more appropriate pilot model would be one that has adjusted to the linear dynamics of the aircraft without saturation. Assuming the theory behind post-transition retention holds, this alternate pilot model would still be valid during the onset period and perhaps would reflect a more accurate OLOP position on the Nichols chart. This thesis

proposes using the Modified Neal-Smith pilot model outlined in MIL-STD-1797A [3]. It will be compared with the results of that obtained from the pure gain model.

Modified Neal-Smith Model

The Modified Neal-Smith pilot model is commonly used for closed-loop pilot-plus-aircraft analysis in computer simulation. The model is based upon achieving certain closed-loop resonance, droop, and bandwidth. The resonance is defined as the maximum closed-loop amplitude and should not exceed 3 dB for Level 1 characteristics and 9 dB for Level 2. Droop is defined as the minimum closed-loop amplitude prior to reaching peak resonance and is limited to a minimum of –3 dB. The bandwidth, as defined for this model, is the frequency at which the closed-loop phase reaches –90 deg. The minimum bandwidth criteria varies with respect to flight phase in the following manner:

Category A: 3.5 rad/sec
Category B: 1.5 rad/sec
Category C: 1.5 rad/sec (2.5 rad/sec for landing phase)

Category A includes maneuvers that require high precision such as formation flying, aerial refueling, and air-to-air combat. Category B includes less aggressive phases of flight such as climb, cruise, and descent. Lastly, Category C includes the terminal phases of flight: takeoff, approach, and landing. This analysis considered only the Category A parameter since the HAVE LIMITS tasks were up-and-away high precision tracking tasks.

The Neal-Smith pilot model has the following transfer function form:

$$\frac{d_{ec}(s)}{q(s)} = \frac{K_p(5s+1)(T_{p_1}s+1)e^{-0.25s}}{s(T_{p_2}s+1)} \tag{20}$$

where K_p = Pilot Gain
T_{p1} = Lead Required
T_{p2} = Lag Required
$e^{-0.25s}$ = Pilot Neuromuscular Delay (empirically determined)

There are no limitations on the values for K_p, T_{p1} or T_{p2}. The goal is to vary these parameters to try and meet the Level 1 closed-loop characteristics outlined above. The *(5s+1)/s* term is included so that the pilot can achieve low level integration if the aircraft model does not have a free '*s*' in it. The chosen values for each HAVE LIMITS configuration are listed in Table 3-4. Configurations 2D and 2DU have similar linear properties with all loops closed thus the same pilot model parameters are used for each.

Table 3-4. Neal-Smith Pilot Model Parameters

Pilot Model Parameters	Configuration	
	2D/2DU	2P
K_p	-.05	-.045
T_{p1}	.06	.61
T_{p2}	.01	.001
Level	1	2

Perhaps the best way to view the performance of the chosen model, and whether or not it meets the criteria, is to view the open-loop aircraft-pilot system on a Nichols chart as shown in Figure 3-4. The chart includes the pertinent closed-loop amplitude and phase lines correlating to the Neal-Smith criteria.

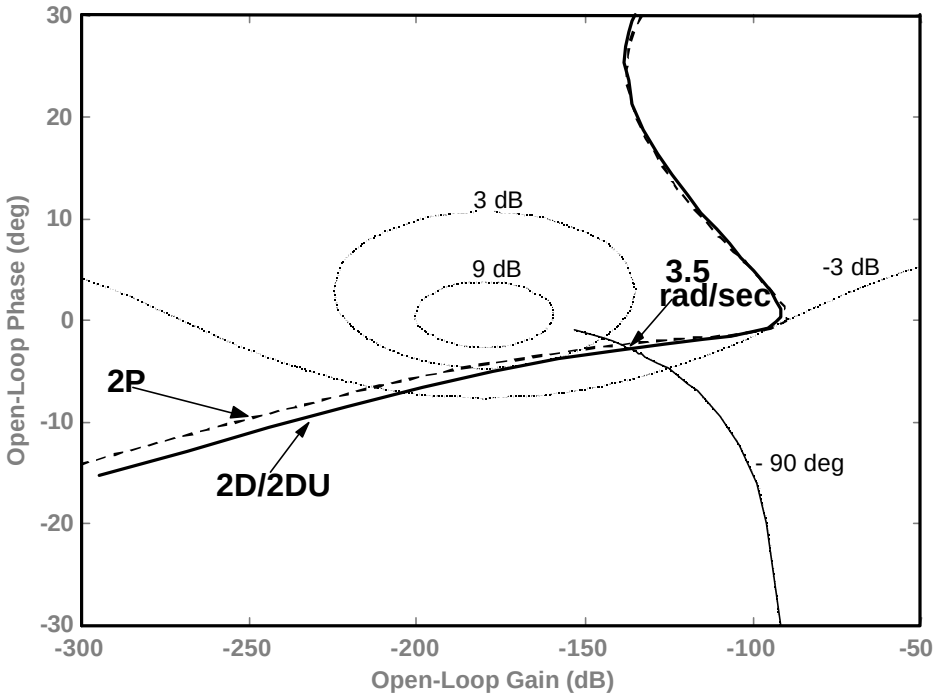

Figure 3-4. Nichols Chart for Modified Neal-Smith Pilot Model

Note that for the 2D/2DU configuration the values chosen result in a closed-loop system that just barely met the Level 1 requirements. Attempts to achieve a more solid Level 1 performance were unsuccessful. Configuration 2P met the bandwidth criteria but not the resonance or droop limits. Attempts at achieving Level 1 properties with configuration 2P were unsuccessful as well due to the lag filter that is included in this system.

Neal-Smith suggested that a pilot may be able to meet the resonance requirements but the amount of lead/lag required by the pilot can still be excessive resulting in lower pilot ratings [23]. This is the original Neal-Smith proposed criterion

from which the modified model was derived and is shown in Figure 3-5. This plot shows closed-loop resonance versus required pilot compensation and once again shows that the 2D/2DU configuration is borderline Level 1/2 while 2P is clearly in the Level 2 region.

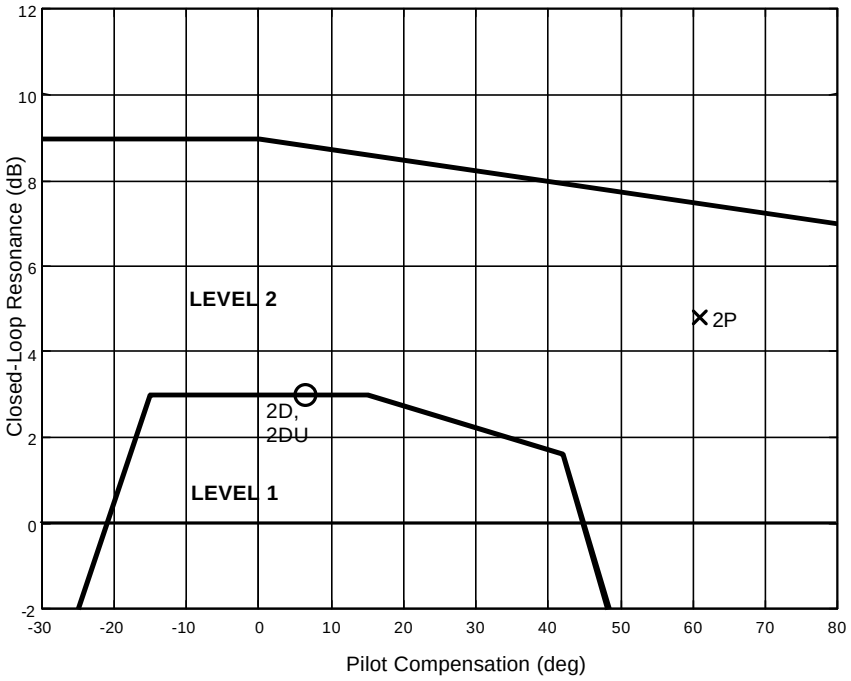

Figure 3-5. Original Neal-Smith Criterion

This study hypothesizes two possible advantages to using the Modified Neal-Smith model versus the simple gain model. First, once the parameters of the Neal-Smith model are picked to meet the closed-loop criteria, there is only one pilot model to be used in the analysis and the gain is automatically incorporated. This is unlike DLR which suggests a wide range of gain values, which could give varying results. In an attempt to validate the OLOP criterion, DLR and FFA, The Aeronautical Research Institute of Sweden, conducted a test involving five pilots and 342 simulator runs [8]. After the runs

were complete, the researchers attempted to find a "suitable" pilot gain that best simulated the actual pilot actions for each run. With these gains, each run could be located in the OLOP chart with conclusive results when compared to the respective PIO ratings. The dilemma then is how would OLOP have predicted PIO susceptibility had the gain values not been known in the first place? Would the results have been as conclusive if the recommended range of gains had been used? If this criterion is to be used in the early design stages of an aircraft, then there will be no flight test and possibly no simulator data from which to extract the appropriate pilot gain. Additionally, it is widely accepted that even a full motion simulator lacks some essential acceleration cues that effect a pilot's response and those gains obtained in a simulator can differ quite a bit from those in the actual airplane.

Second, the Neal-Smith model is a better approximation of the pilot's actions prior to onset, when he/she has adapted to the aircraft's linear dynamics. These pilot dynamics should be a good approximation for the pilot's actions when onset is reached and the jump discontinuity in the Nichols chart occurs.

Determination of Onset Frequencies

The next step in the application of OLOP is to determine the closed-loop onset frequencies for the various rate limits. Recall from Chapter 2 that to determine the onset frequency, ν_{onset}, one must solve the following equation:

$$P_o \cdot \left| \frac{\delta_{RLE}}{P}(j\nu_{onset}) \right| = \frac{R}{\nu_{onset}} \tag{21}$$

The pilot input amplitude, P_o, is multiplied by the magnitude of the transfer function, from pilot input, P, to the input into the rate limiting element, δ_{RLE}, to give the true amplitude into the rate limiter. The authors of OLOP recommended using maximum pilot input amplitude when determining the onset frequencies. Clearly this is a worst case scenario and, in the case of the HAVE LIMITS flight test, produced unreasonable results as will be shown later. The maximum stick deflection for the NT-33A was approximately 3.6", which corresponded to 22 degrees of elevator input. However, various flight test data from HAVE LIMITS showed that the pilots never reached the stick or elevator deflection limits during the tracking exercises. In fact, during some of the more aggressive maneuvering, when the pilots were experiencing rate saturation, the pilots rarely even exceeded ±1". Thus, in this analysis both 3.6" (DLR recommended), and 1" were used to calculate the onset frequencies for comparison.

The Simulink® models used to calculate the onset frequencies for the three configurations are in Figure 3-6 and Figure 3-7. The LINMOD command was used to calculate the transfer function between input-1 (Pilot Input) and output-6 (RLE input)

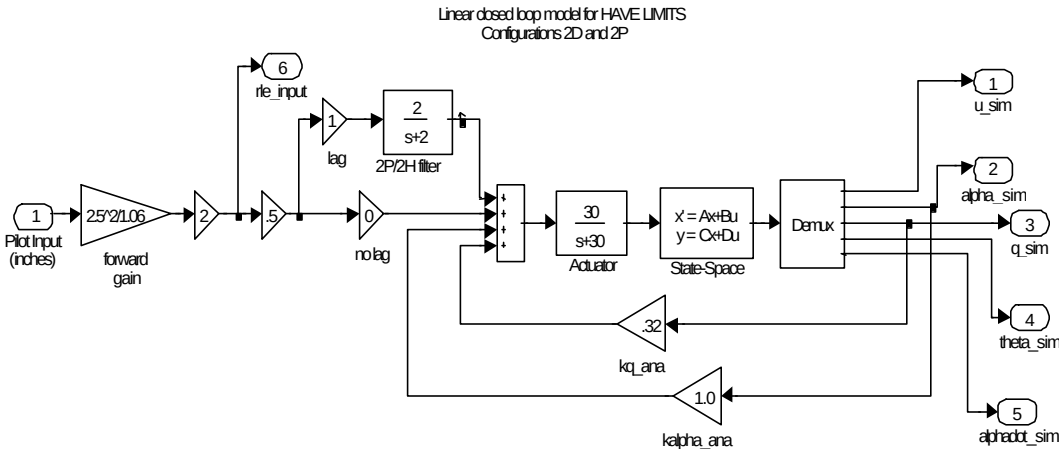

Figure 3-6. Closed-Loop Model, Configuration 2D/2P

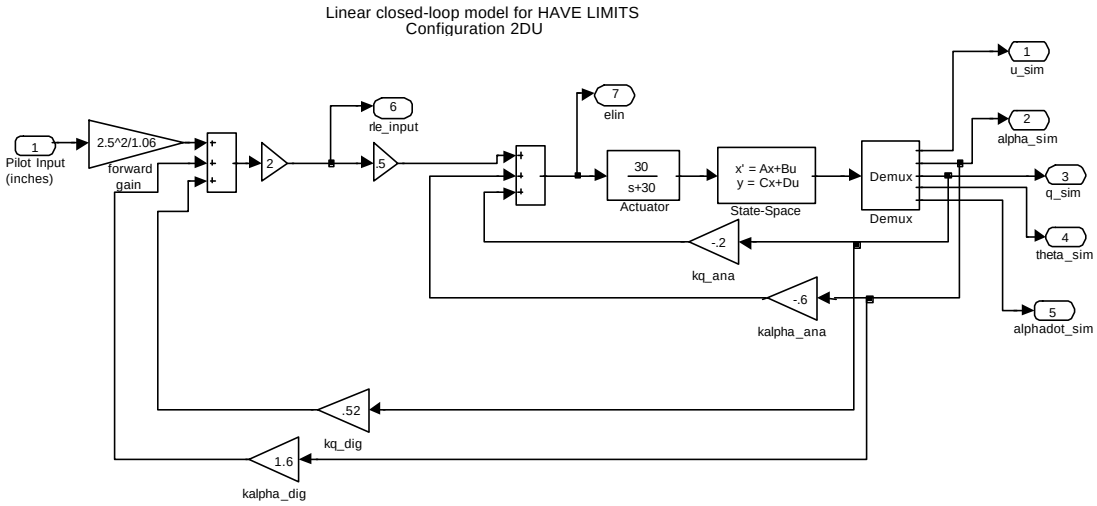

Figure 3-7. Closed-Loop Model, Configuration 2DU

as labeled in the figures. As shown in Chapter 2, the onset frequency can be determined graphically. The onset frequencies for the three configurations are shown in Table 3-5. The graphical technique used to solve for these frequencies is illustrated in Figure 3-8. Notice that the amplitude lines for configurations 2D and 2P are constant with respect to frequency. This reflects the fact that the rate limiter in these configurations is located in the forward path of the flight control system, as can be seen in Figure 3-6. Thus, the rate limiter input amplitude is strictly a function of pilot input amplitude. Configuration 2DU, on the other hand, incorporates the rate limiter in the feedback path, Figure 3-7, so the rate limiter input amplitude is based on the sum of pilot inputs and the digital feedback gains. Also notice as the pilot input amplitude is increased the amplitude lines are shifted up in magnitude and the intersection with the rate limit lines occur earlier giving much lower onset frequencies. This is also illustrated in Table 3-5.

Table 3-5. HAVE LIMITS Onset Frequencies

Rate (deg/s)	Onset Frequencies (rad/sec)			
	Configuration 2D/2P		Configuration 2DU	
	P_o=1.0"	P_o=3.6"	P_o=1.0"	P_o=3.6"
10	.851	.236	2.16	1.10
20	1.70	.471	2.93	1.62
30	2.55	.708	3.49	1.97
40	3.39	.941	4.00	2.26
50	4.23	1.18	4.47	2.50
60	5.09	1.41	4.95	2.69
157	13.3	3.69	11.05	4.19

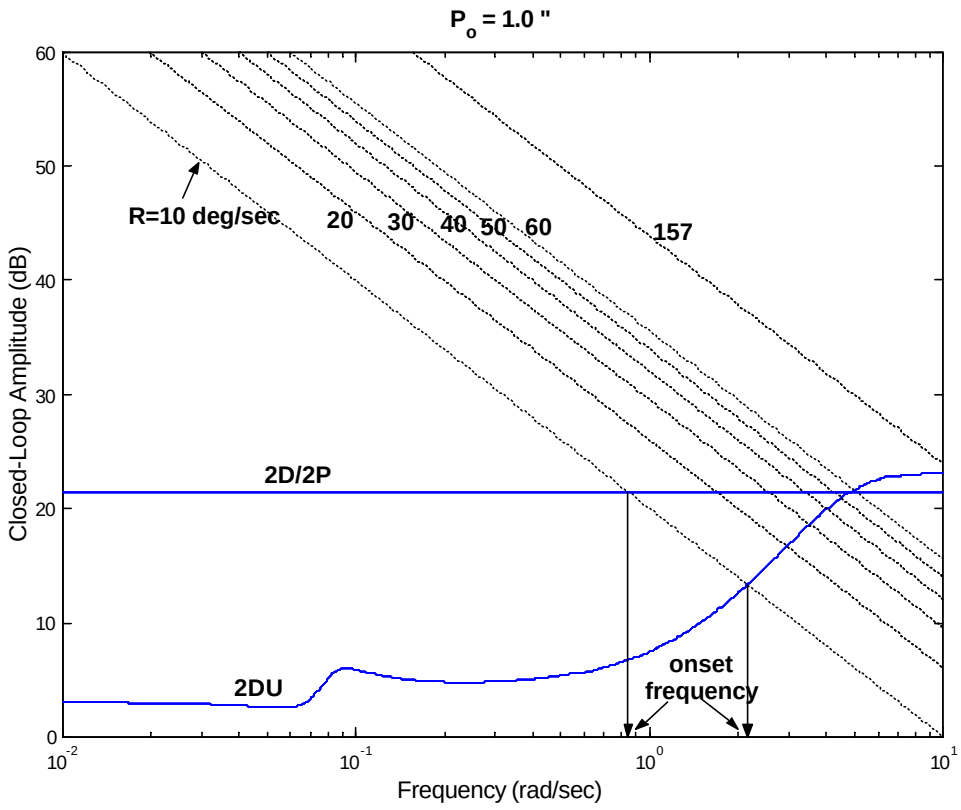

Figure 3-8. Determination of HAVE LIMITS Onset Frequencies

Calculation of OLOP

The final step in determining OLOP for a given system is to calculate the required open-loop transfer function and plot the magnitude and phase for each onset frequency on a Nichols chart. To get the appropriate transfer function required breaking the loop at the position of the rate limiter. Then the output of the rate limiter became the input to the open-loop system, U_{OLOP}, and the output of the system, Y_{OLOP}, the input to the rate limiter. The Simulink® models used to calculate the transfer functions, again using the LINMOD function, are shown in Figure 3-9 and Figure 3-10.

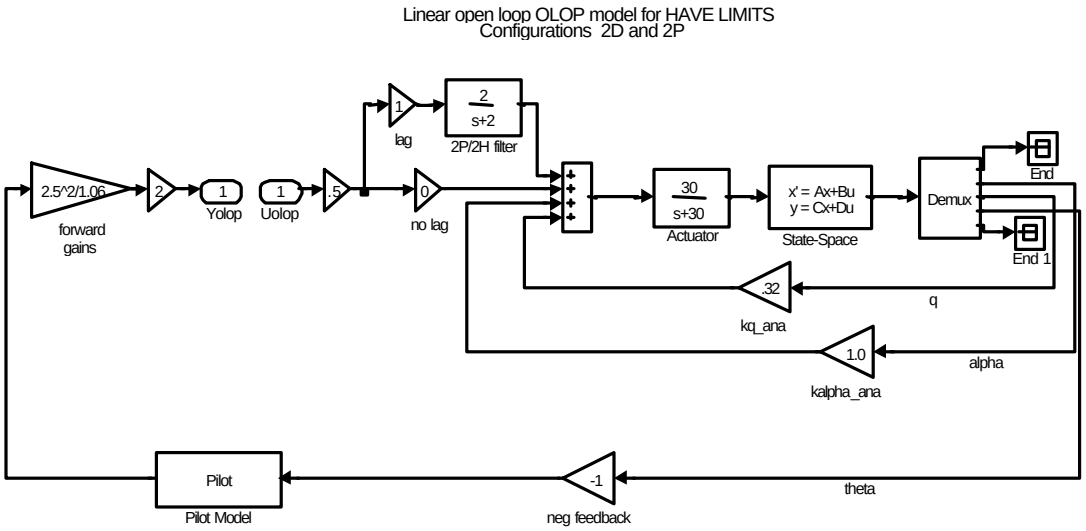

Figure 3-9. Open-Loop Model, Configuration 2D/2P

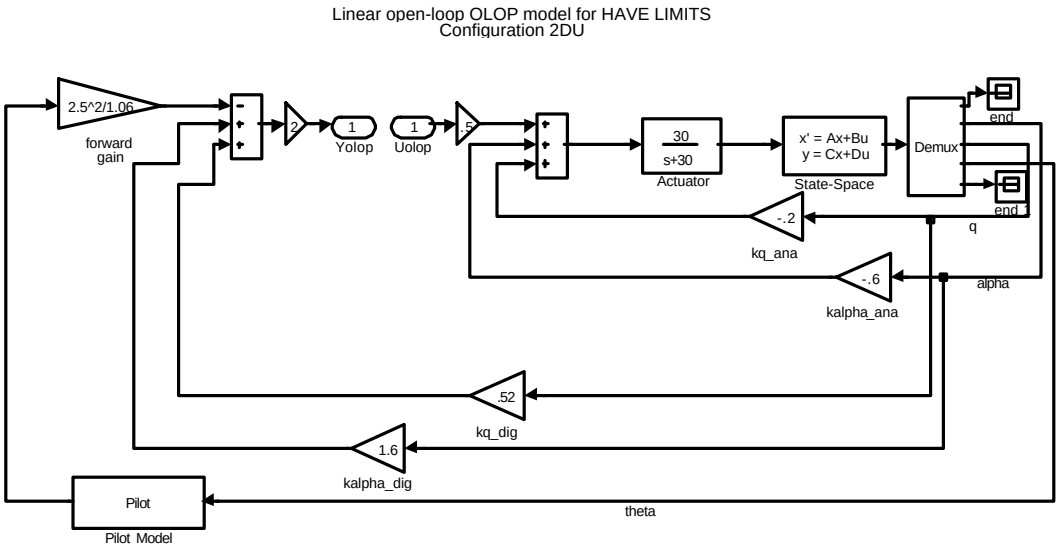

Figure 3-10. Open-Loop Model, Configuration 2DU

Following is a summary of the OLOP results for each configuration. A MATLAB® file called olop.m was used to automate the entire process and is located in Appendix B.

Configuration 2D.

Limited flight test data for this configuration was available but some attempts to match flight test data with simulation results using various pilot gain models were made. This technique was similar to the one used by DLR in their simulator validation [8]. The goal was to find a suitable value for the pilot gain that would yield simulation characteristics that were similar to the actual flight test data in terms of overshoot, damping, etc. The purpose was to see if a simple gain model was suitable and how it compared to the recommended range of gain values. Three separate test runs were examined, each by a different pilot. A simple gain pilot model was appended to Figure 3-6 and then the simulation was conducted with unity pitch angle feedback, θ, and a pitch angle command signal, θ_c. For the three runs, an average suitable gain was calculated to be K_g = -.75, which corresponded to a crossover angle of Φ_c = -142 deg. An example of the simulation results and flight test data is presented in Figure 3-11. This gain value was outside the recommended range of $-130 \leq \Phi_c \leq -90$ degrees and will be referred to as a *very high* gain pilot for this analysis. Note that the overshoots and damping factors in the simulation appear to be less in magnitude when compared to the flight test. Attempts to raise the gain to match the overshoots more closely resulted in unacceptable damping factors. Thus, this value for the pilot gain was deemed reasonable.

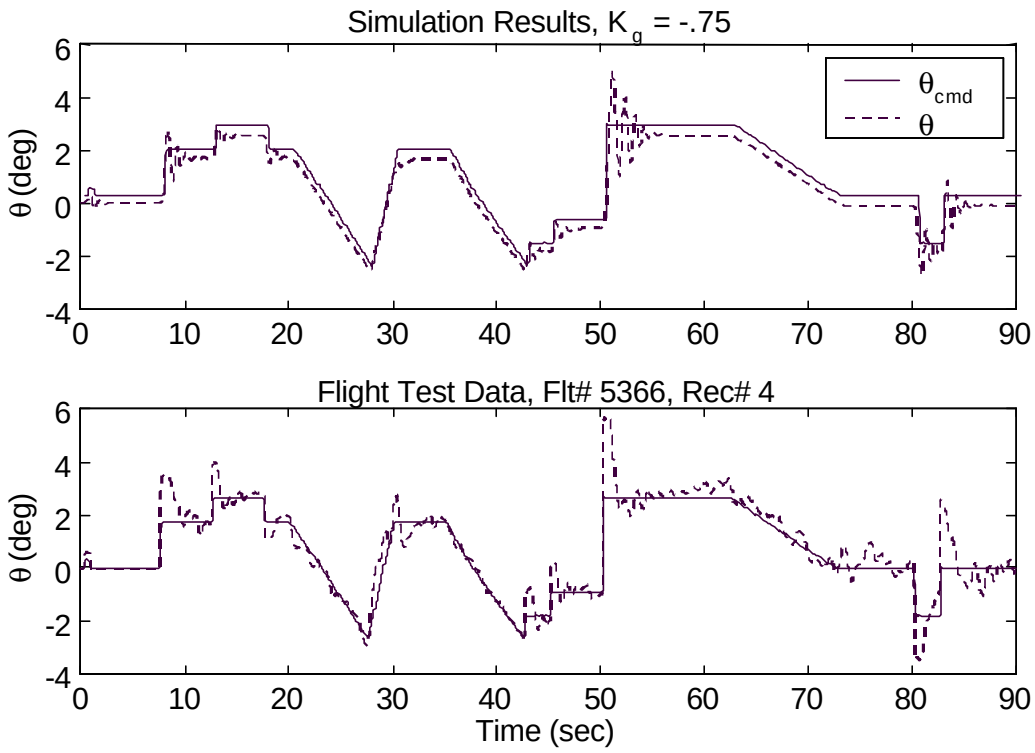

Figure 3-11. Pilot Gain Matching Results

The open-loop frequency response charts and the corresponding OLOPs for Configuration 2D with a stick amplitude of 3.6" are shown in Figure 3-12 and Figure 3-13. Plots for four different pilot model gains are shown (the first three are from the recommended range and the last is the *very high* gain discussed earlier in this section) and also for the Neal-Smith pilot model. The rate limit for each OLOP is depicted. The mean PIO ratings are listed on the Neal-Smith chart and are grouped relative to the tracking task performed (i.e. Dis=Discrete, SOS=Sum-of-Sines). OLOP charts calculated using a stick amplitude of 1" are shown in Figure 3-14 and Figure 3-15. Correlation of the OLOP predictions to the mean PIO ratings from the flight test are listed in Table 3-6.

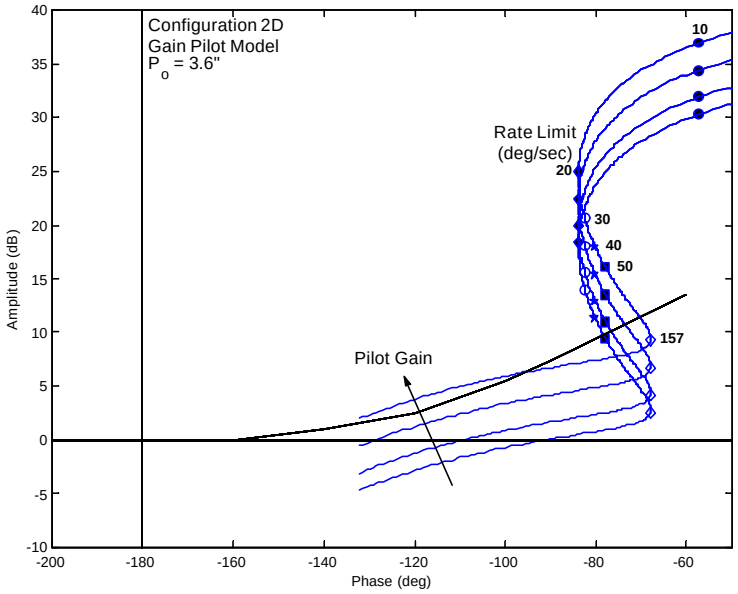

Figure 3-12. Open-loop Frequency Response, 2D, Gain Model, P_o = 3.6”

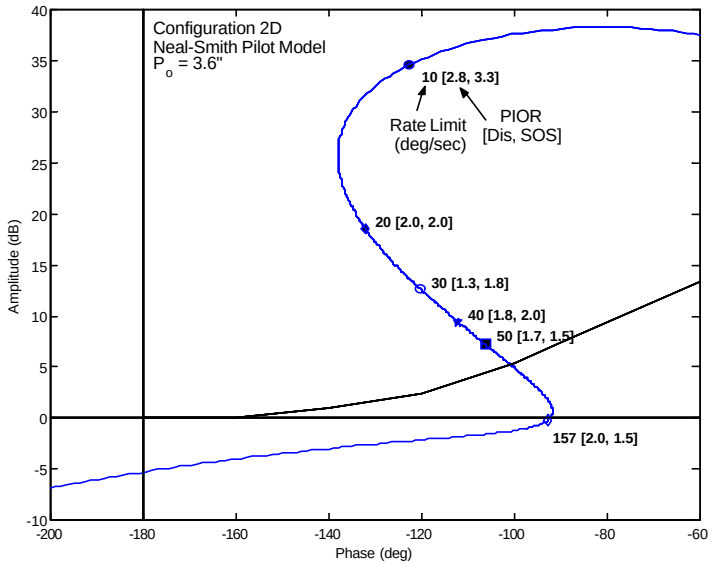

Figure 3-13. Open-loop Frequency Response, 2D, Neal-Smith Model, P_o = 3.6”

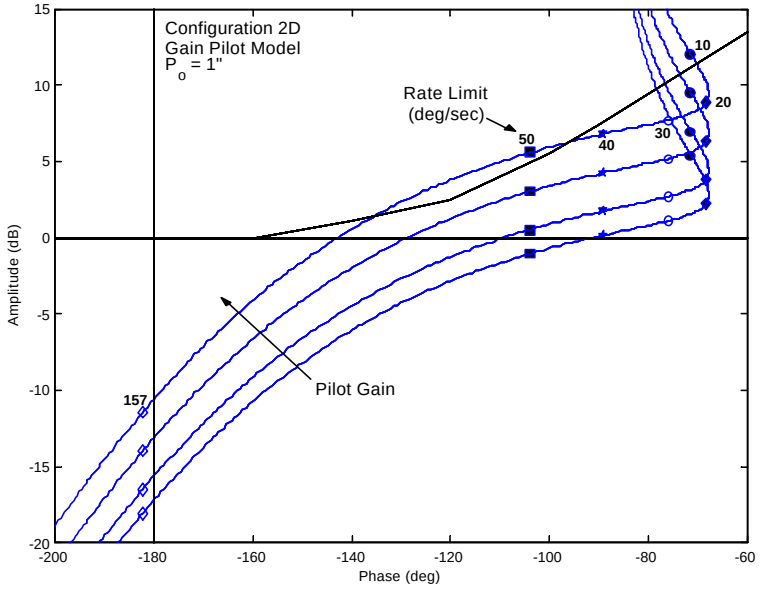

Figure 3-14. Open-loop Frequency Response, 2D, Gain Model, P_o = 1”

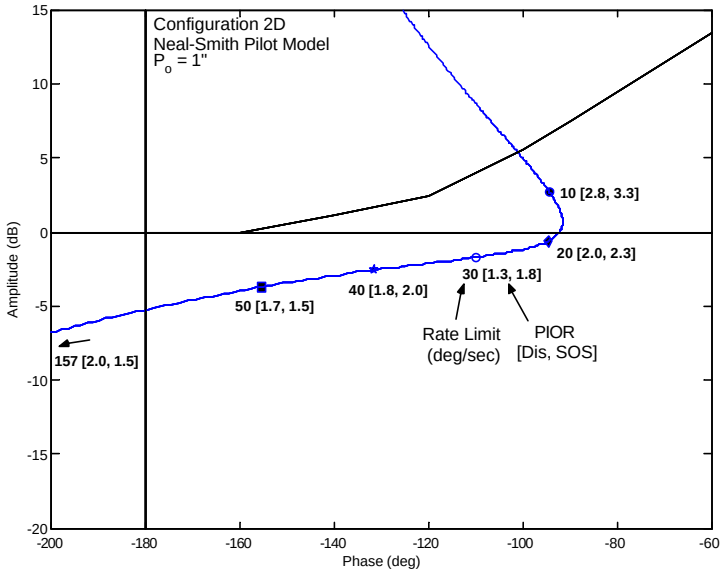

Figure 3-15. Open-loop Frequency Response, 2D, Neal-Smith Model, P_o = 1”

Table 3-6. PIO Ratings and OLOP Comparison, Configuration 2D

	Rate	**10**	**20**	**30**	**40**	**50**	**157**
	PIOR (Dis, SOS)	2.8, **3.3**	2.0, 2.3	1.3, 1.8	1.8, 2.0	1.7, 1.5	2.0, 1.5
	σ (Dis, SOS)	.5 , .6	0 , .6	.6 , 1.0	.8 , .9	.6 , .6	0 , .7
P_o = 1.0"	Neal-Smith						
	Low Gain						
	Medium Gain						
	High Gain						
	Very High Gain	**P**				**P**	
P_o = 3.6"	Neal-Smith	**P**	**P**	**P**	**P**	**P**	
	Low Gain	**P**	**P**	**P**	**P**		
	Medium Gain	**P**	**P**	**P**	**P**	**P**	
	High Gain	**P**	**P**	**P**	**P**	**P**	
	Very High Gain	**P**	**P**	**P**	**P**	**P**	

PIOR = Mean Pilot-Induced Oscillation Rating
Dis = Discrete Tracking Task
SOS = Sum-of-Sines Tracking Task
σ = Standard Deviation
P_o = Pilot Input Amplitude
P = Above OLOP Stability Boundary, i.e. PIO prone

The mean PIO ratings and the standard deviation versus rate limit are contained in the first three rows of Table 3-6. Each are depicted for the two different tracking tasks: discrete (Dis) and sum-of-sines (SOS). The last column (157 deg/sec) essentially represents the unlimited or linear case since rates of this magnitude were never achieved. Shaded blocks are for a mean PIO rating >3 which correlates to PIO. This value was selected based on the PIO rating scale in Appendix A. The transition point from undesirable motions to actual oscillations occurs between PIO ratings of 3 and 4 on the scale. Since these were mean PIO ratings, it was assumed that for a mean >3 the aircraft was rated PIO prone at some point during the test. This same correlation will be used in the flight test.

The rest of the table shows the OLOP results for each pilot model versus rate limit and stick input amplitude. The shaded boxes with a **P** designation are those OLOP points

that were on or above the proposed stability boundary and are thus considered PIO prone. Ideally, for the OLOP criterion to accurately predict the opportunity for PIO, the shaded boxes from the PIO ratings should match with the shaded boxes of the OLOP results in the same column.

Clearly, for a stick amplitude of P_o=3.6" the OLOP results do not correlate well with the PIO ratings for any of the pilot models. In this case, PIO was over-predicted. Examination of Figure 3-12 and Figure 3-13 illustrate how the maximum input amplitude drives nearly all of the OLOPs well above the boundary whereas the configuration was rated PIO prone only for a rate limit of 10 deg/sec. Had the tasks in the flight test required maximum stick amplitudes then perhaps the PIO ratings would have yielded better correlation.

As discussed earlier, a value of P_o=1" was selected as a reasonable value for stick amplitude based on flight test data. The OLOP results correlate much better using this value as can be seen in Figure 3-14 and Figure 3-15. Only the very high gain pilot model shows an OLOP slightly above the boundary for a rate limit of 10 deg/sec, which correlates with the worst mean PIO rating of 3.3. Again, this particular gain value was determined by matching simulation results with flight test data. Notice that because the rate limiter in this case was in the forward loop, a change in pilot gain is simply a vertical shift in amplitude on the Nichols chart. This implies that a simple reduction in pilot gain would move the OLOP below the PIO boundary. Notice also that the OLOP for 50 deg/sec lies slightly above the boundary whereas the mean PIO ratings show a non-PIO aircraft. Lastly, notice how the frequency response curve somewhat parallels the stability

boundary over a wide range of frequencies. This shows that for forward path limiters, the criterion is more sensitive to changes in pilot gain than it is to changes in stick amplitude in these frequency ranges.

The Neal-Smith model shows all OLOPs below the boundary but with the 10 deg/sec point fairly close to it (within 2.5dB). This suggests a small increase in gain or stick input amplitude for this low rate limit would drive this point into the PIO region. A trend of increasing PIO ratings with decreasing rate limits is evident.

A recent study accomplished by DLR analyzing the HAVE LIMITS database presented similar results [10]. Except for small variations in the aircraft and actuator models, essentially the same Nichols plots were produced for this configuration. DLR selected only the high gain pilot model for their analysis and used a stick amplitude of P_o=1.5" (based on simulation analysis). This higher stick amplitude correlated to a lower onset frequency, which had the effect of driving the OLOPs up the curve toward the PIO boundary. Their results showed only the 10 deg/sec OLOP slightly above the boundary that correlated nicely with the flight test data. Analysis of the models for this thesis showed identical results for the 10 deg/sec point when P_o was increased to 1.5" for both the Neal-Smith and the high gain pilot models.

For rate limiting elements in the forward loop, the OLOP criterion is strongly dependent on two closely related variables: pilot gain and stick amplitude. Clearly, if the two values are picked "just right" the OLOP criterion matches well with the flight test data. But with large variations in both values there is potential for widely varying results. One way to minimize the variables is to just pick a pilot model, either a high gain or the

Neal-Smith for example, and then realize that for forward path limiters a reduction in pilot gain will slide the OLOP curve down on the Nichols chart and below the boundary. That leaves stick amplitude as the remaining variable. Stick amplitude is itself a function of stick dynamics, pilot technique, and task. It would be difficult to predict what stick amplitude to use for a given task early in the design stage without the luxury of simulator or flight test data to compare with. Obviously, applying the maximum value, as DLR suggests, would be a worst case scenario but would not necessarily flush out PIO susceptibility using smaller amplitudes. Further discussion on how to address this variable will be presented later in this chapter.

Configuration 2DU.

A similar pilot gain matching technique was used with this configuration as was done with configuration 2D. However, gain values much higher than the medium gain pilot resulted in instabilities in the system and analysis was difficult to perform. Since 2DU and 2D had similar characteristics with all loops closed the same very high gain value was used for this analysis as was used for 2D in addition to the recommended pilot gain values.

The open-loop frequency response charts and the corresponding OLOPs for Configuration 2DU with stick amplitudes of 3.6" and 1" are presented in Figure 3-16 through Figure 3-19. Just as for the 2D case, plots for the four different pilot model gains and for the Neal-Smith pilot model are shown. The rate limit and PIO ratings for each OLOP are depicted. Correlation of the OLOP predictions to the PIO ratings from the flight test are presented in Table 3-7.

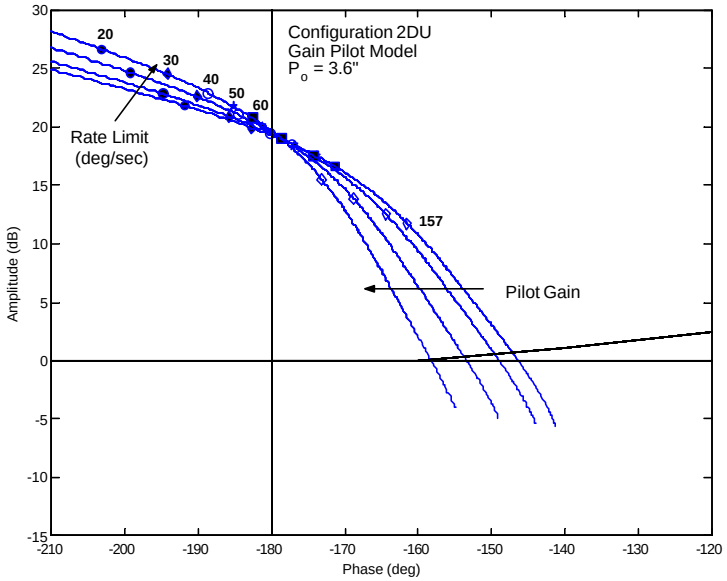

Figure 3-16. Open-loop Frequency Response, 2DU, Gain Model, P_o = 3.6”

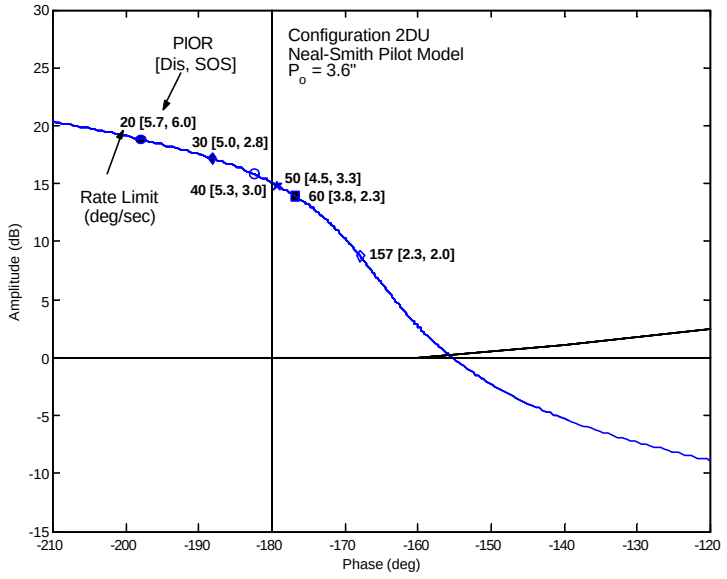

Figure 3-17. Open-loop Frequency Response, 2DU, Neal-Smith Model, P_o = 3.6”

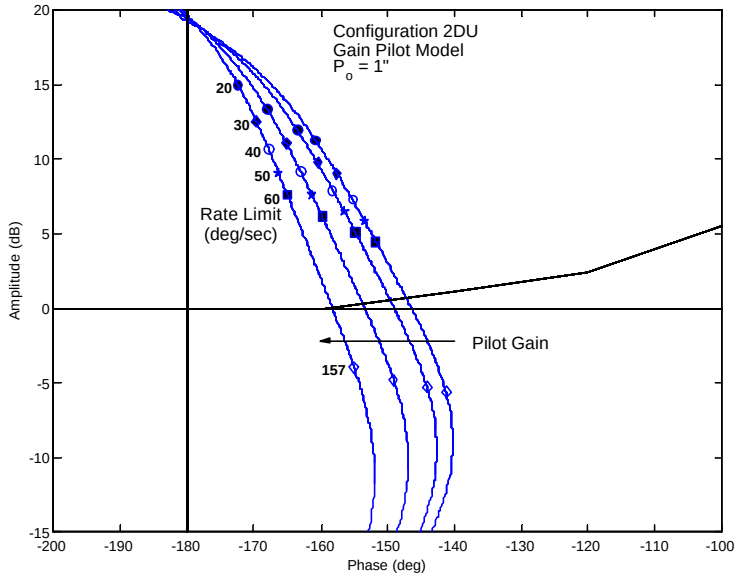

Figure 3-18. Open-loop Frequency Response, 2DU, Gain Model, P_o = 1”

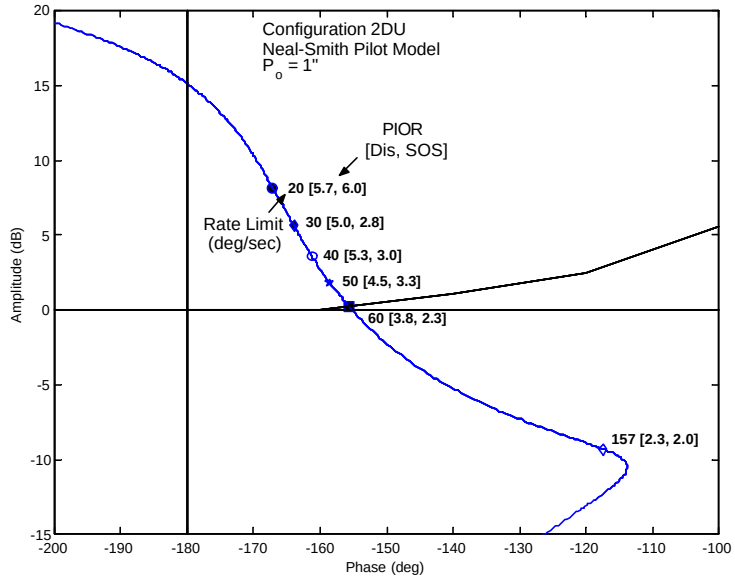

Figure 3-19. Open-loop Frequency Response, 2DU, Neal-Smith Model, P_o = 1”

Table 3-7. PIO Ratings and OLOP Comparison, Configuration 2DU

	Rate	**20**	**30**	**40**	**50**	**60**	**157**
	PIOR (Dis, SOS)	**5.7, 6.0**	**5.0**, 2.8	**5.3,** 3.0	**4.5, 3.3**	**3.8**, 2.3	2.3, 2.0
	σ (Dis, SOS)	.6 , 0	0 , 1.3	.6 , .8	.6 , .6	1.3 , .5	.6 , 0
P_o = 1.0”	Neal-Smith	**P**	**P**	**P**	**P**	**P**	
	Low Gain	**P**	**P**	**P**	**P**	**P**	
	Medium Gain	**P**	**P**	**P**	**P**	**P**	
	High Gain	**P**	**P**	**P**	**P**	**P**	
	Very High Gain	**P**	**P**	**P**	**P**	**P**	
P_o = 3.6”	Neal-Smith	**P**	**P**	**P**	**P**	**P**	**P**
	Low Gain	**P**	**P**	**P**	**P**	**P**	**P**
	Medium Gain	**P**	**P**	**P**	**P**	**P**	**P**
	High Gain	**P**	**P**	**P**	**P**	**P**	**P**
	Very High Gain	**P**	**P**	**P**	**P**	**P**	**P**

PIOR = Mean Pilot-Induced Oscillation Rating
Dis = Discrete Tracking Task
SOS = Sum-of-Sines Tracking Task
σ = Standard Deviation
P_o = Pilot Input Amplitude
P = Above OLOP Stability Boundary – PIO prone

Recall that this configuration consisted of an unstable plant with the rate limiter in the feedback path. One would expect that in the event of rate limiting the system would take on its open-loop characteristics and diverge. The PIO ratings reflect this and tend to get worse as the rate limit decreases. As it turns out in this particular case, all the pilot models for both stick amplitudes accurately predict PIO but further examination of the Nichols charts is necessary.

For P_o=3.6”, the OLOPs are well above the boundary including the 157 deg/sec point. This can be somewhat misleading since the PIO ratings for that rate limit do not show PIO tendencies. This can be explained by the fact that the OLOP criterion only predicts PIOs in the presence of rate limiting. Since commanded input signals never exceeded this very high rate limit, the OLOP point is meaningless. It merely says that if

rate limiting *had* occurred at this limit value and stick amplitude, then a PIO may have been likely.

For P_o=1", the OLOPs correlate quite well for all the pilot models. By examining Figure 3-19, one could argue that the Neal-Smith model correlates the best because the 60 deg/sec OLOP is just on the boundary. The mean PIO rating for the discrete task at this rate limit is 3.8, suggesting that this is possibly the transition point from a non-PIO aircraft to one that is PIO prone. As the rate limit decreases the OLOPs are driven deeper into the PIO region correlating to the increase in PIO ratings. If this was the transition point (60 deg/sec), it again shows that using maximum stick amplitude can over-predict PIO, by examination of Figure 3-16, where this point is still well above the boundary.

Note that for this configuration, with the rate limiter in the feedback path, variation in pilot gain has less impact on the position of OLOP in the Nichols chart as opposed to forward path limiters (see Figure 3-18). Thus the selected pilot gain is less critical. In fact, DLR came to the same conclusion regarding pilot model sensitivity after a recent flight test of their own stating "…in the longitudinal axis, the sensitivity to changes of pilot gain is rather low, such that an inaccuracy in determining the gain does not significantly change the OLOP location" [12]. However the stick amplitude still had a significant impact as it did for configuration 2D.

Configuration 2P.

A similar pilot gain matching technique was used with this configuration as was done with configuration 2D. A gain value of K_g = -.62, which corresponds to a crossover angle of Φ_c= -142 degrees, was determined to be a suitable average gain based on three separate test records. As before, this gain value will be referred to as the very high gain.

The open-loop frequency response charts and the corresponding OLOPs for Configuration 2P with stick amplitudes of 3.6" and 1" are presented in Figure 3-20 through Figure 3-23. Just as for the 2D case, plots for the four different pilot model gains and for the Neal-Smith pilot model are shown. The rate limit and PIO ratings for each OLOP are depicted. Correlation of the OLOP predictions to the PIO ratings from the flight test are contained in Table 3-8.

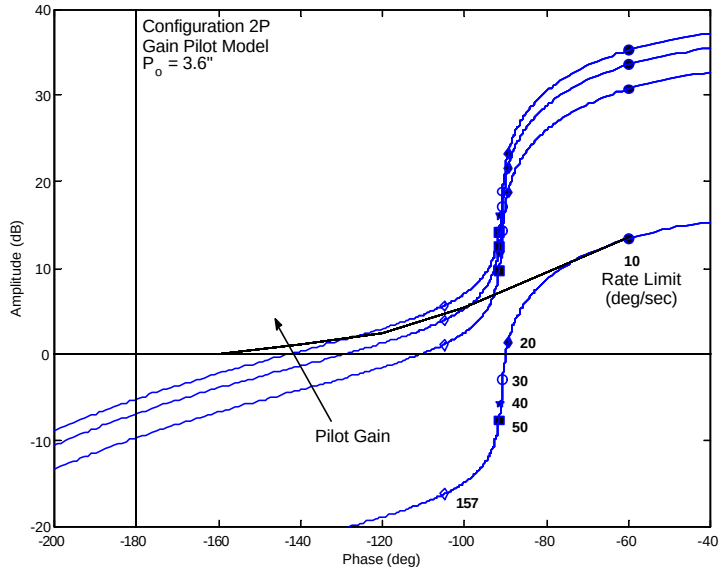

Figure 3-20. Open-loop Frequency Response, 2P, Gain Model, P_o = 3.6”

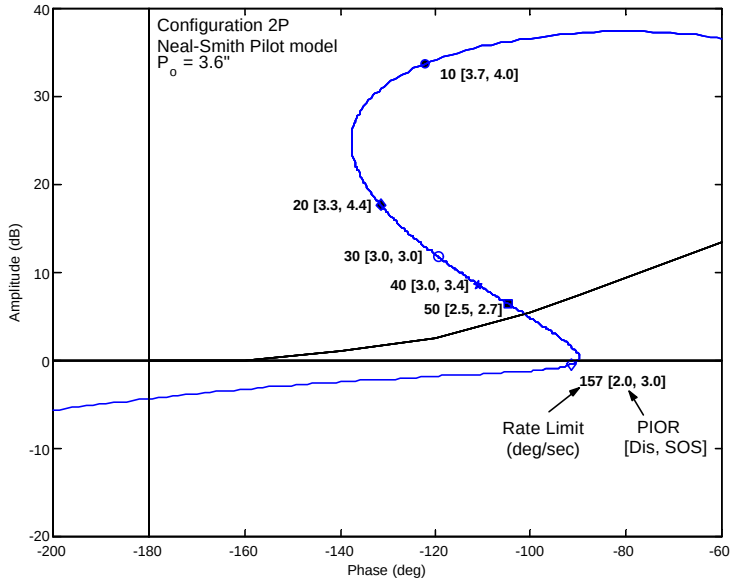

Figure 3-21. Open-loop Frequency Response, 2P, Neal-Smith Model, P_o = 3.6”

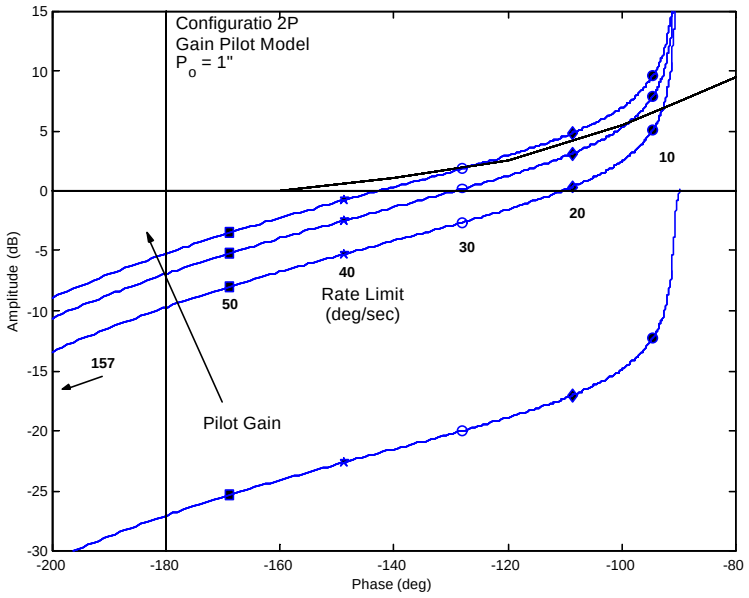

Figure 3-22. Open-loop Frequency Response, 2P, Gain Model, P_o = 1”

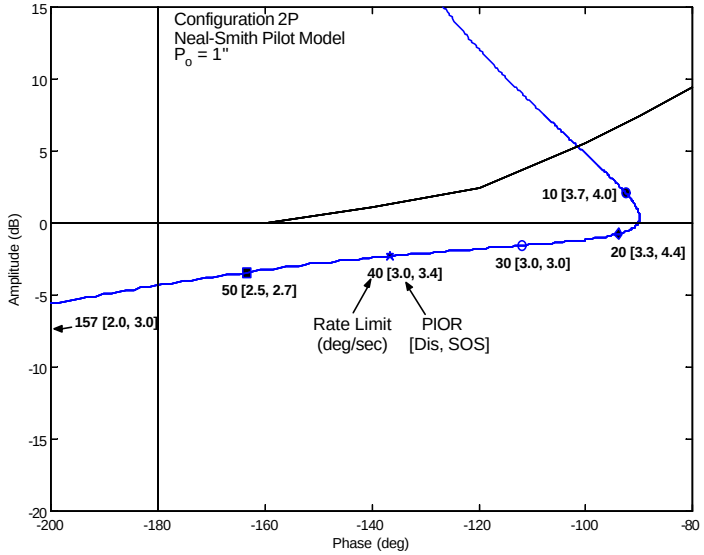

Figure 3-23. Open-loop Frequency Response, 2P, Neal-Smith Model, P_o = 1”

Table 3-8. PIO Ratings and OLOP Comparison, Configuration 2P

	Rate	**10**	**20**	**30**	**40**	**50**	**157**
	PIOR (Dis, SOS)	**3.7, 4.0**	**3.3, 4.4**	3.0, 3.0	3.0, **3.4**	2.5, 2.7	2.0, 3.0
	σ (Dis, SOS)	1.2, 0	1.1, .6	0, 0	.8 , .5	.6 , .5	0 , 0
P_o = 1.0"	Neal-Smith						
	Low Gain						
	Medium Gain						
	High Gain	**P**					
	Very High Gain	**P**	**P**	**P**			
P_o = 3.6"	Neal-Smith	**P**	**P**	**P**	**P**	**P**	
	Low Gain	**P**					
	Medium Gain	**P**	**P**	**P**	**P**	**P**	
	High Gain	**P**	**P**	**P**	**P**	**P**	
	Very High Gain	**P**	**P**	**P**	**P**	**P**	**P**

PIOR = Mean Pilot-Induced Oscillation Rating
Dis = Discrete Tracking Task
SOS = Sum-of-Sines Tracking Task
σ = Standard Deviation
P_o = Pilot Input Amplitude
P = Above OLOP Stability Boundary – PIO prone

Recall that this configuration was identical to 2D with a first order lag added to the forward path. This additional lag resulted in a requirement for more pilot compensation and a Level 2 Neal-Smith rating. It was also predicted to be PIO prone using other linear methods [15]. Flight test data for the unlimited case somewhat confirms those predictions by garnering a mean PIO rating of 3.0 for the sum-of-sines task; a full rating and a half greater than that obtained for the 2D configuration.

Certainly, the presence of rate limiting could have increased the severity or likelihood of PIO but it could not be singled out as the sole cause for this configuration. The OLOP criterion could be used in this case to examine the degradation in PIO susceptibility due to rate limiting above and beyond the unlimited configuration. Although there was some variance in the PIO ratings for the various rate limits, one could conclude that the 10 and 20 deg/sec rate limits had the most significant effect shown by

an increase in the mean PIO ratings of approximately a factor of one. Thus, these two OLOPs should be on or near the boundary. Examining Figure 3-22 shows that the high gain and the very high gain pilots correlate best with the flight test results. Again, as was seen with 2D, the OLOP curves tend to parallel the boundary. Examining Figure 3-23 shows that the Neal-Smith model does not do as well for this particular case using this stick amplitude. Once again, as with configuration 2D, the pilot gain and stick amplitude had a dramatic effect on the OLOP results for forward path limiters

A New Metric: Stick Ratio (SR)

The application of OLOP is dependent on three major factors: pilot model, rate limit, and stick input amplitude. The pilot model affects the general shape and position of the curve on the Nichols chart. The rate limit and input amplitude affect the position of the OLOP along that curve. Since the rate limit is inherent to the actuator design it is assumed known. That leaves the pilot model and the stick amplitude as the remaining variables. As was shown in the evaluation of the HAVE LIMITS data, variations on these variables can have drastic effects on the position of the OLOP. The analysis showed that choosing either the Neal-Smith or the high gain (Φ_c = -130 deg) pilot model yields similar results. Thus, at this point, using either model seems reasonable with the caveat that for rate limiters in the forward path, the OLOP is very sensitive to gain variations.

Once a pilot model is chosen, the remaining variable is the stick input amplitude. In order to try and eliminate only picking the maximum input amplitude, as DLR

suggests, a new metric called *stick ratio* (SR) is introduced. Stick ratio is defined as the percentage of maximum input amplitude required to drive the OLOP above the PIO boundary on the Nichols chart. An example of this concept is illustrated in Figure 3-24. The OLOP chart for the 2DU Configuration with a 60 deg/sec rate limit using the Neal-Smith pilot model is shown. Here the stick amplitude has been varied to yield stick ratios between 20% and 25%. At SR≈24%, the OLOP crosses the stability boundary. This study hypothesizes that perhaps there is a correlation between stick ratio and PIO likelihood. If only a small stick ratio is required to drive the OLOP into the PIO region, possibly representing stick inputs that are achieved on a regular basis during high precision or operational tracking, then PIO would be encountered more frequently.

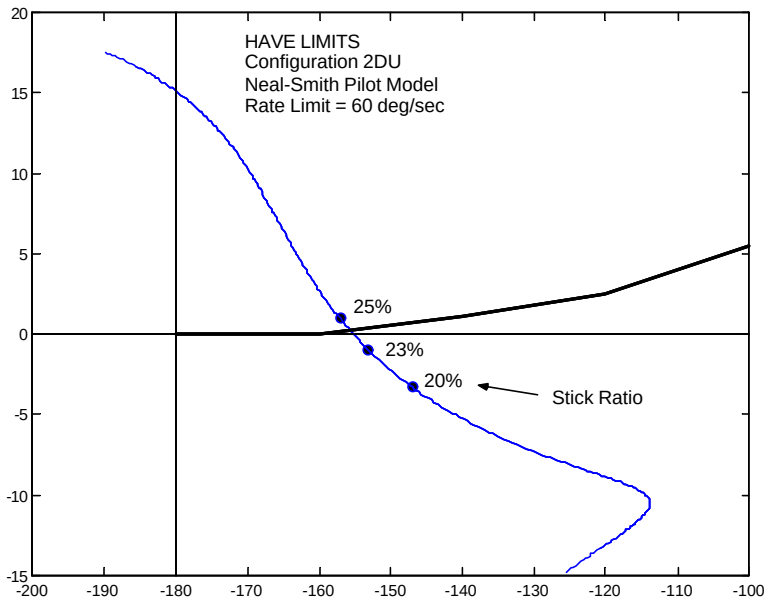

Figure 3-24. Stick Ratio Illustration

On the other hand, if a relatively large stick ratio were required then, depending on the task of course, the likelihood of PIO would be less. Thus, the use of stick ratio would help flush out those configurations that may be PIO prone for stick amplitudes less than the maximum value.

This new metric was applied to the HAVE LIMITS configurations 2D and 2DU utilizing the Neal-Smith pilot model and is shown in Figure 3-25. Recall that the given tasks for HAVE LIMITS required a maximum stick input of approximately 1" or SR≈30%. If, for a given configuration and rate limit, the stick ratio required to drive the OLOP above the stability boundary was below this value then PIO would likely be encountered. This was the case for the 2DU configuration. Even though the given task required the use of only 30% of available stick amplitude, these smaller inputs, in conjunction with rate limiting, were enough to put OLOP in the dangerous PIO region. This was reflected by the mean PIO ratings >3 for all rate limits. Conversely, configuration 2D only encountered the PIO region for the lowest rate limit of 10 deg/sec. For the higher rate limits, even though rate limiting may have occurred, the associated stick amplitudes used were not high enough to drive the OLOP into the PIO region. Mean PIO ratings for this configuration were <3.0 for the higher rate limits.

If the given task had required maximum stick amplitudes then, according to OLOP, both configurations would have been PIO prone for all rate limits. Thus, the major players in whether or not a configuration is PIO prone are the given task, the amount of stick authority given to the pilot, and pilot technique.

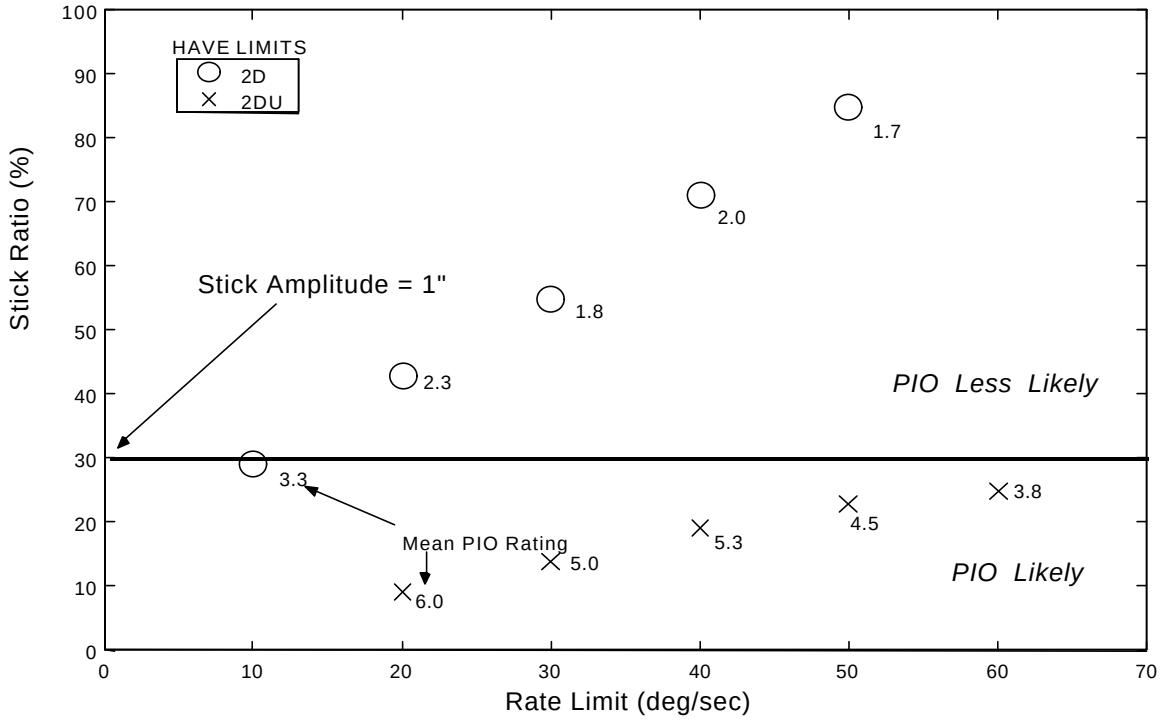

Figure 3-25. HAVE LIMITS Stick Ratio Plot

Configuration 2DU was obviously a worst case scenario because only a small stick ratio was required to make it PIO prone. Configuration 2D was at the other end of the spectrum, especially for the higher rate limits. In this case, if the given task represented the anticipated stick inputs needed to accomplish a typical mission for this aircraft, one could say that 2DU was PIO prone and 2D was not (except for the lowest rate limit).

By looking at the full range of stick inputs, it becomes clear that PIO can be encountered without utilizing full stick deflection. Examining the stick ratio concept can help flush out those amplitudes that drive the OLOP into the PIO region. If the stick ratio

is small, then these amplitudes would most likely be encountered during a typical mission and the aircraft would encounter PIO in the presence of rate limiting. If the stick ratio is large, then perhaps these amplitudes would only rarely be encountered during a typical mission. This aircraft is still PIO prone for maximum inputs combined with rate limiting, but the likelihood of achieving these amplitudes would be much less than that with a small stick ratio making the aircraft less PIO prone. One would have to look at the broad range of expected tasks needed to accomplish the mission for a given aircraft design and exercise engineering judgement as to whether or not it is susceptible to PIO due to rate limiting. Further investigation into this concept will be examined in the following sections and the flight test.

HAVE LIMITS Conclusions

The OLOP criterion was used to evaluate the three configurations from the HAVE LIMITS database. When the maximum stick amplitude (3.6") was applied, OLOP over-predicted PIO for all configurations. After applying OLOP using a stick amplitude more representative of what actually occurred in the flight test (1"), correlation between OLOP predictions and pilot ratings improved. This demonstrated the strong influence of stick amplitude on the criterion and illustrated a limitation to its use as a prediction tool. A new metric, *stick ratio*, was introduced to try to evaluate the likelihood of PIO versus the full range of stick amplitudes using OLOP. Preliminary analysis seemed to indicate good correlation between stick ratio and PIO susceptibility based on this flight test data.

The analysis included an examination of the full range of DLR recommended gain pilot models, a flight test derived gain model, and the Modified Neal-Smith model. The flight test derived gain model (very high) was slightly outside of the recommended range of gain models. For the forward path limiters (2D and 2P) the high gain and the Neal-Smith models showed good correlation with pilot ratings while the very high gain model fared slightly better. For the feedback limiter case (2DU) all pilot models correlated well, with the Neal-Smith model providing perhaps the best correlation. Changes in pilot gain had a dramatic effect on the position of the OLOPs relative to the stability boundary for forward path limiters. The changes were less dramatic for the feedback limiter. Based on this analysis, only the high gain and Neal-Smith models will be used from this point forward since both have given promising results. However, one needs to keep in mind the effect of pilot gain when evaluating forward path limiters.

A major limitation to this analysis should be noted. Although this was the largest database examining rate limiting effects, only a small amount of clean flight test data was available. Better flight test data would have been helpful to determine if in fact rate limiting had occurred for each run. Thus, some PIO ratings included in this analysis may have been given in the absence of rate limiting, and would therefore be meaningless when trying to correlate with OLOP. Hopefully, these were only few and far between. Plus, the analysis still seemed to show positive trend information. Additionally, using 1" for stick amplitude was based on examination of these limited time histories. A more thorough analysis would involve examination of each and every run to look at actual stick amplitudes. Determining whether or not sufficient rate limiting occurred and actual stick amplitudes for OLOP correlation will be addressed in the flight test.

IV. Analysis of HAVE FILTER

As with HAVE LIMITS, the OLOP criterion was applied to the HAVE FILTER TMP database and the methodology and results are presented in this chapter. Both feedback and forward path configurations were evaluated in addition to configurations with multiple limiters. A stick ratio analysis was performed as well.

HAVE FILTER Overview

The HAVE FILTER TMP was conducted on 1-18 September 1998, at the Calspan flight research facility in Buffalo NY [1]. The purpose of the TMP was to examine the prevention of PIO/departure due to rate limiting using a non-linear rate limiter pre-filter (RLPF). Three USAF TPS students flew the flight test on the Variable Stability In-Flight Simulator (VISTA) NF-16D. Each test pilot had primarily a fighter background. A total of four calibration and nine test sorties were flown.

Before the RLPF was implemented into the test aircraft, some baseline configurations were flown with rate limiters in the forward and feedback paths. These configurations were ideal for OLOP analysis and are shown in Figure 4-1 and Figure 4-2. The Baseline configuration consisted of several components: unstable bare airframe dynamics (pole at s = +1.34 with a time to double amplitude of 0.5 seconds), q and α feedbacks generating the overall HAFA1 (Highly Augmented Fighter Aircraft) and HAFA2 dynamics, and a rate limited (60 deg/sec) actuator model in the feedback loop. The Baseline + SWRL (Software Rate Limiter) configuration was created by adding the

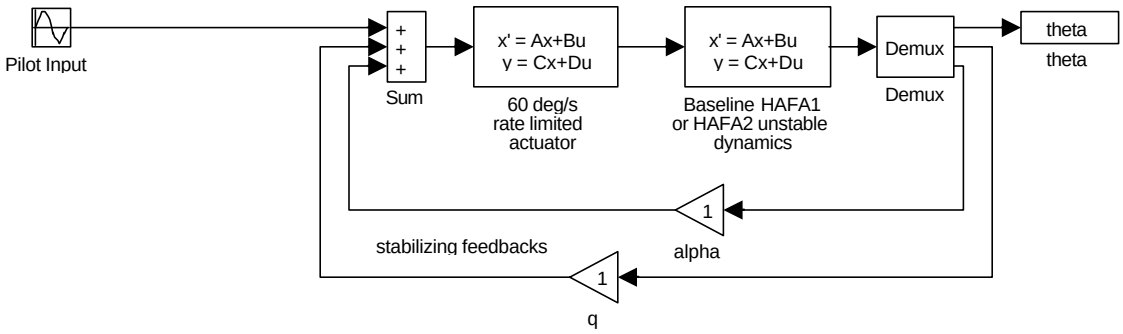

Figure 4-1. Baseline Configuration

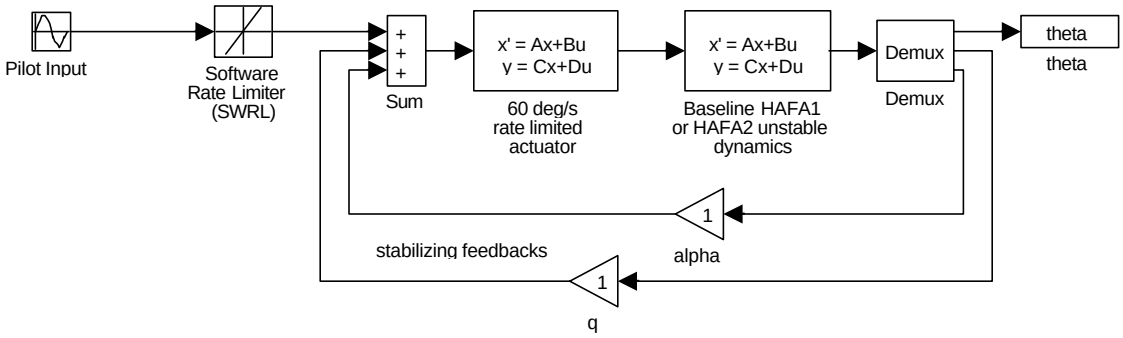

Figure 4-2. Baseline + SWRL Configuration

SWRL to the pilot command path in conjunction with the Baseline configuration. The SWRL settings tested were 20, 30, 35, 40, and 50 deg/sec. Table 4-1 contains the various LOES short period approximation parameters for HAFA1 and HAFA2. Using the Control Anticipation Parameter (CAP), HAFA1 was predicted to have Level 1 flying qualities while HAFA 2 was predicted to be Level 3. In addition, HAFA2 was predicted to be potentially PIO prone due to its poor linear qualities.

Table 4-1. VISTA Longitudinal Aircraft Dynamics

LOES Short Period Model Form: $\frac{q}{d_e}(s) = K_q \frac{(T_{q2}s+1)e^{-ts}}{(s^2+2z_{sp}w_{sp}s+w_{sp}^2)}$		
Configuration	**HAFA1**	**HAFA2**
$\omega_{sp\ (rad/sec)}$	4.64	1.8
ζ_{sp}	.7	.654
$T_{\theta 2}$	.65	.65
K_q	18.998	21.816
τ	.156	.156

The evaluation pilots evaluated the handling qualities for each configuration in three different phases. Phase 1 consisted of non-specific maneuvers to get a feel for how the aircraft performed. Phase 2 involved tracking a HUD generated command bar using the Handling Qualities During Tracking (HQDT) technique [3]. The HUD generated task was similar to the discrete task used in HAVE LIMITS (see Figure 3-1) but with twice the amplitude to ensure rate limiting was achieved. PIO ratings were assigned after each task. Phase 3 consisted of a HUD tracking task as well but the pilots used less aggressive operational tracking techniques. Only the PIO ratings from Phase 2 were used in the OLOP analysis because of the aggressive nature of the task and the higher probability of encountering rate limiting.

Aircraft and Pilot Models

The Simulink® models shown in Figure 4-1 and Figure 4-2 were provided by Calspan for the OLOP analysis. Included (not shown in the diagram) were the forward stick gains for the two configurations converting stick displacement (inches) to commanded elevator input (degrees). For HAFA1 the gain was 20.0 deg/in and for

HAFA2 the value was much lower at 5.7 deg/in. The side stick controller was used and had a pitch deflection range of ±.75 in.

This analysis compared the Modified Neal-Smith and the high gain (Φc = -130 deg) pilot models. Only the high gain model was chosen instead of the full range of gains suggested by DLR. The HAVE LIMITS analysis showed that the high gain and the Neal-Smith correlated best with pilot ratings. The parameters for the two pilot models are listed in Table 4-2 (see equation 20 for Neal-Smith pilot model equation).

Table 4-2. Pilot Model Parameters for HAVE FILTER

Pilot Model Parameters	Configuration	
	HAFA1	HAFA2
K_p	-.0105	-.0063
T_{p1}	.195	1.5
T_{p2}	.01	.01
K_g	-.113	-.071

Determination of Onset Frequencies

The next step in the OLOP process was determining the onset frequencies for the various rate limits and configurations utilizing equation 21 from the previous chapter. Again, the issue of input amplitude was in question. Upon examination of the flight test data provided by the Air Vehicles Directorate, Air Force Research Lab (AFRL), maximum stick deflection was regularly achieved during the more aggressive portions of the HQDT task. Pilots frequently commented that they achieved stop-to-stop or bang-bang at the termination of the maneuver. Thus, for this OLOP analysis, maximum stick deflection (P_o = .75") was used. The onset frequencies were calculated and are shown in

Table 4-3. Notice that the higher forward gain for HAFA1 correlated to lower onset frequencies than HAFA2 for a given configuration and rate limit. Also, it should be noted that for the SWRL + Baseline configuration, only the SWRL was considered in the analysis even though the 60 deg/sec rate limited actuator was still included in the feedback loop. This highlighted one of the limitations of OLOP, that it can only handle one rate limiter at a time for a given flight control system. This can give confusing results that will be presented later in the chapter.

Table 4-3. HAVE FILTER Onset Frequencies

Rate (deg/s)	Onset Frequencies (rad/sec)			
	Configuration Baseline		Configuration Baseline + SWRL	
	HAFA1	HAFA2	HAFA1	HAFA2
20	N/A	N/A	.835	2.93
30	N/A	N/A	1.25	4.39
35	N/A	N/A	1.45	5.14
40	N/A	N/A	1.67	5.84
50	N/A	N/A	2.08	7.29
60	2.87	7.29	N/A	N/A

Calculation of OLOP

The final step in the analysis was calculating the appropriate open-loop transfer function, plotting it on a Nichols chart, and examining the OLOP position versus the stability boundary. As with HAVE LIMITS, the system loop was broken at the position of the rate limiter and the LINMOD function was used to obtain the open-loop transfer function. Following is a summary of the analysis of the two configurations.

Baseline Configuration.

The open-loop frequency response charts and the corresponding OLOPs for the Baseline configuration are shown in Figure 4-3 and Figure 4-4. The OLOPs for both pilot models are presented and the mean PIO rating from the Phase 2 task is shown.

The HAFA1 aircraft showed good correlation for both pilot models between the mean PIO rating (5.2) and the OLOP position, which was well above the boundary. In the flight test, rate limiting was encountered regularly and all three pilots experienced divergent PIO.

The HAFA2 mean PIO rating did not correlate well with the OLOP prediction. The OLOP was well below the boundary but the mean PIOR of 3.6 showed that PIO was encountered. However, upon further examination of the flight test data, the pilots rarely activated the rate limiter in the feedback loop for this configuration. This was likely due to the low gain setting on the command path from the pilot. Thus, the PIO ratings were due to the poor linear handling qualities and not rate limiting. Therefore, OLOP was meaningless for this particular configuration when trying to correlate with pilot ratings.

Sample time histories from one of the more aggressive pilots for both configurations are shown in Figure 4-5 and Figure 4-6. Stick position in inches, pitch angle (θ) and tracking command (θ_{cmd}) in degrees, and rate limiter input (RLE_{in}) and output (RLE_{out}) in degrees are displayed on the three plots. The time history covers a similar portion of the tracking command where a large input was demanded from the pilot.

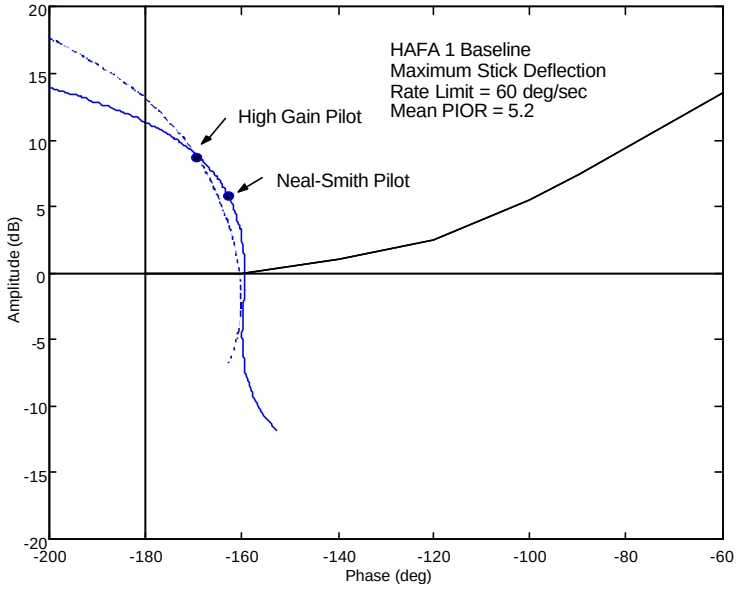

Figure 4-3. Baseline Open-Loop Frequency Response, HAFA1, P_o = .75”

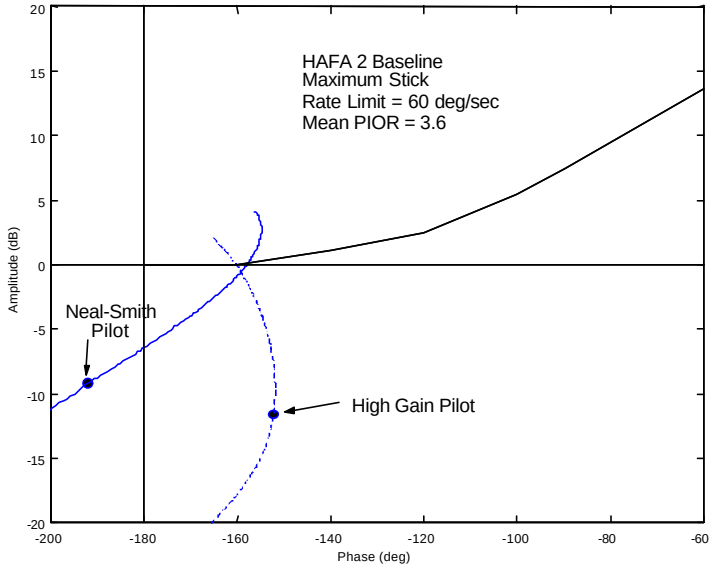

Figure 4-4. Baseline Open-Loop Frequency Response, HAFA2, P_o =. 75”

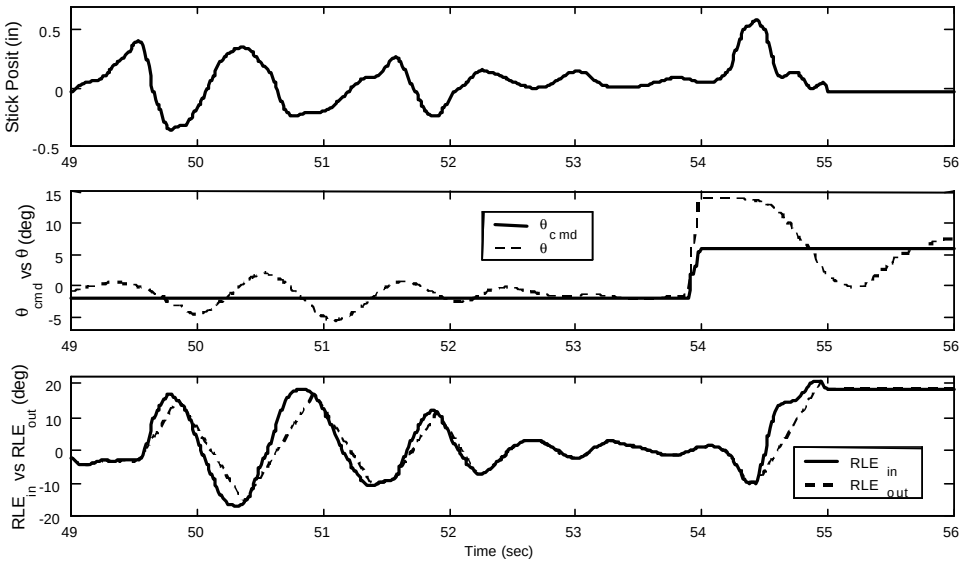

Figure 4-5. HAFA1 Baseline Configuration Sample Time History

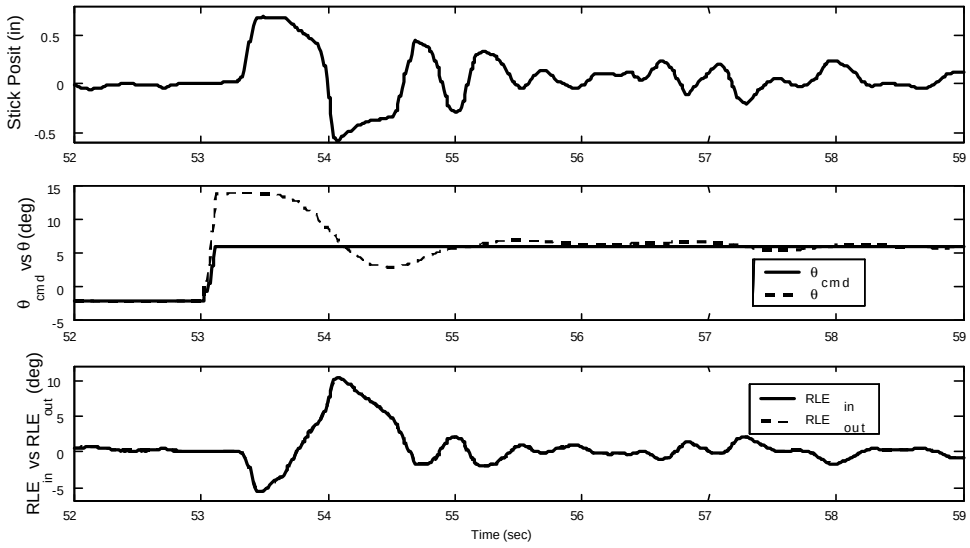

Figure 4-6. HAFA2 Baseline Configuration Sample Time History

The time histories clearly show the propensity for HAFA1 to encounter rate limiting, with less than maximum stick inputs, by examining the classic sawtooth pattern in the rate limiter output. On the other hand, the same pilot, with nearly full stick deflections, did not rate limit the HAFA2 configuration at a similar point in the task.

Baseline + SWRL Configuration

The open-loop frequency response charts and the corresponding OLOPs for the various SWRL settings are shown in Figure 4-7 and Figure 4-8. The mean PIO rating from the Phase 2 evaluation is displayed next to the SWRL setting value. Again, both pilot models are shown for comparison.

The OLOPs for HAFA1 are all clearly below the boundary except for the lowest SWRL setting of 20 deg/sec. However, the PIO ratings increase as the rate limit increases. This may be counterintuitive at first and appears not to correlate well with OLOP. The explanation for these results lies in the fact that the flight control configuration contained two rate limiters, one in the forward and one in the feedback path. Even though the SWRL settings were set at a rate lower than that of the feedback limiter (60 deg/sec), the SWRL output signal, summed with the feedbacks, was still enough to rate limit the feedback limiter too. This occurred for SWRL settings as low as 30 deg/sec and the pilots experienced bounded and divergent PIO several times as with the Baseline configuration. Only the lowest SWRL setting of 20 deg/sec was sufficient enough to prevent the feedback limiter from activating.

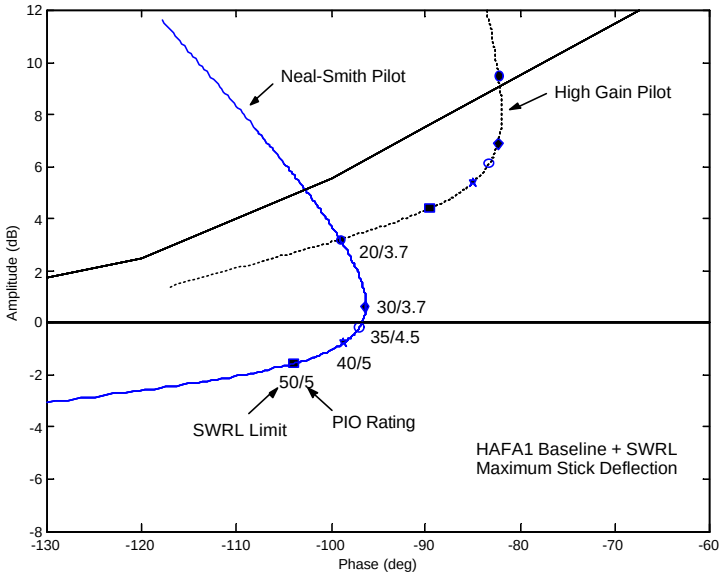

Figure 4-7. Baseline + SWRL Open-Loop Frequency Response, HAFA1, P_o = .75”

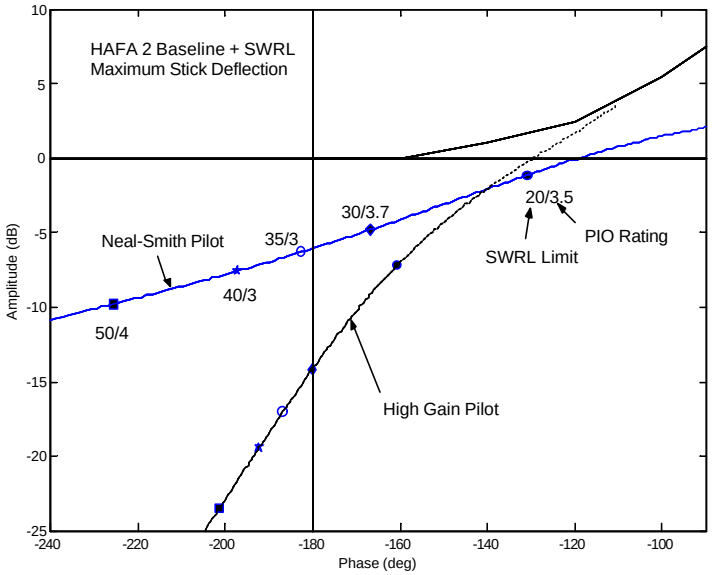

Figure 4-8. Baseline + SWRL Open-Loop Frequency Response, HAFA2, P_o = .75”

Thus, for the SWRL settings ≥ 30 deg/sec, with the feedback limiter invoked, previous OLOP analysis shown in Figure 4-3 would also apply which showed the aircraft to be PIO prone. This correlates with the higher PIO ratings for those SWRL settings. Then the only valid OLOP that can be used for correlation with pilot ratings in Figure 4-7 is for the lowest SWRL setting because it is the only rate limiter contributing to PIO susceptibility. The PIO rating of 3.7 suggests that it should be on or above the boundary. It appears that for this case, the high gain model gives slightly better correlation between the OLOP and the PIO rating than the Neal-Smith model. Figure 4-9 shows a sample time history that illustrates the simultaneous activation of the feedback and forward path limiters with a SWRL setting of 35 deg/sec.

Although the OLOPs for HAFA2 in Figure 4-8 were below the boundary the aircraft still seemed to be PIO prone. This is actually good correlation for OLOP. Recall that the aircraft received a nominal mean PIO rating of 3.6, without rate limiting present, due to the poor linear dynamics. The mean PIO ratings with the SWRL in place are nearly the same as the nominal value for all of the SWRL settings. This suggets that even with rate limiting present due to the SWRL, the effects on the overall dynamics were not enough to further degrade the aircraft's PIO susceptibility. Thus, for an aircraft with poor linear dynamics, the introduction of rate limiting does not necessarily make the aircraft more PIO prone.

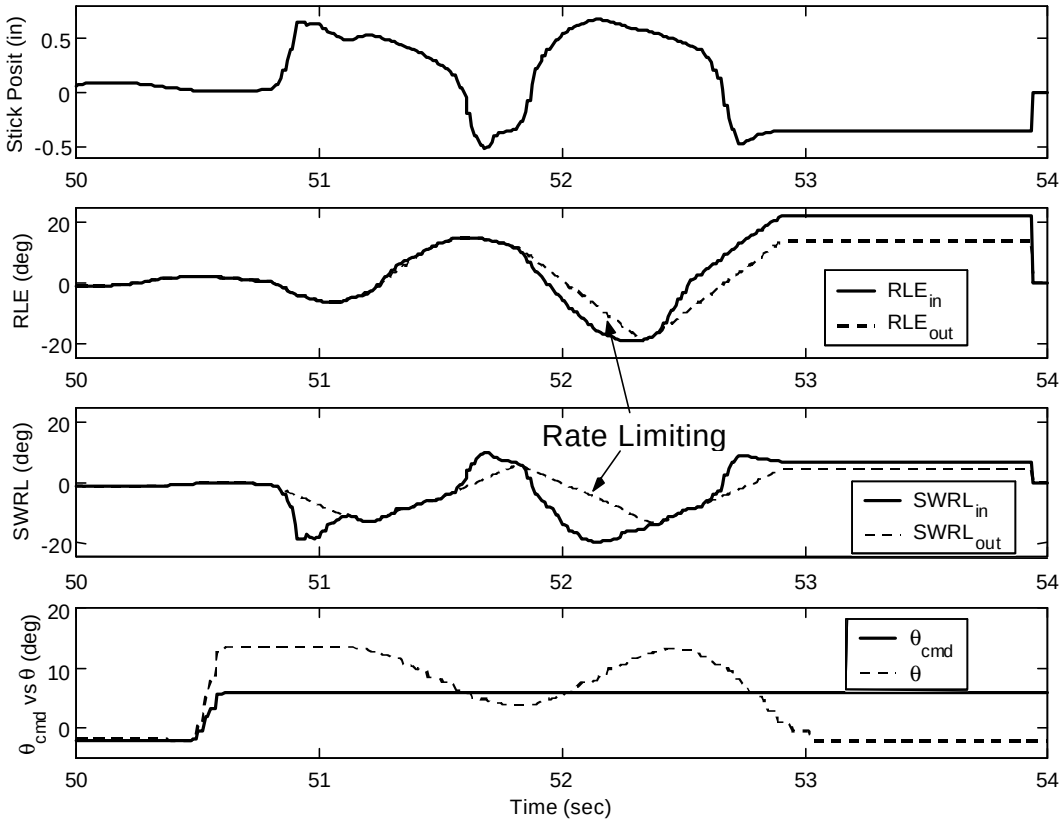

Figure 4-9. HAFA1 Baseline + SWRL Configuration Sample Time History

Stick Ratio Analysis

DLR suggests using the maximum stick amplitude in the OLOP application, which was shown to be unreasonable for the HAVE LIMITS TMP analysis. The introduction of s*tick ratio* (SR) was introduced to examine the PIO susceptibility of an aircraft versus its full range of stick amplitudes. Even though maximum stick amplitude proved to be a reasonable assumption for the HAVE FILTER TMP, examining the stick

ratio for the various configurations gives further insight into the PIO susceptibility of each configuration. The stick ratio analysis for the HAVE FILTER configurations using both pilot models is presented in Figure 4-10.

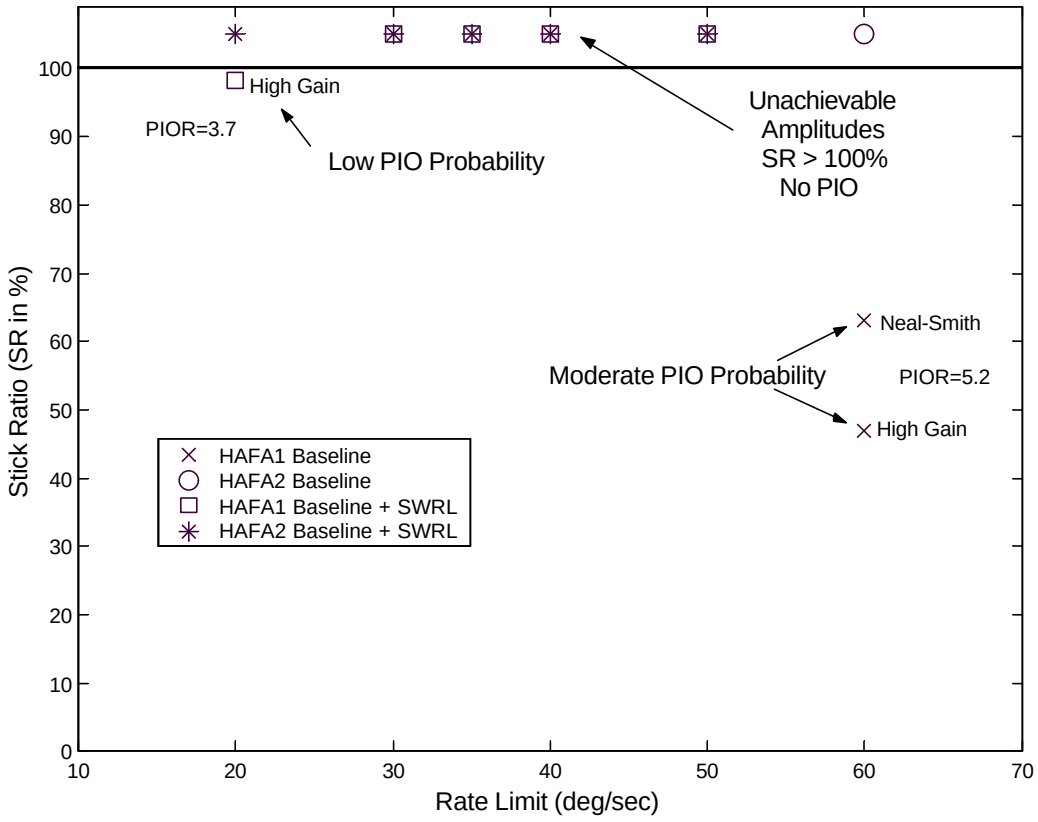

Figure 4-10. HAVE FILTER Stick Ratio Plot

Since many of the OLOPs in the analysis were below the stability boundary with maximum stick deflection applied, a stick ratio greater than 100% would be required to drive those points above the boundary. Since a SR>100% is not possible, these particular points show that, with maximum stick inputs applied and with rate limiting present, these

configurations should not be more PIO susceptible due to rate limiting. This proves to be the case for the HAFA2 Baseline and all but one of the Baseline + SWRL configurations.

The HAFA1 Baseline +SWRL configuration, with the lowest rate of 20 (deg/sec), barely plots below the 100% line utilizing the high gain pilot model. Only the high gain model showed the OLOP to be above the stability boundary (see Figure 4-7) for this configuration. This configuration could be analyzed to have low PIO probability because it would take nearly full stick amplitude and the presence of rate limiting to bring it into the dangerous region above the stability boundary. However, as was the case with this test, maximum amplitude was achieved and PIO encountered. Once again, engineering judgement will have to be made when relating stick amplitudes to actual mission tasks.

For the HAFA1 Baseline configuration, utilizing either pilot model, one could conclude that this configuration had a moderate probability for PIO. This is because it only took approximately a SR≈50-60% to make this configuration PIO prone. Again, are these stick amplitudes anticipated? For this TMP, with a very aggressive pilot technique (HQDT), these amplitudes were regularly achieved which garnered high PIO ratings for this configuration.

Once again, analyzing a particular configuration for PIO susceptibility using stick ratio highlights the difficulty of predicting what kind of stick amplitudes are anticipated. In contrast to HAVE LIMITS, the given task for HAVE FILTER demanded full deflection from the pilots, but was it representative of a typical mission? Is it reasonable to assume that a SR=50% will be reached during a typical mission? Since stick amplitude will be a function of the task, pilot aggressiveness, and the given

configuration; engineering judgment will have to be used when labeling an aircraft as PIO prone based on its stick ratio value.

HAVE FILTER Conclusions

The OLOP criterion was used to analyze several configurations from the HAVE FILTER TMP. OLOP accurately predicted the PIO susceptibly of the HAFA1 Baseline configuration with the limiter in the feedback loop. Unfortunately, this was the only rate limit value examined with the feedback limiter. Although the correlation for HAFA1 looked promising for both pilot models there was insufficient data to provide any trend information.

The HAFA2 Baseline configuration never achieved rate limiting, so the OLOP analysis was not applicable except to highlight the configuration's PIO susceptibility due to its linear characteristics.

Analysis of the HAFA1 Baseline + SWRL configuration highlighted the effects of having multiple rate limiters in a flight control system. Even though the SWRL was set at a much lower rate than the feedback limiter, the presence of feedback signals was still enough to activate both limiters simultaneously. This eliminated all but one of the points for correlation with OLOP. With this very limited data, it appeared that the high gain pilot model correlated better than the Modified Neal-Smith. Since OLOP only allows for the analysis of one limiter at a time, both limiters need to be evaluated separately in the event that both are activated.

OLOP analysis of the HAFA2 Baseline + SWRL configuration showed that the mere presence of rate limiting did not necessarily degrade the PIO susceptibility of an aircraft that already had poor linear characteristics. Since the OLOPs were below the boundary, without an increase in PIO ratings from the baseline case, this was considered good correlation.

Lastly, the stick ratio metric was applied to analyze the PIO susceptibility of each configuration versus stick amplitude. Again, this highlighted the need for sound engineering judgement when analyzing stick amplitudes versus mission related tasks.

V. Analysis of Large Aircraft Rate Limit (LARL) Program

This chapter presents the methodology and results from applying the OLOP criterion to the LARL Flight Test Program database. This analysis was limited to forward path limiters only on a large transport aircraft and was the final analysis conducted prior to conducting the flight test. A stick ratio analysis was performed as well.

LARL Overview

The LARL Program was conducted on 17-23 June 1998 at the Calspan flight research facility in Buffalo, NY [26]. The purpose of the program was to study the effects of rate limiting on a large transport category airplane. The experiment utilized the USAF Total In-Flight Simulator (TIFS) aircraft with rate limiting in the pitch command path. Three veteran test pilots with varying backgrounds conducted the evaluations. A total of eight sorties were flown.

The test configuration was very similar to that of the HAVE FILTER Baseline + SWRL configuration (see Figure 4-2). The differences were that the bare airframe dynamics were a generic large four-engine transport category, the actuator was rate limited at 50 deg/sec, and the SWRL settings tested were none, 5, 10 and 17.5 deg/sec. Again, q and α feedbacks were used to generate two overall sets of dynamics. The short period characteristics are shown in Table 5-1. LARL1 was predicted to have Level 1 flying qualities while LARL2 was borderline Level 1/2.

Table 5-1. LARL Short Period Characteristics

Config	ω_{sp} (rad/sec)	ζ_{sp}
LARL1	2.73	.70
LARL2	1.90	.73

The evaluation pilots rated the handling qualities of these two configurations after following HUD generated tracking commands. The HUD tracking tasks were the same as those from HAVE LIMITS and are depicted in Figure 3-1. Cooper-Harper and PIO ratings were assigned for each test run.

Upon examination of flight test data provided by Air Vehicles Directorate, AFRL, the actuator in the feedback loop was never rate limited with the given configurations and task, even when the SWRL setting was unlimited. Therefore, the OLOP analysis was only applicable to the SWRL in the forward path.

Aircraft and Pilot Models

The Simulink® model for the LARL program was provided by the Air Vehicles Directorate, AFRL. The test program used a side stick controller and a wheel column for pitch and roll commands. The forward gains were normalized so that the maximum available pitch input amplitude command of P_o=20 deg was the same for both controllers.

As with HAVE FILTER, this analysis compared the OLOP results using both the Modified Neal-Smith and the high gain pilot models. The parameters for the two pilot models are shown in Table 5-2 (see Eq. 20 for the Neal-Smith Pilot Model equation).

Table 5-2. Pilot Model Parameters for LARL

Pilot Model Parameters	Configuration	
	LARL1	LARL2
K_p	-.6	-1.6
T_{p1}	1	.33
T_{p2}	.001	.02
K_g	-17.4	-6.8

Determination of Onset Frequencies

The next step in the OLOP analysis was the determination of the onset frequencies. Examination of the flight test data showed large variations in input amplitude used by the pilots with respect to the various SWRL settings. Initially, the analysis used the suggested maximum input, P_o=20 deg, and then the range of input amplitudes was examined with the stick ratio metric. The onset frequencies are listed in Table 5-3. Note that with the normalized forward gains, the onset frequencies are the same for each configuration.

Table 5-3. LARL Onset Frequencies

Rate (deg/s)	Onset Frequency (rad/sec)
5	.250
10	.499
17.5	.875

Calculation of OLOP

The final step in the OLOP analysis was breaking the loop at the SWRL position and plotting the respective OLOPs on the Nichols chart. Following is an analysis of the two configurations.

LARL1 Configuration.

The open-loop frequency response and the corresponding OLOPs for configuration LARL1 are shown in Figure 5-1. The OLOPs for both pilot models are shown with the rate limit and the mean PIO ratings for the two tasks.

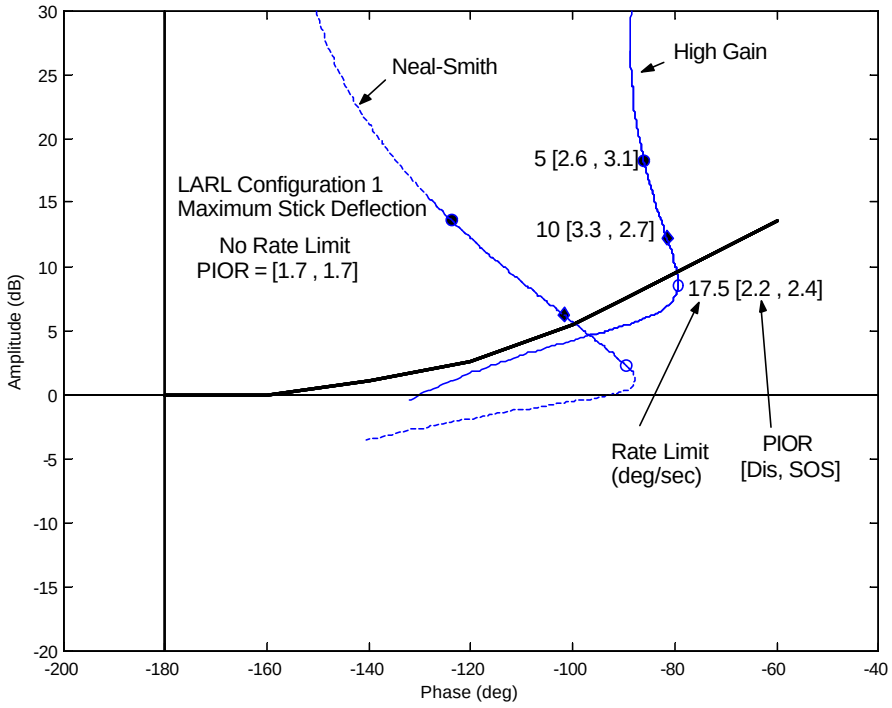

Figure 5-1. LARL1 Open-Loop Frequency Response, P_o=20 deg

A mean PIO rating of 1.7 for both tasks with no rate limit set on the SWRL showed a non-PIO prone aircraft. The OLOP analysis predicted that if rate limiting were achieved with maximum stick amplitudes the aircraft would be more PIO prone as the SWRL settings decreased. The mean PIO ratings for the lower SWRL settings seem to correlate well with OLOP because at least one of the mean ratings was >3.0, indicating PIO. The OLOP corresponding to the highest rate limit, 17.5 deg/sec, does not cross the boundary for either pilot model. This would suggest that there would be little or no degradation to the nominal PIO characteristics. The PIO ratings show slight degradation, but no PIO. There does not appear to be an advantage to using one pilot model over another for this configuration. Correlation was acceptable for both models.

As was seen with previous analysis, the OLOPs will remain close to the boundary for lower amplitudes because the Nichols plot, especially for the high gain pilot, nearly parallels the boundary. Thus, maximum amplitudes may not be necessary to still encounter the effects of being close to the boundary.

LARL2 Configuration.

The open-loop frequency response and the corresponding OLOPs for configuration LARL2 are shown in Figure 5-2. The OLOPs for both pilot models are shown with the rate limit and the mean PIO ratings for the two tasks.

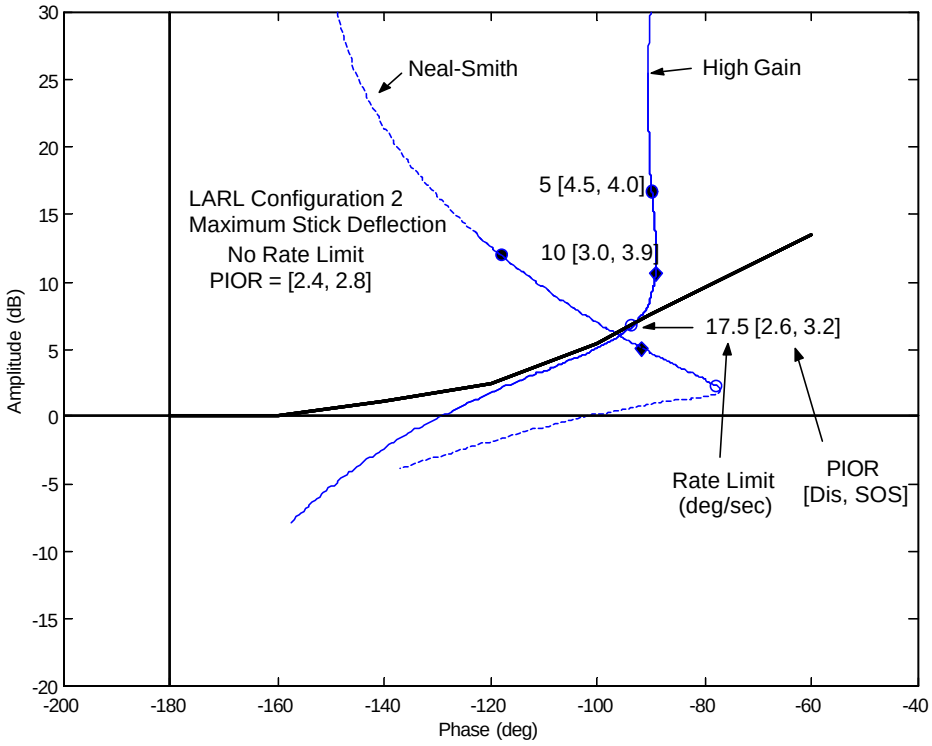

Figure 5-2. LARL2 Open-Loop Frequency Response, P_o=20 deg

During the flight test, this configuration received Level 1 and 2 ratings and slightly higher mean PIO ratings (2.4, 2.8) than LARL1 with no rate limit on the SWRL. The OLOP analysis for this configuration was very similar to that for LARL1. The flight test data correlated well with the OLOP positions, especially for the high gain pilot model. The lowest rate limit increased the PIO ratings by a factor of about 1.5 whereas the highest rate limit showed only a slight increase in PIO ratings.

Stick Ratio Analysis

The stick ratio analysis for the LARL configurations is presented in Figure 5-3. The high gain pilot model was used for generating the plot. The analysis shows that the LARL2 configuration was just slightly more susceptible to PIO due to rate limiting than LARL1.

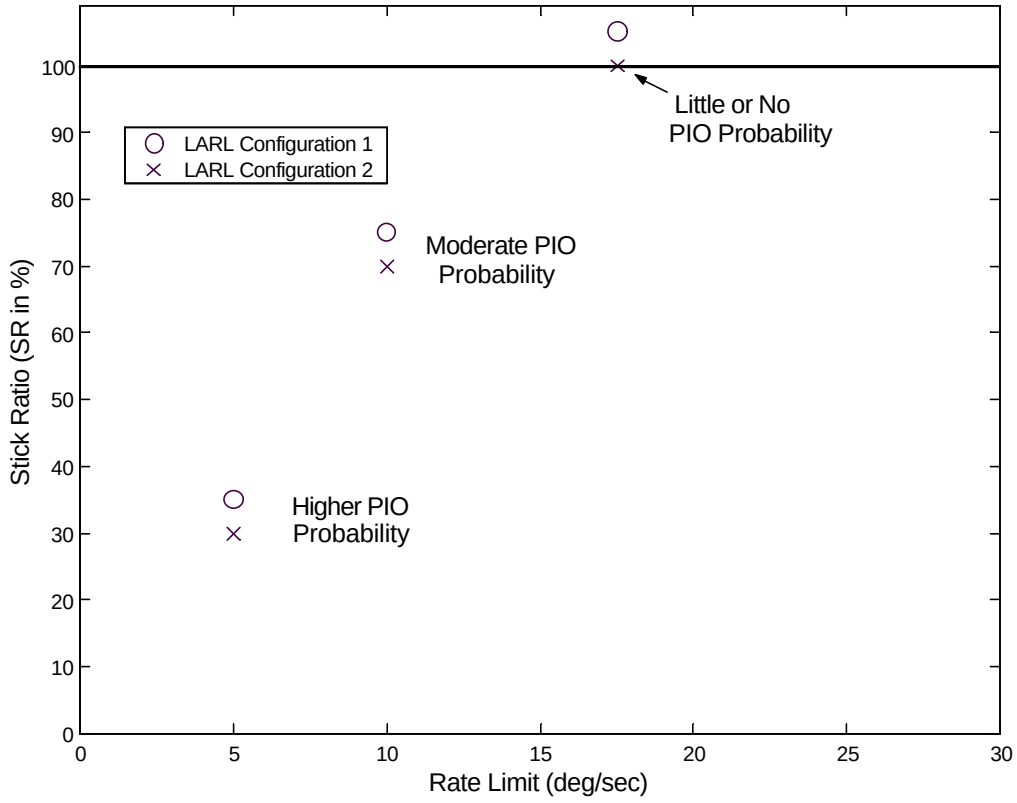

Figure 5-3. LARL Stick Ratio Plot

As one would expect, the lower rate limits are more susceptible to PIO. In fact, for the lower settings, the pilots used much higher amplitudes than those used for the same task but with a higher rate limit. This exacerbated the rate limiting effects as is

illustrated in Figure 5-4. Included are sample time histories of aircraft pitch angle (θ) versus tracking command (θ_{cmd}), and pilot input ($SWRL_{in}$) versus SWRL output ($SWRL_{out}$). The two time histories are test runs by the same pilot and the same task on configuration LARL2 but with different SWRL settings. With a setting of 5 deg/sec, the SWRL was rate limited nearly the entire time. This was a classic example of amplitude attenuation caused by rate limiting and the pilot trying to compensate for it with larger inputs. For this case, the pilot inputs nearly reached the maximum value of 20 degrees. In contrast, for a limit of 17.5 deg/sec, rate limiting occurred only for short time periods and the pilot input amplitudes were much less than those for the lower SWRL setting.

Recall that in the development of the stick ratio metric, the stick ratio value was based on the point at which the OLOP crossed the boundary into the PIO region. The stick ratio for the 17.5 deg/sec rate limit is at or greater than 100% suggesting that it would be highly unlikely to encounter PIO. But, as discussed earlier, although the OLOP lies below the boundary it was still within close proximity. Thus, it becomes important not to look at the stick ratio value alone but also to examine the Nichols chart in conjunction with it. The boundary should not be considered as a cliff between PIO and no PIO but rather as a region around which PIO susceptibility increases. This concept is explored further in the flight test chapter.

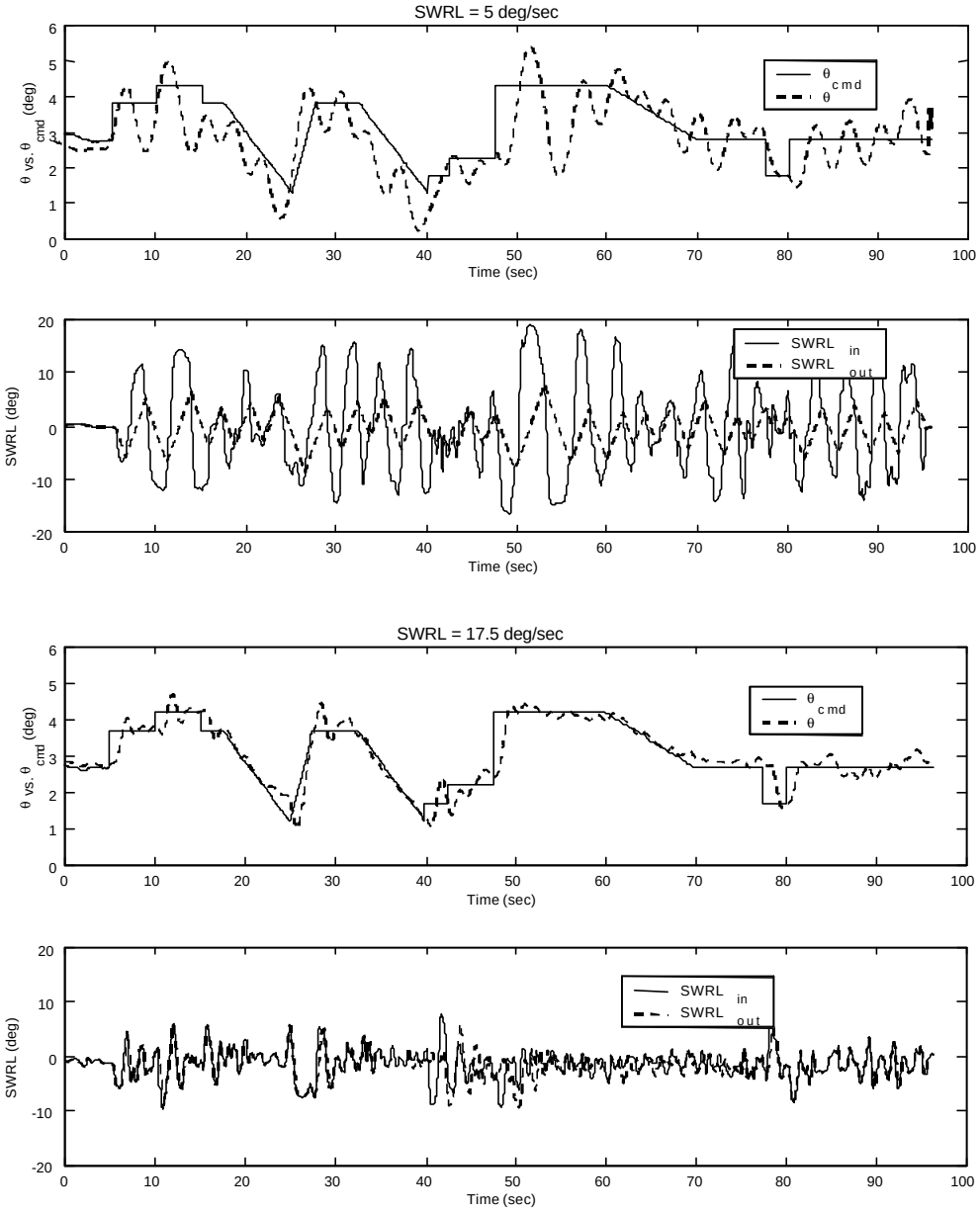

Figure 5-4. LARL2 Sample Time Histories

LARL Conclusions

The OLOP criterion was successfully used to analyze the LARL flight test program. The criterion correctly predicted the degradation in PIO characteristics due to very low SWRL settings for both configurations. The analysis reinforced the use of the stick ratio plot in conjunction with the Nichols chart to fully explore PIO probability with respect to stick amplitude. This was especially important when a significant portion of the frequency response curve paralleled the stability boundary. A high stick ratio value did not necessarily equate to an absence of PIO.

Examining the sample time histories illustrated the wide range of input amplitudes that were used during the test for identical tasks but with different rate limits. This further stressed the importance of analyzing the full range of stick inputs using stick ratio and not just the maximum value.

The high gain pilot model appeared to give only slightly better correlation for limiters in the forward path than did the Neal-Smith model. As noted in HAVE LIMITS, changes in pilot gain would have dramatic effects on the results.

Additionally, only maximum pilot amplitude was used for the analysis whereas time history study showed that pilots used a wide variety of amplitudes depending on the rate limit value. Again, this shows the need for sound engineering judgement when evaluating stick amplitudes versus mission tasks and their use with OLOP.

VI. Flight Test

Approach

The objective of this study was to validate the OLOP criterion and help pave the way for its use as a design tool for the prediction of PIO due to non-linear rate limiting. The analysis of the HAVE LIMITS, HAVE FILTER, and LARL flight test programs highlighted some limitations in the application of OLOP. Specifically, the choice of pilot model and stick amplitude had dramatic effects on the results, sometimes yielding an over-prediction of PIO. Based on the analysis of these three test programs, the proposed method for the application of OLOP would be to apply it using both the high gain and Neal-Smith pilot models. Stick amplitude would remain as a variable and could be evaluated against PIO likelihood using the stick ratio concept.

To further reinforce these concepts, a flight test was conducted. Due to a limited number of sorties, the scope of the flight test was limited only to those configurations with rate limiting elements in the feedback loop. These configurations appeared to have the most dramatic PIO occurrences because at the onset of rate limiting the aircraft dynamics suddenly took on their original bare airframe characteristics. Conversely, for the forward path limiters, rate limiting simply introduced additional phase lag and attenuation but the underlying dynamics remained unchanged. These cases appeared to be more predictable and less dramatic to the pilot. Additionally, pilot gain had a dramatic effect on the OLOP analysis for forward path limiters, whereas it was shown to be less of

a factor for limiters in the feedback path. This left stick amplitude as the major contributing factor for the feedback limiter case.

The first two flight tests analyzed in this report that examined feedback limiting, HAVE LIMITS and HAVE FILTER, only examined unstable plant dynamics which were then augmented to a stable configuration with feedbacks. OLOP successfully predicted the PIO tendencies of these configurations. This test program evaluated four different plant dynamics, three which were stable and one unstable, which required augmentation. The OLOP criterion was applied to see if it could filter out which of these configurations might be PIO prone due to rate limiting. For the flight test, OLOP was not used as a prediction tool per se. The idea was to give the criterion as much accurate information as possible; to include stick amplitude values at the onset of rate limiting that were obtained from flight test data. Then the dependence on the pilot model could be assessed against how well the criterion correlated with the pilot ratings. Additionally, if correlation was good, then this would provide support for the concepts derived from the previous analyses.

Flight Test Overview

Four flight control configurations with a variable rate limited stabilator and stabilizing feedback gains were evaluated using a Heads-Up Display (HUD) generated tracking task on the NF-16D Variable Stability In-Flight Simulator Test Aircraft (VISTA). Ground tests and calibration sorties were accomplished at Veridian Flight

Research Facility in Buffalo NY, between 20 and 28 September 2000. Twelve test sorties, totaling 15.4 hours, were flown from 3-16 October 2000 at Edwards AFB CA.

All testing was conducted at 15,000 ft Pressure Altitude and 300 KCAS. Each configuration was tested with a rate limited stabilator; limit values varied between 10-60 deg/sec. The closed-loop dynamics of each configuration were identical. Thus, the pilot was blind as to what configuration was being flown until rate limiting occurred. The safety pilot implemented configuration changes in-flight between test points and knew which configuration was being flown. The test team pilots and their experience are listed in Table 6-1.

Table 6-1. Team Test Pilots

Pilot	Designation	Operational Aircraft Experience	Total Flight Hours
Gregory P. Gilbreath, Capt, USAF	Pilot 1	A-10	1,500+
Luciano Ippoliti, Capt, Italian AF	Pilot 2	AMX	1,000+
Daniel S. Ormsby, Capt, USAF	Pilot 3	C-5	2,400+

Flight Test Configurations

The desired configurations for the flight test consisted of the following elements: four different longitudinal plant dynamics to be simulated by VISTA, a rate limited stabilator actuator, and stabilizing feedback gains generating identical closed-loop dynamics. The configuration block diagram is shown in Figure 6-1. The feedback gains used to create the closed-loop dynamics for each configuration are listed in Table 6-2. The center stick was used for all test sorties with a linear stick gradient of 8 lbs/in and deflection limits of ±4 in. A forward gain (K_s) of 4.6 deg/in was used prior to the

feedback summing junction. A software rate limiter on VISTA simulated the rate limited actuator. This was done to reduce the amount of phase lag in the overall system. Although it was not quite representative of an actual rate limited actuator, it still produced the same effects (phase lag, amplitude attenuation) and should not effect OLOP analysis. The actuator model was provided by Veridian and used in OLOP analysis in conjunction with LOES models (Equation 22).

Actuator Dynamics:
$$\frac{d_e}{d_{ec}} = \frac{14944751.528}{s^2 + (2)(.74)(71.4)s + 71.4^2}\left(\frac{\text{deg}}{\text{deg}}\right) \qquad (22)$$

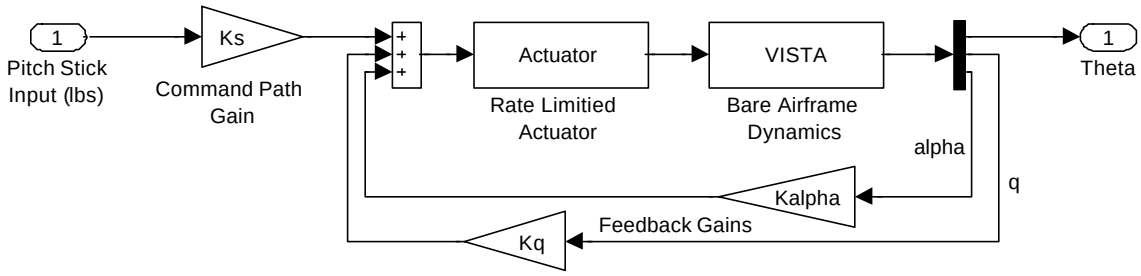

Figure 6-1. Flight Test Configuration Block Diagram

Table 6-2. Feedback Gains

Configuration	K_{alpha} (deg/deg)	K_q (deg/deg/s)
A	.0776	.449
B	.901	.601
C	.698	.391
D	1.05	.623

Table 6-3. Desired Longitudinal Dynamics.

Configuration	Short Period Frequency (rad/sec)	Short Period Damping	T_{q2} (sec)
A (Low Damping)	3.4	.21	.84
B (Marginally Stable)	.78	.78	.84
C (Sluggish)	2.4	.64	.84
D (Unstable)	Time to Double = 1.0 sec		.84
Closed-Loop	5.0	.8	.80

The desired longitudinal short period frequencies, damping ratios, and numerator time constants ($T_{\theta 2}$) for each of the bare airframe dynamics and for the overall closed-loop dynamics are listed in Table 6-3. These configurations were chosen because the majority of OLOP research done by DLR had been in the lateral-directional axis. This test focused on the longitudinal axis. Additionally, the only data analyzed to this point using OLOP, for limiters in the feedback loop, were those with unstable plant dynamics. Limited data exists where rate limiting occurred inside feedback loops with a *stable* bare airframe.

The overall closed-loop dynamics for each configuration were identical and representative of a typical modern fighter with solid Level 1 characteristics. Thus the pilot was, in effect, blind to which set of plant dynamics was present until rate limiting was encountered.

Test Aircraft Description

The NF-16D Variable Stability In-Flight Simulator Test Aircraft (VISTA, USAF S/N 86-0048) was a modified F-16D Block 30, Peace Marble II (Israeli version) aircraft

with a Digital Flight Control System (DFLCS) using Block 40 avionics and powered by an F100-PW-229 engine. To allow a command/safety pilot to fly from the aft cockpit, all necessary controls were moved from front to aft cockpit. The aft cockpit had conventional F-16 controls except the throttle was driven by a servo, which followed electrical commands of the front cockpit when the VISTA Simulation System (VSS) was engaged. Primary VSS controls, displays, and system engagement were located in the aft cockpit. The front cockpit included the VSS control panel needed to engage the variable feel center stick or sidestick, but the VSS system could only be engaged from the aft cockpit. Front cockpit Multi-Function Displays (MFDs) reflected the aft cockpit MFDs and could be used for simulation configuration controls if necessary. Other modifications to the aircraft included a higher flow rate hydraulic system with increased capacity pumps and higher rate actuators as well as modifications to electrical and avionics systems required to support VSS operations. The aircraft was configured with a centerline fuel tank and no other stores for this test.

Flight Test Objectives

The overall test objective was to conduct a limited evaluation of the ability of the OLOP criterion to predict PIO tendencies caused by actuator rate limiting. This evaluation would help determine whether the OLOP criterion could be used as a reliable design tool. The specific objectives were as follows:

1) Verify that the four desired flight test configurations and the desired rate limits were properly implemented on VISTA.

2) Evaluate the ability of OLOP criterion to accurately predict PIO in presence of rate limiting.

All test objectives for the flight test were met.

Flight Test Procedures

Configuration Verification.

Veridian pilots flew two calibration sorties to collect data to verify that the four desired aircraft configurations were implemented on VISTA correctly. Additionally, proper operation and scoring of the HUD tracking task was evaluated.

Veridian pilots performed programmed step inputs and manual frequency sweeps. Data obtained from these inputs were used to construct time history and frequency response plots for both bare airframe open-loop and closed-loop dynamics. Veridian and the test team used this data to construct Lower Order Equivalent System (LOES) matches in both the time and frequency domain. LOES dynamics were compared to dynamics requested by the test team for each of the configurations to see if desired characteristics were achieved. Additionally, LOES dynamics were implemented in the aircraft model used for OLOP analysis. Samples of rate limiting for each of the rate limit values were also obtained from several test sorties for verification.

OLOP Evaluation.

A programmable HUD tracking task was used in determining PIO susceptibility for each configuration. The task contained both pitch and roll commands as shown in

Figure 6-2. Test pilots conducted Phase 1, 2, and 3 handling qualities evaluations for each point in the test matrix, as described below.

Phase 1: Pilots performed pitch captures and pitch step inputs, progressing from small to large amplitude. Pilots performed gentle maneuvering to get a feel for the aircraft handling qualities and how it might perform during Phase 2 and 3.

Phase 2: Pilots performed a pitch only HUD tracking task using the Handling Qualities During Tracking (HQDT) technique [3]. During the task, pilot comments were recorded and a PIO rating assigned using the scale in Appendix A. Pilots started with small, low frequency inputs and smooth tracking. Frequency was gradually increased followed by an increase in amplitude during more aggressive tracking to examine non-linear rate limiting effects. This technique modeled a gain only, reactionary pilot.

Phase 3: Pilots performed a combined pitch and roll task using normal piloting technique while striving to achieve the following performance criteria:

Desired: Track target inside a 10 mil diameter circle 50% of the time.
Adequate: Track target inside a 20 mil diameter circle 50% of the time.

Timing for task scoring began at the start of the tracking task. After the task, the pilot assigned a PIO rating and Cooper-Harper Level using rating scales in Appendix A. See Figure 6-3 for an illustration of the target reticle in the programmable HUD.

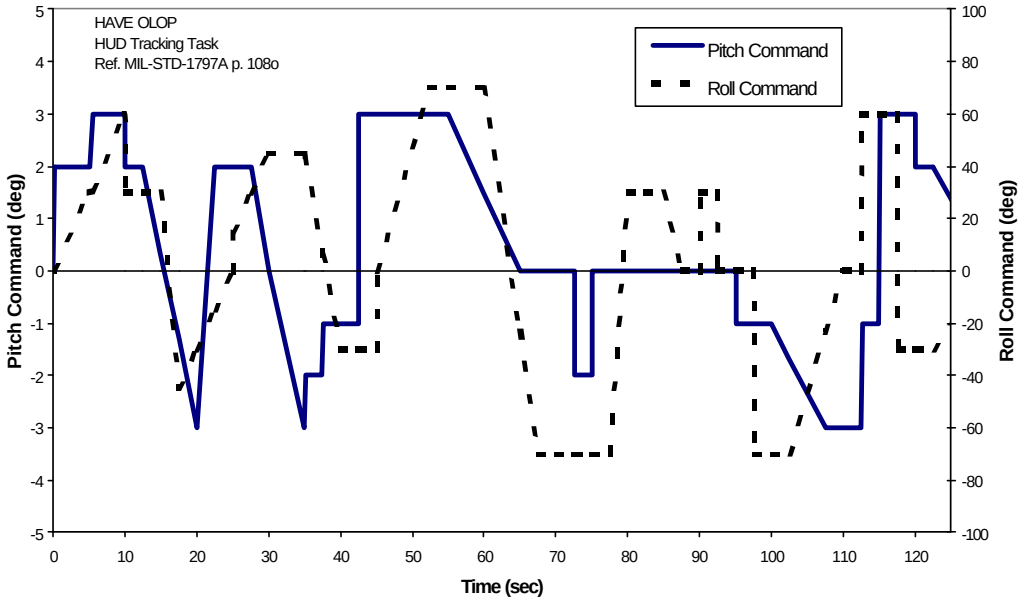

Figure 6-2. HUD Tracking Task

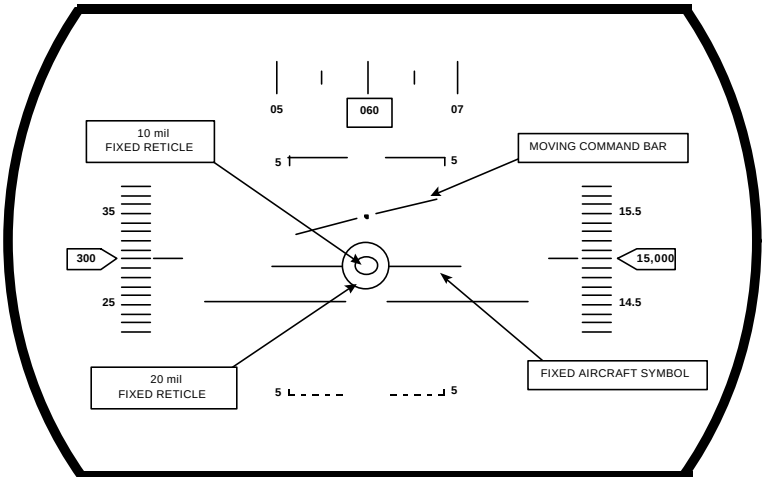

Figure 6-3. HUD Symbology

During calibration sorties and the first test sortie, various gains were evaluated which were used as a multiplier on the task magnitude. The purpose of changing task magnitude was to ensure rate limiting occurred during some portion of the task. If rate limiting did not occur then the test point would not be valid for use with OLOP. Rate limiting was easily achieved for Phase 2 HQDT even for the highest rate limit of 60 deg/sec. Thus, the nominal pitch task, as shown in Figure 6-2, was used for Phase 2. For Phase 3, the test team and Veridian determined that a gain of +0.5 would be used as a multiplier for both the pitch and roll task for rate limit values of 10, 20, and 30 deg/sec. For 40, 50, and 60 deg/sec rate limits, a gain value of +1.5 would be placed on the pitch command while the nominal roll command was left as is. Additionally, the sign of the roll gain was randomly changed between a positive and negative value to minimize task predictability. These gains proved to be effective in achieving rate limiting without creating an unrealistic task or demanding an unusual amount of pilot aggressiveness.

PIO ratings and comments during execution of the HUD tracking task were obtained. The test team determined that if a satisfactory amount of rate limiting was present, then the OLOP calculation would be compared to PIO ratings assigned by pilots and evaluated in accordance with Table 6-4.

Table 6-4. OLOP Evaluation Criteria

OLOP Calculation	Assigned PIO Rating	Evaluation
PIO Predicted	PIOR ≥ 4	Satisfactory
	PIOR ≤ 3	Unsatisfactory
PIO Not Predicted	PIOR ≥ 4	Unsatisfactory
	PIOR ≤ 3	Satisfactory

Data Analysis.

Each test point was evaluated to see if sufficient rate limiting had occurred. This proved to be a challenging part of the analysis requiring engineering judgement. The test team decided a full cycle of rate limiting was desired in order to call the test point valid for use in OLOP analysis. The amount of rate limiting achieved was evaluated using the rating scale in Table 6-5. If the test point was rated as either Rate Limit Rating 1 or 2 then it was used in OLOP analysis. Rate Limit Rating 3 points were omitted.

Table 6-5. Rate Limit Rating

Rate Limit Rating	
1	Satisfactory: Rate limit > 1 cycle
2	Marginal: Intermittent rate limit >1 cycle
3	Unsatisfactory: Minimal or no rate limit

A sample time history assessed as having a Rate Limit Rating of 1 for a Phase 3 task is presented in Figure 6-4. Shown are the stabilator rate (deg/sec), stick deflection (in), and the points during the task where rate limiting was achieved (indicated by the circles on the stick deflection trace). For this example, the aircraft was configuration C with a 10 deg/sec rate limit. Several cycles of the characteristic square wave shape of the stabilator rate leaves no doubt that rate limited dynamics were being experienced. From this trace one could also extract the maximum stick deflection for use in the OLOP analysis. The peak longitudinal stick deflection, with rate limited dynamics, occurred between 58 and 59 seconds into the task (1.23 inches).

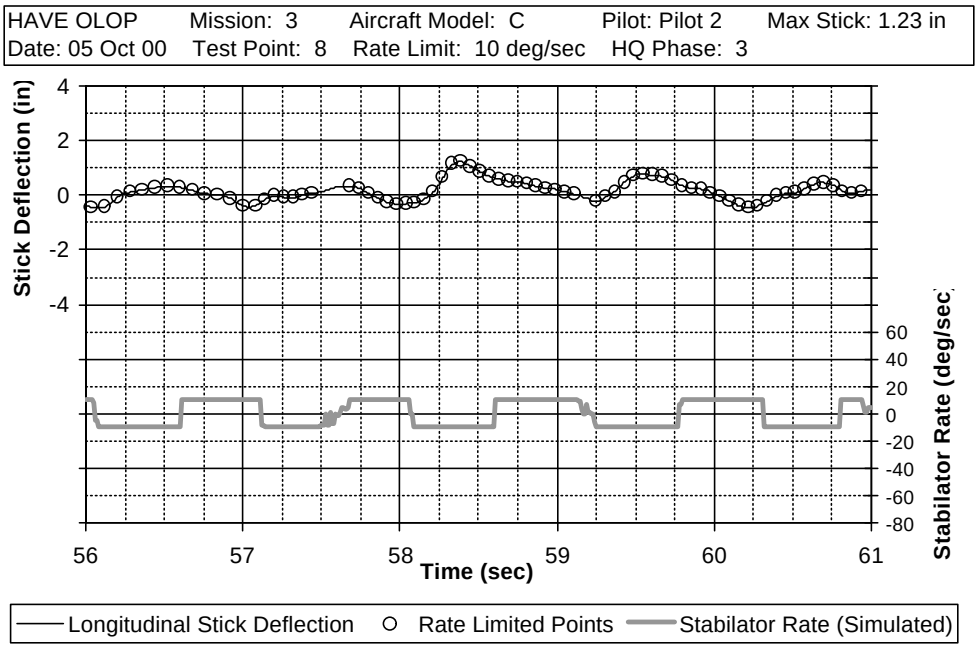

Figure 6-4. Sample Time History, Rate Limit Rating 1

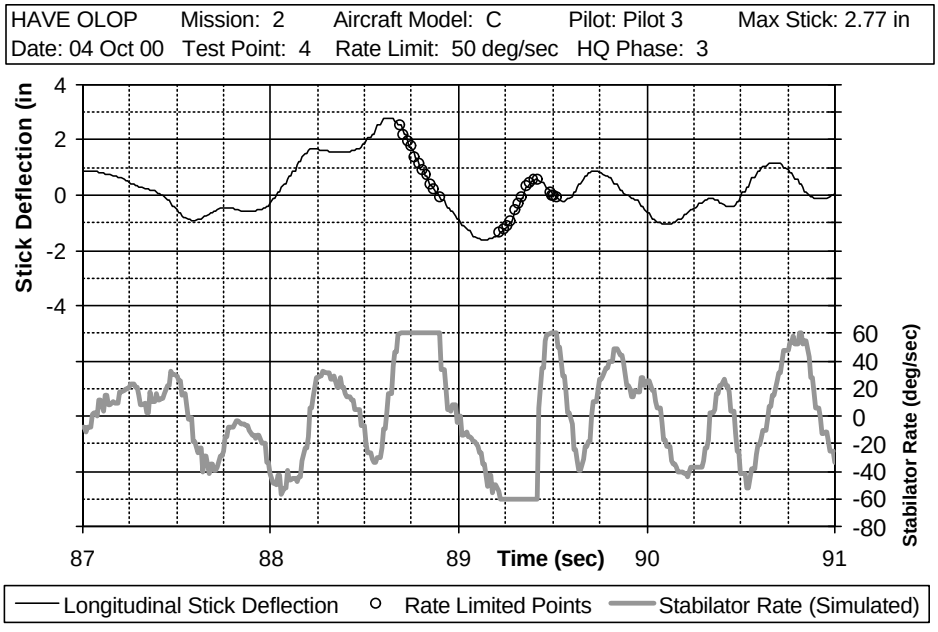

Figure 6-5. Sample Time History, Rate Limit Rating 2

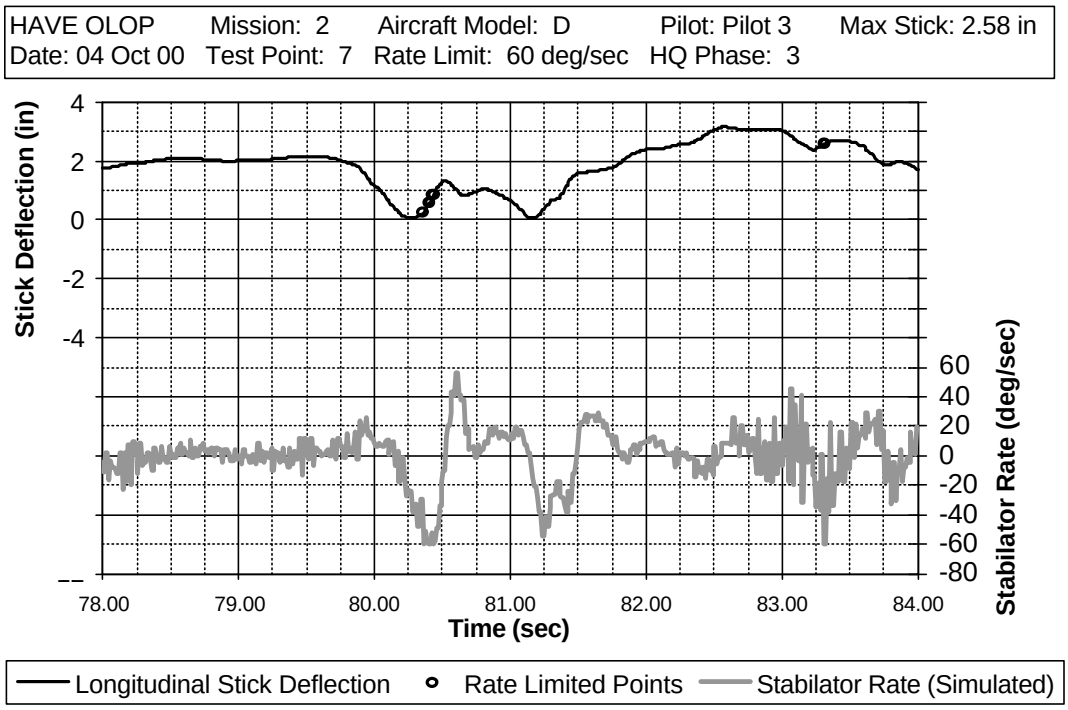

Figure 6-6. Sample Time History, Rate Limit Rating 3

A sample time history of a Rate Limit Rating 2 test point is shown in Figure 6-5. The aircraft was Configuration C with a 60 deg/sec rate limit. Just before the 89 sec point in the task, the pilot got on the rate limit, but the rate limit was not achieved during the middle portion of the stick cycle, then it was back on for the following stick reversal. This was assessed as a complete cycle of rate limiting with intermittent rate limited dynamics. The resulting maximum rate limited stick deflection was 2.77 inches.

An example of a Rate Limit Rating 3 point is shown in Figure 6-6. The aircraft was Configuration D with a 60 deg/sec rate limit. The pilot encountered momentary rate limiting during certain control movements, but never for an entire stick cycle. Since no

complete cycle of rate limiting was found during this run, this point was not used for OLOP correlation.

Once a Rate Limit Rating was established for a given test point, the maximum stick amplitude achieved during rate limiting was determined from time histories. The stick amplitude, rate limit value, aircraft model obtained from the calibration sorties, and appropriate pilot model were used to generate the OLOP positions on the Nichols chart.

As with previous analysis, two pilot models were used: the high gain pilot, as defined by DLR, and the Modified Neal-Smith pilot. However, both models were not used on every test run. Since the pilot technique used in Phase 2 simulated a pure gain pilot (i.e. not using any compensation and very aggressive), the test team used the high gain pilot model for the Phase 2 OLOP analysis only. Phase 3, on the other hand, allowed pilots to use normal piloting technique and compensation. Thus the test team used the Modified Neal-Smith pilot model for this analysis. Following are the two pilot models.

Neal-Smith Pilot Model:
$$Pilot = \frac{-.052(5s+1)(.11s+1)e^{-.25s}}{s(.01s+1)}\left(\frac{in}{\deg}\right) \qquad (23)$$

High Gain Pilot Model (F_c = -130°):
$$Pilot = -.46\left(\frac{in}{\deg}\right) \qquad (24)$$

As with previous analysis, a MATLAB® routine similar to the one in Appendix B was used for the analysis. A block diagram, similar to the one in Figure 3-10 used for HAVE LIMITS, was used to obtain the OLOP frequency response.

Flight Test Results

Configuration Validation

The four configurations were verified using the calibration flight data. The parameters requested by the test team versus results from the LOES matches are shown in Table 6-6.

Table 6-6. Desired versus LOES Dynamics

Configuration	**Short Period Frequency (rad/sec)** Desired/LOES Match	**Short Period Damping** Desired/LOES Match	**T_{q2} (sec)** Desired/LOES Match
A	3.4/3.4	.21/.15	.84/.86
B	.78/.78	.78/.78	.84/.86
C	2.4/2.15	.64/.6	.84/.86
D (Unstable)	Time to Double = 1.0/0.6 sec		.84/.85
Closed-Loop	5.0/5.0	.8/.7	.80/.85

As shown in Table 6-6, the LOES dynamics differed slightly from the desired dynamics. However, they were considered satisfactory for the test. As a result, the linear aircraft model was changed to match LOES results for OLOP analysis. The following 2nd order short period LOES models were generated for the bare airframe (A thru D) and the closed-loop dynamics which were used in the OLOP analysis:

A:
$$\frac{q}{d_{hs}} = \frac{-1.0(.86s+1)e^{-.040s}}{s^2+(2)(.15)(3.4)s+3.4^2}\left(\frac{\text{deg/sec}}{\text{deg}}\right) \tag{25}$$

B:
$$\frac{q}{d_{hs}} = \frac{-15(.86s+1)e^{-.040s}}{s^2+(2)(.78)(.78)s+.78^2}\left(\frac{\text{deg/sec}}{\text{deg}}\right) \tag{26}$$

C:
$$\frac{q}{\delta_{hs}} = \frac{-2.85(.86s+1)e^{-.040s}}{s^2+(2)(.6)(2.15)s+2.15^2}\left(\frac{\text{deg/sec}}{\text{deg}}\right) \tag{27}$$

D:
$$\frac{q}{\delta_{hs}} = \frac{-10.9(.85s+1)e^{-.040s}}{(s+2.13)(s-1.284)}\left(\frac{\text{deg/sec}}{\text{deg}}\right) \tag{28}$$

Closed-Loop Dynamics:
$$\frac{q}{\delta_{hs}} = \frac{-.72(.85s+1)e^{-.040s}}{s^2+(2)(.7)(5)s+5^2}\left(\frac{\text{deg/sec}}{\text{deg}}\right) \tag{29}$$

A sample time history of pitch rate for configuration A, open-loop, from a step input is shown in Figure 6-7. Both the time history data from the calibration flight and the data from the LOES model, derived by Veridian, are shown.

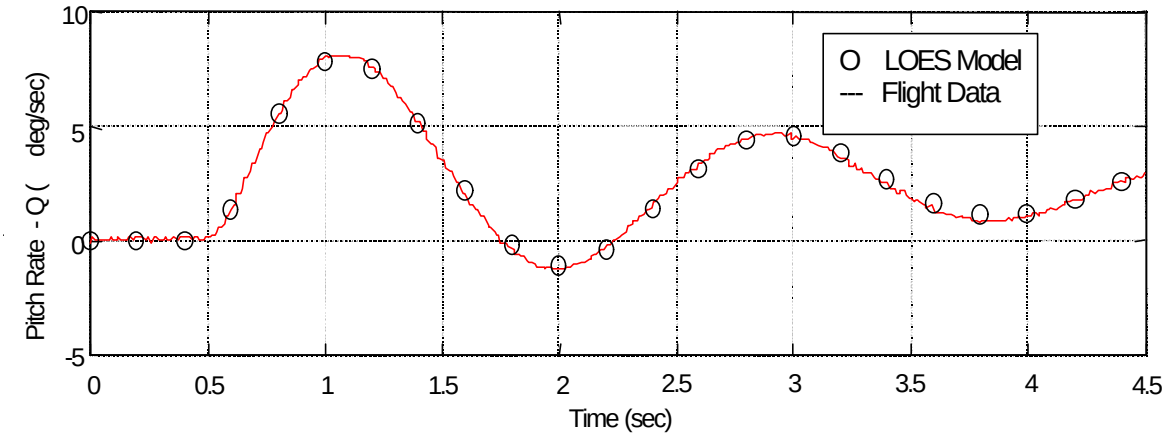

Figure 6-7. Time History Match, LOES vs Flight Data, Config. A, Open-Loop

The test team assessed this match was satisfactory. Satisfactory time history and frequency response matches were obtained for all configurations. There were some discrepancies at the lower frequencies due to phugoid effects. Higher order models (to include phugoid) were examined to try an obtain better frequency response matches. Although this was accomplished with success, the addition of these modes had little impact on the OLOP analysis for these configurations. The major influencing factors for OLOP with limiters in the feedback loop were the short period dynamics and the strength of the feedback signals. Therefore, 2^{nd} order short period approximations were considered sufficient for use in the OLOP analysis. A complete summary of the configuration validation is provided in Reference [13].

To ensure desired rate limits were achieved, several time histories from the test sorties were examined to compare with desired rate limits. The test team assessed that the rate limits satisfactorily matched for all desired rate limit values.

OLOP Evaluation.

The total number of evaluations flown for each test point for both Phase 2 and 3 are shown in Table 6-7 and Table 6-8. The number of evaluations are presented by their Rate Limit Rating as discussed in the previous section. The goal of this test was to obtain a minimum of 3 evaluations (one per pilot) of Rate Limit Rating 1 for each test point for both Phase 2 and 3. Although not statistically significant, this number of evaluations was deemed reasonable in order to assess the PIO susceptibility of a each test point given the limited number of pilots and sorties available to the test program.

The desired number of Rate Limit Rating 1 evaluations was easily achieved for Phase 2 as shown in Table 6-7. The number of Rate Limit Rating 1 points for Phase 3 were fewer, particularly at the higher rate limits, as shown in Table 6-8. However, by combining Rate Limit Rating 1 and 2 points, 3 evaluations were obtained for each test point in Phase 3. Due to several evaluations garnering a Rate Limit Rating of 3 by Pilot 3, six test points (not indicated in the table) received evaluations from only two pilots that could be used in the OLOP analysis. All other test points received evaluations from all three pilots. Pilot 3 had primarily a transport background and tended to be less aggressive than the other two pilots which resulted in less rate limiting at the higher rate limit values.

Table 6-7. Number of Evaluations, Phase 2 Points

Phase 2		Aircraft Model												Priority Level
		A			B			C			D			
Rate Limit Rating		1	2	3	1	2	3	1	2	3	1	2	3	
Rate Limit	10	3			3			3			3			1
	20	3			3			3			4			3
	30	6			3			5			4			2
	40	5			3			3			4			2
	50	3	1		4			3			3			3
	60	3	2	2	5			3	2	1	4			1

Table 6-8. Number of Evaluations, Phase 3 Points

Phase 3		Aircraft Model												Priority Level
		A			B			C			D			
Rate Limit Rating		1	2	3	1	2	3	1	2	3	1	2	3	
Rate Limit	10	3			3			3			3			1
	20	3			3			3			3			3
	30	6	1	1	3			5		1	3			2
	40	5			2	1	1	2	2		3	1	1	2
	50	2		1	2	2	2	1	2	1	1	2		3
	60	3	1	3	3		4	1	3	1	2	1	3	1

A summary of PIO ratings, pilot comments, and OLOP Nichols charts are presented for each configuration. A complete summary of all pilot comments is contained in Reference [13]. A flight log and a complete mission data summary are contained in Appendix C.

Configuration A.

Configuration A was a lightly damped bare airframe with natural frequency of 3.4 rad/sec and a damping ratio of 0.15. PIO ratings are plotted against both rate-limit and pilot in Figure 6-8 for Phase 2 and Figure 6-9 for Phase 3. The shaded symbols indicate a match with the OLOP criterion while open symbols show disagreement with OLOP. Perfect correlation would be indicated by all symbols being shaded for these figures.

For Phase 2, the pilots agreed that configuration A was PIO prone for rate limits below 40 deg/sec. Pilots noted that small amplitude response was good but easily developed into bounded or divergent PIO with larger stick amplitudes. OLOP correlated with each of these ratings. As the rate limit increased to 40 deg/sec and higher, some pilots still experienced PIO while others did not. OLOP correlated when the pilots found PIO but did not correlate when PIO did not occur. For the non-PIO cases, pilots commented that they could feel the non-linear effects causing some out-of-phase response, but no PIO. Although these cases did not agree with OLOP they were all within one rating of PIO. Also, pilots noted throughout the test that it was sometimes difficult to distinguish between a PIO rating of 3 vs. 4 using the HQDT technique.

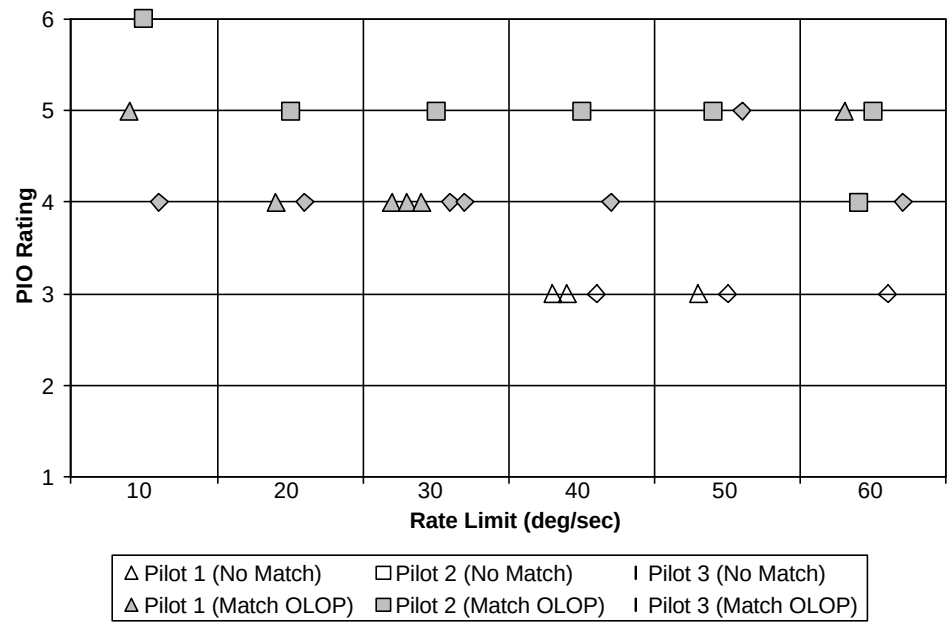

Figure 6-8. Pilot PIO Ratings, Configuration A, Phase 2

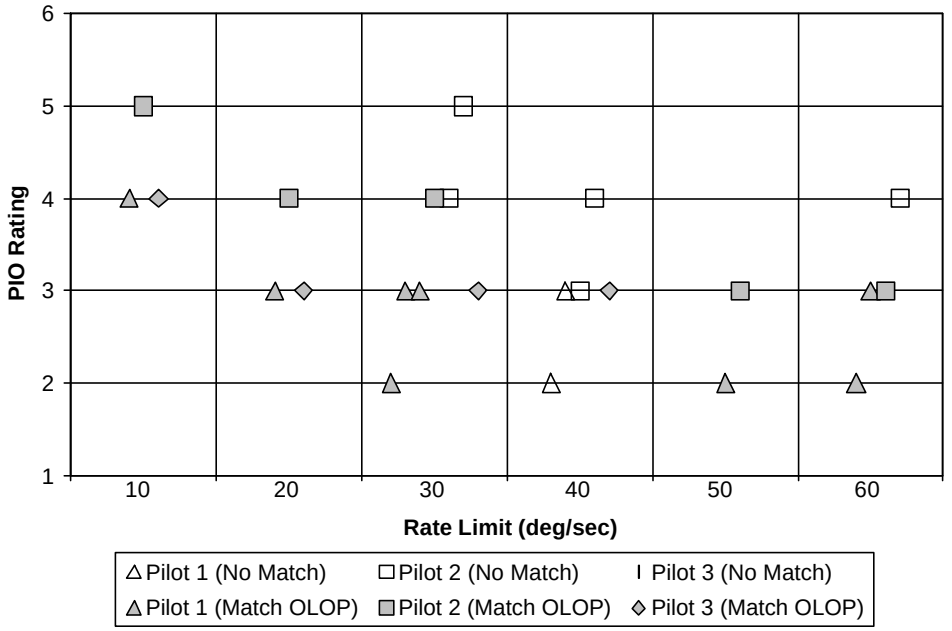

Figure 6-9. Pilot PIO Ratings, Configuration A, Phase 3

Similar comments and trends were apparent for Phase 3. Examining the 20 deg/sec case shows the importance of stick amplitude when using OLOP. Two pilots noted annoying pitch bobbles, but no PIO for this case. On the other hand, Pilot 2 reported abandoning the task under tight control (PIO rating = 4). After examining the time histories and using the respective stick amplitudes for each pilot, OLOP correlated with each of these ratings. As with Phase 2, increasing the rate limit led to a wider variability in ratings and disagreements with OLOP.

The OLOP Nichols chart for Configuration A for both Phase 2 and 3 is shown in Figure 6-10. Individual data points are displayed by pilot, indicated by the shape of the symbol. If the symbol is filled in, the pilot rated that particular point as PIO prone and vice versa if the symbol is empty. For perfect correlation, all symbols above the stability boundary would be shaded and all symbols below the boundary would be open.

As will be seen for all configurations, no points were collected below the OLOP stability boundary for Phase 2. This was driven by the HQDT technique, which called for pilots to explore large amplitudes and the subsequent non-linear effects. Often, this led to divergent PIO as indicated by the points well above the boundary. Attempts were made on later test sorties for pilots to terminate HQDT at smaller amplitudes and rate the configuration in the hope that the point would fall below the OLOP stability boundary and round out the data. This resulted in some points closer to the boundary but never below. A curious group of points that did not correlate lie around 5dB and -160°. Pilot comments for these points were very similar. Pilots could definitely feel the non-linear effects and phase lag, but they did not feel as though these effects were a PIO.

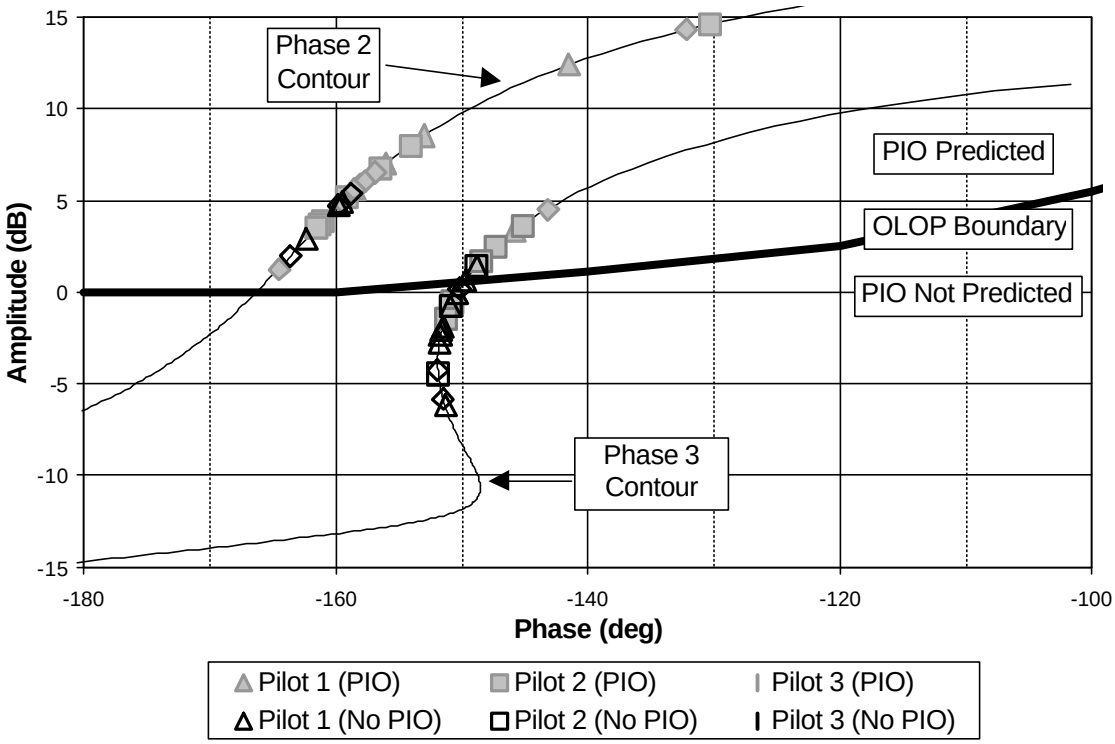

Figure 6-10. OLOP Nichols Chart, Configuration A

Phase 3 points provided a much better distribution across the boundary showing good trend information. As the points moved further away from the boundary, either above or below, correlation improved. For this and the other configurations, it was found that most of the points that did not correlate lie within approximately ±3dB of the stability boundary. This may in fact support the current position of the stability boundary and the fact that it is the transition point from non-PIO to PIO. If this were the case, it would be expected that most pilot rating scatter would occur around this boundary.

Configuration B.

Configuration B was a marginally stable bare airframe with a very low natural frequency of 0.78 rad/sec. The PIO ratings are plotted by rate limit and pilot for Phase 2 and 3 tasks in Figure 6-11 and Figure 6-12.

Pilot comments for Phase 2 indicated that all rate limited cases were PIO prone. For the lowest rate limit, two pilots commented that the VSS departed using normal control inputs without even starting HQDT (PIO rating = 6). As the rate limit increased, pilots were able to evaluate the configuration for longer periods of time but they always resulted in a PIO as input frequency gradually increased. OLOP matched 100% for all Phase 2 runs.

For Phase 3, pilot comments and ratings became more varied as rate limits increased. Results and OLOP correlation were very similar to Phase 2 for rate limits of 10-40 deg/sec. Only one of four runs for the 50 deg/sec case correlated. The furthest outlier came from Pilot 1 who noted that reducing his gain was necessary to maintain control, however based on his stick amplitude, OLOP did not predict PIO.

The OLOP Nichols chart for both Phase 2 and 3 is presented in Figure 6-13. The trend from the Phase 3 data was somewhat encouraging. As OLOP increased in amplitude along the Phase 3 contour, above the boundary, correlation improved. The non-correlated cases for the 50 and 60 deg/sec rate limits lie within ±3 dB of the boundary. For the Phase 2 points, the correlation was 100%, but again no points fell below the boundary. Still, the Phase 2 results are promising, with 100% correlation even within 3 dB of the boundary.

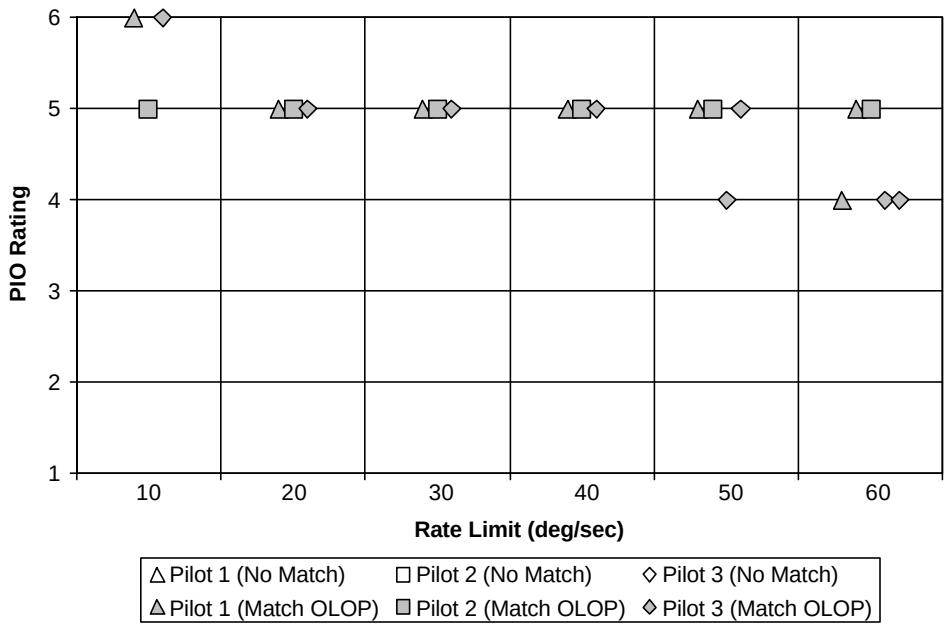

Figure 6-11. Pilot PIO Ratings, Configuration B, Phase 2

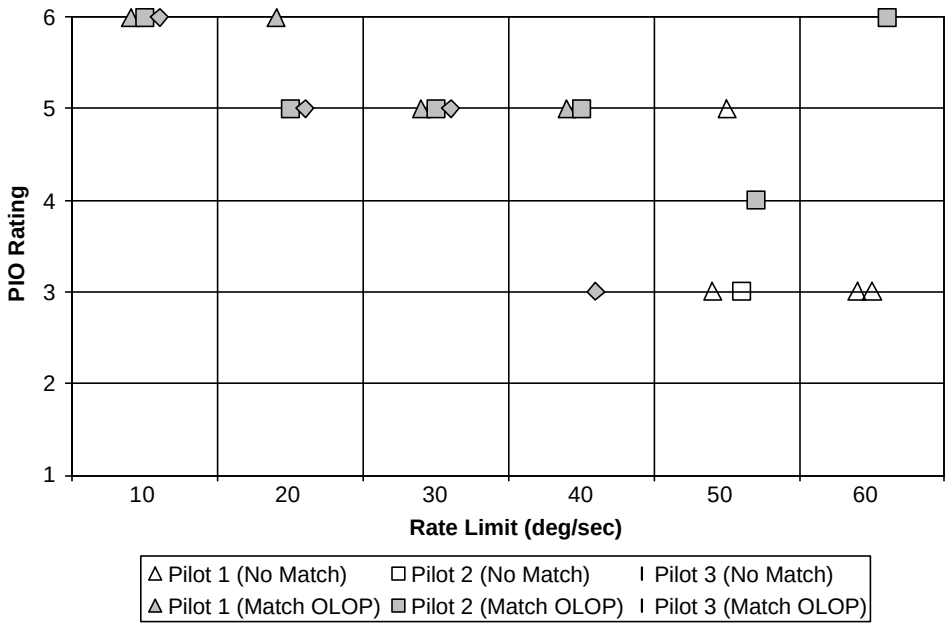

Figure 6-12. Pilot PIO Ratings, Configuration B, Phase 3

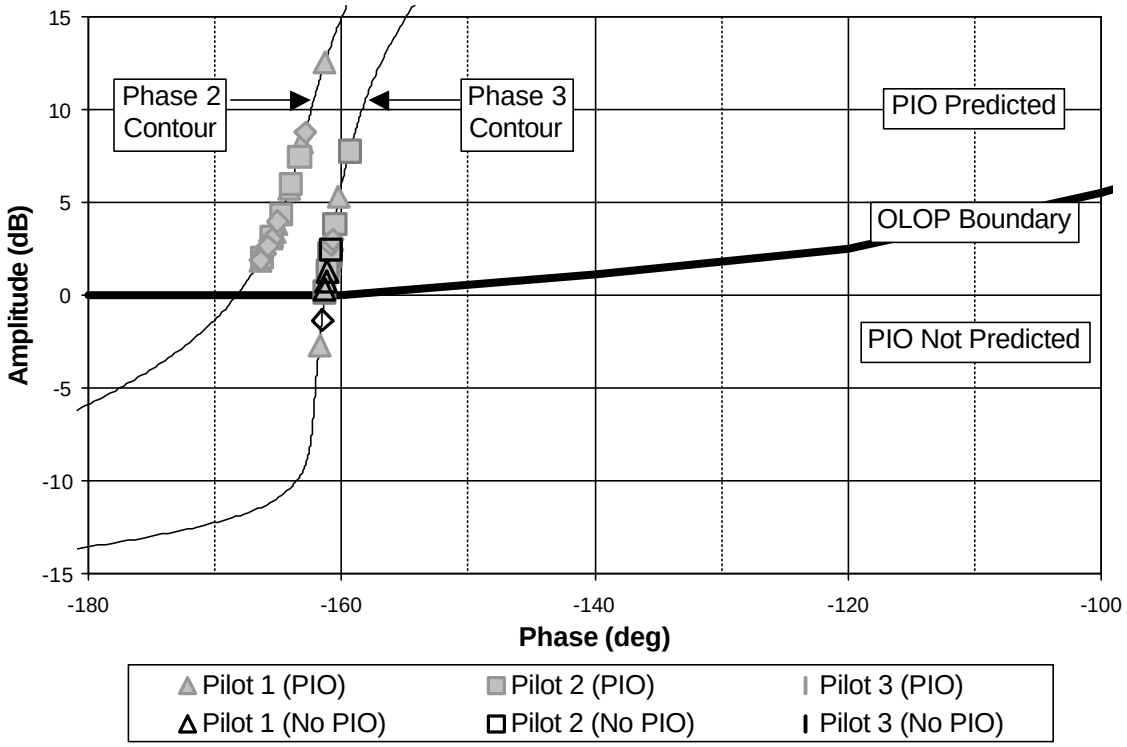

Figure 6-13. OLOP Nichols Chart, Configuration B

Configuration C.

This configuration's bare airframe was characterized by a relatively low short period frequency of 2.4 rad/sec but was well damped with a damping ratio of 0.64. The PIO ratings are presented by rate limit and pilot for Phase 2 and 3 tasks in Figure 6-14 and Figure 6-15.

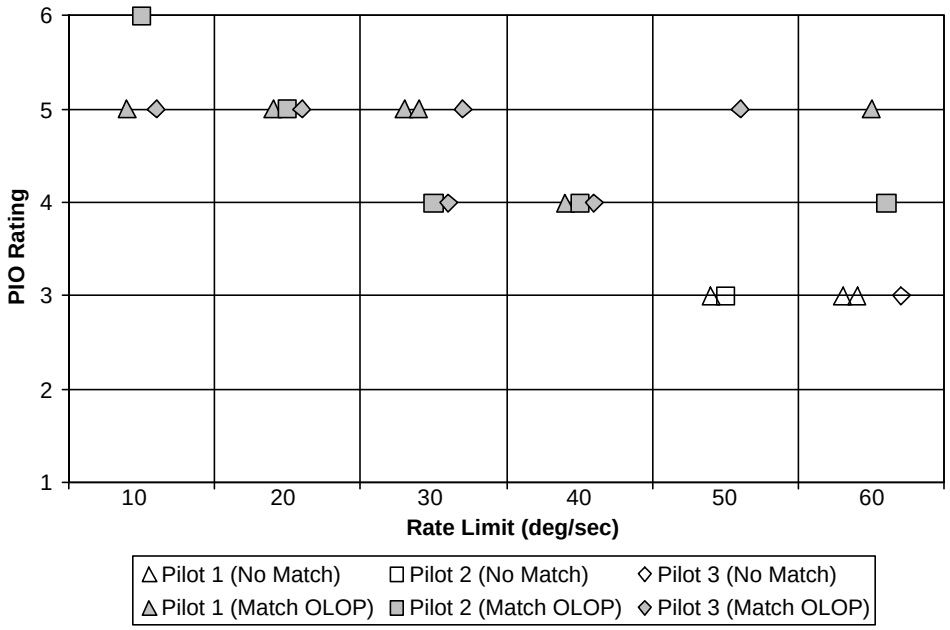

Figure 6-14. Pilot PIO Ratings, Configuration C, Phase 2

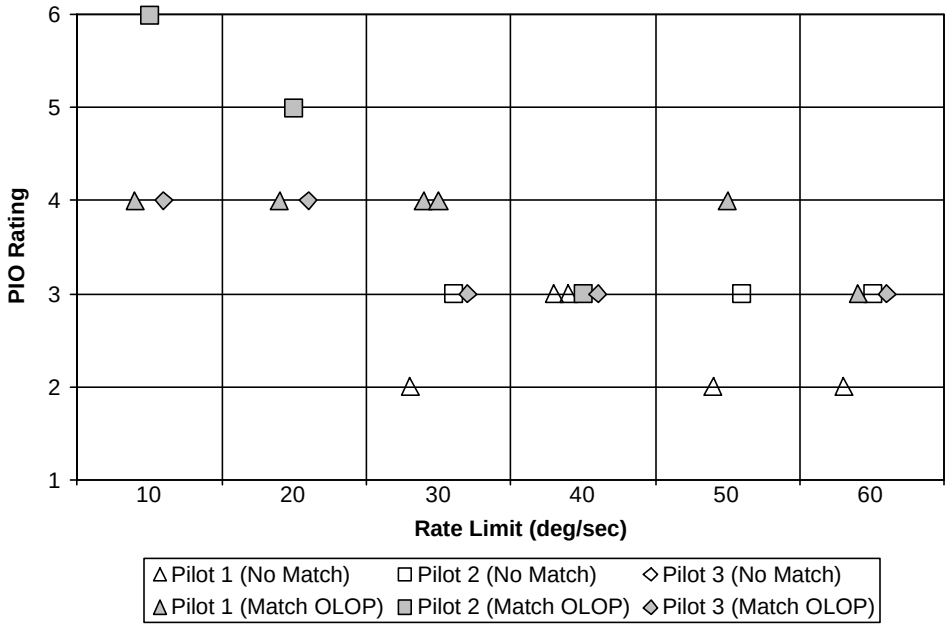

Figure 6-15. Pilot PIO Ratings, Configuration C, Phase 3

Pilot comments for Phase 2 indicated the configuration was PIO prone for rate limits less than 50 deg/sec. For the 10 and 20 deg/sec cases, pilots experienced a divergent PIO excited by small amplitude and higher frequency inputs. During the 30 and 40 deg/sec evaluations, all three pilots reported PIO with increasing amplitude inputs. The OLOP criterion agreed with each rating. There was more rating scatter for the 50 and 60 deg/sec cases. All three pilots experienced PIO using tight control and larger stick amplitudes. Smaller stick amplitudes showed a tendency to be out of phase and induce undesirable motions, but no PIO. OLOP matched the pilot ratings 100% for the PIO cases. OLOP did not match any cases where PIO was not experienced (0% correlation) but was within one pilot rating of PIO.

For Phase 3, all pilots experienced PIO for the 10 and 20 deg/sec cases. OLOP agreed with each rating. Again, as the rate limit increased, pilot ratings and comments became more varied. Unlike Phase 2, there were 5 cases were PIO was not experienced and OLOP agreed. For rate limits greater than 30 deg/sec, pilots noted a tendency to induce undesirable motions and bobbles, even for larger stick amplitudes, but only once was PIO experienced. OLOP correlated with that pilot's rating as well.

The OLOP Nichols chart for Configuration C for both Phase 2 and 3 is presented in Figure 6-16. Again, all but one of the points that did not correlate lie within ±3dB of the boundary. The pilot comments for the furthest outlier (4dB, -157°) were similar to Configuration A for these points in that pilots could feel non-linear effects but did not feel they were bad enough to rate it as a PIO event.

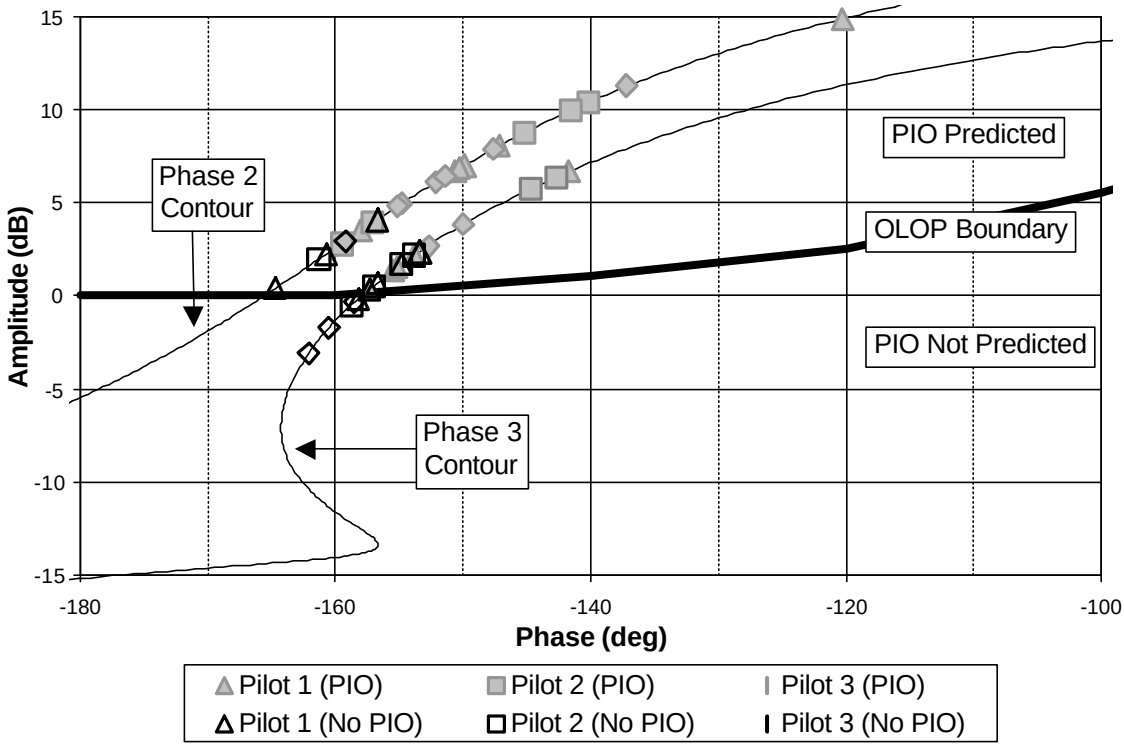

Figure 6-16. OLOP Nichols Chart, Configuration C

Trend data for Phase 3 looks promising and is similar to that of Configuration A. Trend data for Phase 2 appears to mirror that of Phase 3 as the points approach the boundary. However, further points need to be collected below the boundary for Phase 2 in order to make a more definitive conclusion.

Configuration D.

Configuration D was an unstable bare airframe with a time to double amplitude of approximately 0.6 sec. The PIO ratings are plotted against both rate limit and pilot for Phase 2 and 3 in Figure 6-17 and Figure 6-18.

Pilot evaluations of Phase 2 points indicated the configuration was PIO prone for all rate limits. Pilot 2, however, did have one run (50 deg/sec) where he did not experience PIO. He commented that he experienced several bobbles and undesirable motions, but no PIO. Upon examination of the time histories, this point was very interesting. The pilot in fact was on the rate limit for several cycles, lasting approximately 5 seconds. Thus, he was essentially flying the unstable open-loop airplane but still rated it as a PIO rating of 3. He rated his workload as intolerable and rated the aircraft as Level 3. Except for that one rating, OLOP correlated 100%.

Pilot evaluation of Phase 3 points indicated the configuration was PIO prone for rate limits from 10 to 40 deg/sec. Pilot comments were more varied as the rate limit increased to 50 and 60 deg/sec. At 50 deg/sec, two of three ratings assessed the configuration as PIO prone. Pilot 3 reported some bobbles, but never had to back out of the loop. All ratings matched OLOP. Finally, for the 60 deg/sec points, PIO was reported and predicted on 2 of 3 runs. The one rating that did not match OLOP was from Pilot 3 who experienced bobbles and undesirable motions, but no PIO.

The OLOP Nichols chart for Configuration D for both Phase 2 and 3 is shown in Figure 6-19. As with configuration B, all Phase 2 and most Phase 3 points are well above the boundary. Again, the correlation is good above the boundary with scatter within ± 3dB. Unfortunately, very minimal trend information can be gathered from this data due to lack of points below the boundary.

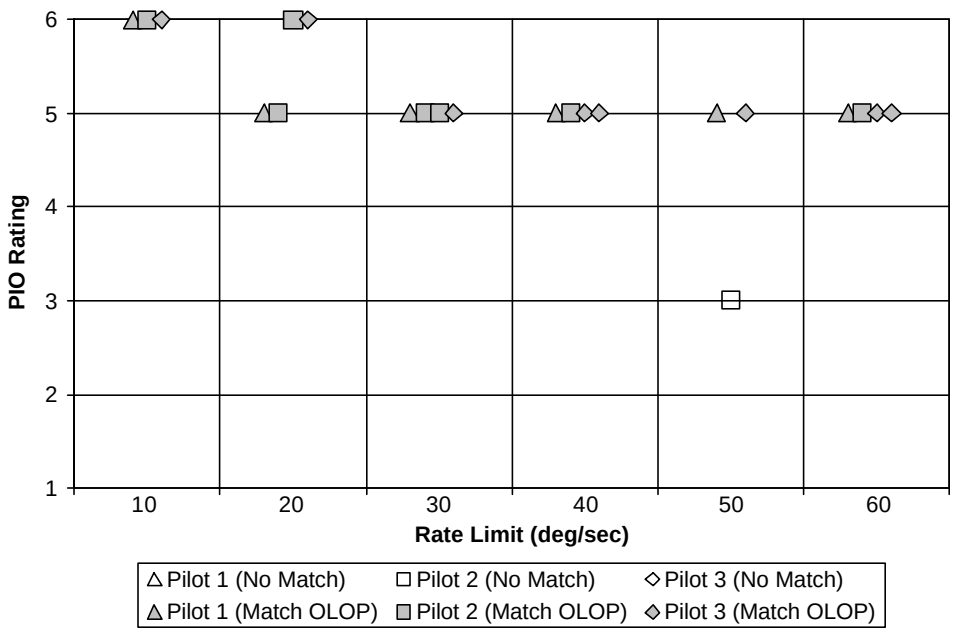

Figure 6-17. Pilot PIO Ratings, Configuration D, Phase 2

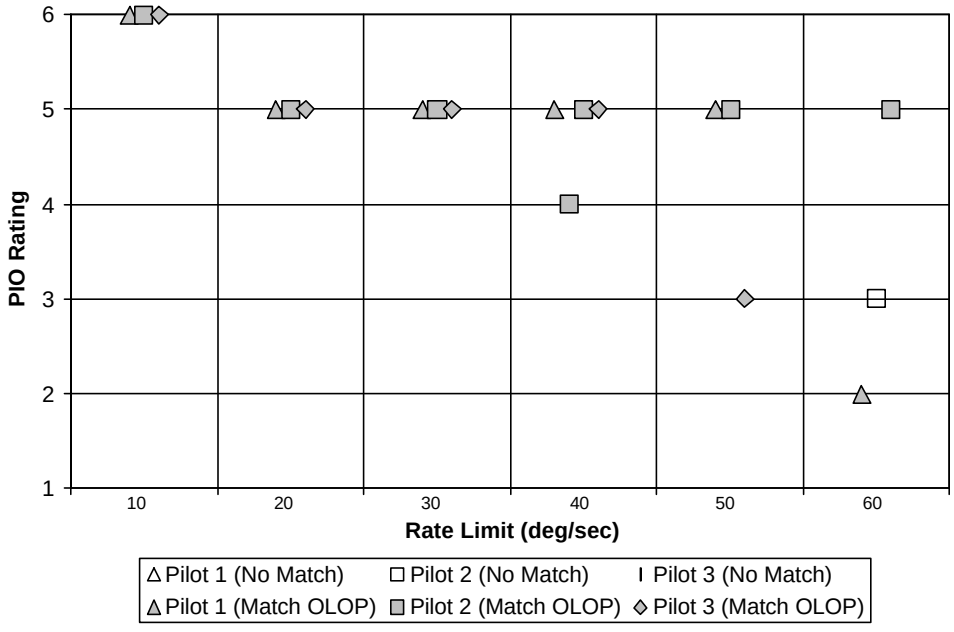

Figure 6-18. Pilot PIO Ratings, Configuration D, Phase 3

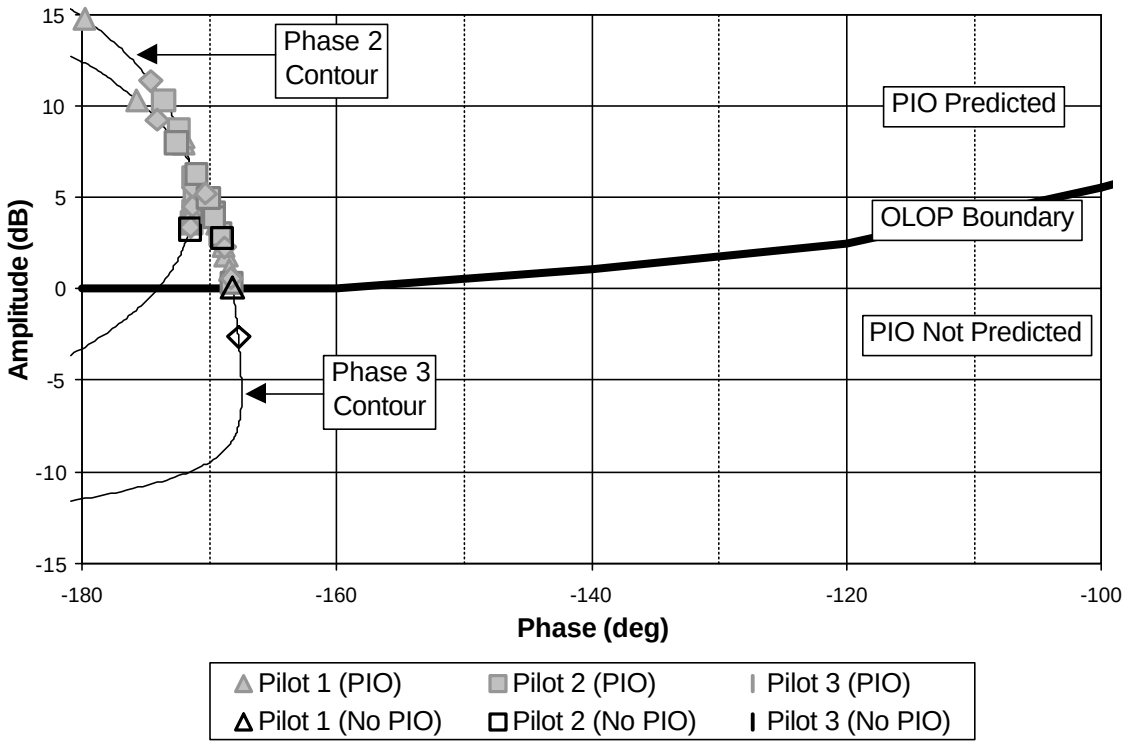

Figure 6-19. OLOP Nichols Chart, Configuration D

Overall Correlation.

Correlation percentages for both Phase 2 and 3 and an overall correlation for the criterion is presented in Table 6-9. The table breaks down the overall statistics into two categories: those test points where the pilots assessed PIO, and those points where no PIO was assessed. Numbers in parentheses represent the 95% confidence bound in percent (using a binomial distribution) for the calculated correlation. In this manner, pilot PIO ratings were used as truth.

For Phase 2, OLOP correlated 100% when the pilots experienced PIO (79 cases). On the other hand, for the 12 cases when PIO was not found OLOP did not correlate. Of

those 12 points, 9 were within ±3dB of the stability boundary. Although overall correlation for this phase was 87%, the distribution of data points was very uneven with most of them being PIO cases versus non-PIO. Additionally, there were no points below the stability boundary and minimal trend data could be gathered from the Nichols charts. In general, pilots found that the HQDT technique was valuable for investigating the effects of rate limiting but was sometimes difficult to use for evaluating PIO susceptibility using the given PIO rating scale.

For Phase 3, OLOP correlated 90% when PIO was found (48 cases) and 56% when PIO was not found (36 cases). For this phase there was a much better distribution of PIO cases versus non-PIO. In addition, all of the points that did not correlate for this phase where within ±3dB of the stability boundary. Examination of the Nichols charts showed definite trend information. Configurations were rated as more PIO prone as the OLOP position moved well above the stability boundary and vice versa. These results give strong support for using the Neal-Smith pilot model with OLOP given the Phase 3 task and the PIO rating scale used. Combining the results from Phase 2 and 3, the overall success rate was 81% for the criterion.

Table 6-9. Overall OLOP Correlation by Phase

All Configs	Correlation						Overall Correlation		
	PIO			No PIO					
	# PIO	# OLOP Matches	% (± 95% bound)	# No PIO	# OLOP Matches	% (± 95% bound)	# Ratings	# OLOP Matches	% (± 95% bound)
Phase 2	79	79	100 % ± 0 %	12	0	0 % ± 0%	91	79	87 % ± 7 %
Phase 3	48	43	90 % ± 9 %	36	20	56 % ± 17 %	84	63	75 % ± 9 %
Overall	**127**	**122**	**96 % ± 3 %**	**48**	**20**	**42 % ± 14 %**	**175**	**142**	**81 % ± 6 %**

Correlation with the OLOP results by pilot is presented in Table 6-10. The criterion fared well for all three pilots when PIO was observed and OLOP predicted it. Each pilot was at or above 90%. Results were not as good for the non-PIO cases where only Pilot 3 fared better than 50%. This is not surprising considering the small number of instances for each pilot compared to the PIO instances. The overall correlation for all the pilots was between 74% and 92%, therefore there was some obvious pilot variability but no one pilot could have had a significant impact over another on the results.

Table 6-10. OLOP Correlation by Pilot

Pilot	Correlation						Overall Correlation		
	PIO			No PIO					
	# PIO	# OLOP Matches	% (± 95% bound)	# No PIO	# OLOP Matches	% (± 95% bound)	# Ratings	# OLOP Matches	% (± 95% bound)
Pilot 1	41	40	98 % ± 5 %	25	9	36 % ± 20 %	66	49	74 % ± 11 %
Pilot 2	47	43	91 % ± 8 %	11	3	27 % ± 31 %	58	46	79 % ± 11 %
Pilot 3	39	39	100 % ± 0 %	12	8	67 % ± 31 %	51	47	92 % ± 8 %
Overall	**127**	**122**	**96 % ± 3 %**	**48**	**20**	**42 % ± 14 %**	**175**	**142**	**81 % ± 6 %**

The objective of this flight test was not to use OLOP to predict PIO per se, but to feed it accurate information in order to determine its reliability. This would help support its use as a design tool using the methods proposed in this thesis. Compared to a recent study on PIO criteria [22], these overall correlation results would rank second among a group of seven other PIO prediction criteria. Although promising, the criterion still has a major variable that cannot be overlooked: stick amplitude.

Stick Ratio Analysis.

A stick ratio (SR) analysis for the four flight test configurations using the Modified Neal-Smith pilot model is presented in Figure 6-20. Included on the chart are the stick activity bands obtained for each rate limit setting from the flight test data. The bands reflect the range of stick amplitudes that the pilots used, in conjunction with rate-limiting, during the Phase 3 task. This chart illustrates several insights as to how OLOP might be used as a design tool.

First, if OLOP had been used to predict PIO using maximum stick amplitude (i.e. SR=100%) it would have predicted PIO for all but one of the configurations. Only Configuration A, with a 60 deg/sec rate limit, would not be PIO prone because the stick ratio required an amplitude beyond that available to the pilot. Obviously for these configurations using maximum stick amplitude over-predicted PIO because of the 84 Phase 3 runs, only 43 reported PIO.

Further examination of the stick activity bands shows that pilots only approached maximum stick amplitude for the highest rate limit. For the two lowest rate limits, the pilots only used slightly more than half the available stick amplitude. But for these two rate limits pilots still reported PIO in all but 2 of 24 runs. This shows that PIO can still be a problem even with relatively small stick amplitudes and that the analysis of stick amplitude is critical when using OLOP.

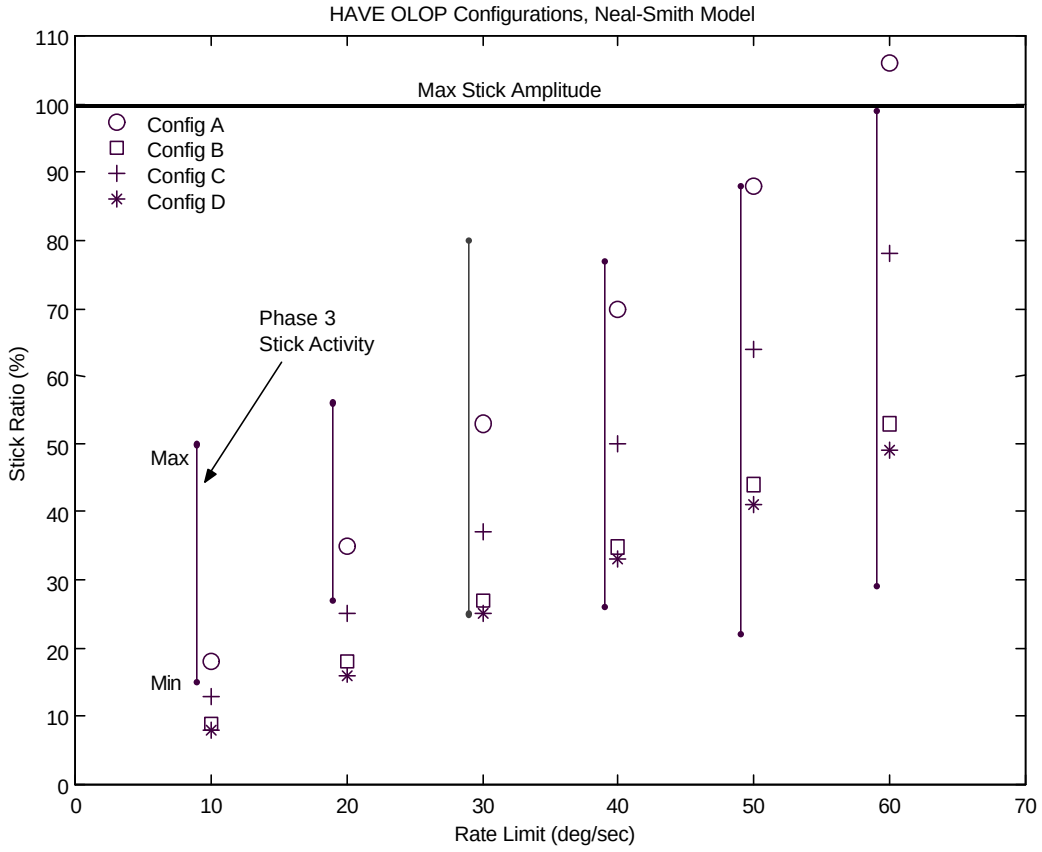

Figure 6-20. Stick Ratio Chart for Flight Test Configurations, Phase 3

Next, as an example of how a designer might use this as a design tool, lets examine Configuration A, with a 50 deg/sec rate limit (SR=88%). If this were the design to be evaluated for PIO due to rate limiting then the designer would have to estimate what stick amplitudes might be expected during a typical mission task using simulations, a ground based simulator, or an in-flight simulator. Lets assume that the stick activity band shown for this rate limit value represents the expected stick amplitudes. In this case, the designer may conclude that his design is virtually PIO free because nearly all of the stick activity is less than the stick ratio.

On the other hand, if the designer was evaluating Configuration D for the same rate limit (SR=41%) and stick activity, then his conclusions would be somewhat different. In this case, approximately two-thirds of the stick activity yields stick ratios greater than the design stick ratio. This clearly shows that expected stick amplitudes could easily drive this configuration into the dangerous PIO region.

VII. Conclusions and Recommendations

A critical examination of the Open-Loop Onset Point (OLOP) criterion was presented in this thesis. The objective was to evaluate the criterion's ability to predict PIO in the presence of rate limiting and determine its potential as a design tool. The criterion was applied to three previous flight tests examining rate limiting: the HAVE LIMITS, HAVE FILTER, and Large Aircraft Rate Limit (LARL) programs. OLOP was applied using the recommended range of pilot model gains and the Modified Neal-Smith pilot model for comparison. These analyses uncovered some limitations regarding the use of the OLOP criterion as a design tool and set the stage for a limited flight test.

Analysis of HAVE LIMITS offered several insights into the OLOP criterion and its application to rate limiters in both the forward and feedback paths of a flight control system. First, OLOP over-predicted PIO for all three configurations when the maximum stick amplitude was applied. When flight test representative stick amplitudes were used, which were much less than the maximum, correlation improved. Although maximum stick amplitude may have represented the worst case scenario, it did not help uncover PIO tendencies due to rate limiting for stick amplitudes less than maximum. Because stick amplitude was such a volatile factor in the use of OLOP a new metric, *stick ratio*, was introduced as a complementary tool. Stick ratio analysis appeared to correlate well with PIO ratings from this test and reinforced the idea that the full range of stick amplitudes needs to be examined when using OLOP as a prediction tool. The metric was successfully applied to the two other test programs and was examined further in the flight test.

Second, the HAVE LIMITS analysis included an examination of the recommended gain pilot models and the Modified Neal-Smith pilot model. It was shown that changes in pilot gain had a dramatic effect on the OLOP positions relative to the stability boundary for forward path limiters. The changes were less dramatic for the feedback limiter case. The high gain and Neal-Smith pilot models yielded reasonably good correlation to pilot ratings when using the smaller stick amplitude. Therefore, they were the only models considered for the remainder of the thesis research.

Analysis of the HAVE FILTER program offered more insight into both forward and feedback path limiters in addition it highlighted the effects of having two limiters active at the same time. OLOP correctly predicted the PIO susceptibility of the one feedback limiter configuration (HAFA1). When OLOP was applied to HAFA1 with a forward path limiter added, correlation with pilot ratings was poor. This was because both the forward and feedback limiters were often engaged simultaneously for this configuration. This showed the need to conduct OLOP analysis separately for each limiter location and to assess which will have the more negative effect if activated. Analysis of the second configuration (HAFA2) with the forward path limiter yielded good correlation with OLOP. Although this configuration was already PIO prone due to poor linear characteristics, OLOP was successfully used to see if rate limiting would further degrade its PIO susceptibility.

Analysis of the LARL program offered additional insight into forward path limiters on large aircraft. The same conclusions for forward path limiters from HAVE LIMITS and HAVE FILTER were reinforced.

A flight test was developed to further examine OLOP's viability as a design tool. Based on the analysis of these three test programs, the premise for the application of OLOP was to apply it using both the high gain and Neal-Smith pilot models. Because stick amplitude was shown to be critical to the OLOP prediction, it would remain as a variable that a designer would have to contend with, perhaps using stick ratio. If the flight test yielded accurate predictions using actual stick amplitudes then recommendations could be developed on how to use OLOP in the design phase.

The flight test was accomplished on the VISTA NF-16D examining four configurations involving feedback limiters. Overall, OLOP correlated with pilot ratings 81% of the time. For Phase 2, using the HQDT technique and the high gain pilot model, correlation was 87% but most of the data points represented PIO cases (79) versus non-PIO (12). Additionally, there were no points below the boundary for this phase yielding minimal trend information. Pilots also commented that although valuable for examining the effects of rate limiting, HQDT was sometimes difficult to use for evaluating PIO with the given the PIO rating scale.

For Phase 3, the distribution of PIO cases (48) versus non-PIO (36) was much better yielding a correlation rate of 75%. In addition, all of the points that did not correlate with OLOP were within ±3dB of the stability boundary. This showed that the boundary cannot be treated as a definitive break between the PIO and non-PIO regions but rather as a transition region about which PIO may occur. The results also showed good trend information and strong support for using the Neal-Smith pilot model with OLOP.

Based on the results of this research, the Modified Neal-Smith pilot model is considered appropriate to use with the OLOP criterion. The model is widely accepted and perhaps best represents the pilot prior to the onset of rate limiting. Results using this model in conjunction with the Phase 3 data were promising. Because it is simple to calculate, the high gain pilot model can still be used as well to represent the pilot in the worst case scenario. However, because of the minimal effect of pilot gain on the OLOP analysis for feedback limiters, it is not recommended to use the range of pilot gains as suggested by DLR. When analyzing forward path limiters on the other hand, pilot gain variations may be considered.

The OLOP criterion can be a useful design tool but with limitations. The designer will have to use engineering judgement when using this tool to determine whether a redesign is necessary versus the calculated risk of reaching a specific amplitude and hence, a dangerous PIO situation. The criterion itself is fairly easy to use and implement with control system software such as MATLAB® and Simulink®. Traditional linear techniques should still be applied to examine PIO susceptibility prior to using OLOP. Based on this study the following steps are recommended when using OLOP as a design tool.

1. Apply the OLOP criterion to the desired flight control system design using the DLR-defined high gain pilot model and the Modified Neal-Smith pilot model applying maximum stick deflection. If OLOP is clearly below the boundary for both pilot models then PIO is unlikely.

2. If OLOP lies above the boundary for both pilot models, recalculate using predicted stick amplitudes perhaps obtained from simulation, ground based simulators, or in-flight simulators. Stick ratio could be used as a complementary tool at this point.

3. If OLOP lies above the boundary, using anticipated stick amplitudes, for the high gain pilot model but not the Neal-Smith pilot model, then perhaps the following conclusion could be made: PIO is not likely under normal operational maneuvers; however, a momentary high gain maneuver could result in a PIO.

4. If OLOP is within ±3dB of the stability boundary then the occurrence or absence of PIO is difficult to predict with any certainty.

Recommendations for further research are as follows: The focus of this study was on the longitudinal axis. It is desirable that a design tool could be applied to all aircraft modes of motion. Thus a flight test examining the lateral-directional axis would help further validate the criterion and would complement simulator work that DLR has accomplished in this axis as well [8]. Another flight test involving forward path limiters in the longitudinal axis, using the data analysis techniques from HAVE OLOP, would complement the flight test data presented here for feedback limiters. Data from the HAVE OLOP flight test could be used to further examine pilot model identification. Simulator studies could be conducted and compared to flight test data to examine the viability of predicting stick amplitudes that will be experienced in flight.

Appendix A: Pilot Rating Scales

Pilot-Induced-Oscillation (PIO) Scale	
Description	**Rating**
No tendency for pilot to induce undesirable motions	1
Undesirable motions tend to occur when pilot initiates abrupt maneuvers or attempts tight control. These motions can be prevented or eliminated by pilot technique.	2
Undesirable motions easily induced when pilot initiates abrupt maneuvers or attempts tight control. These motions can be prevented or eliminated, but only at sacrifice to task performance or through considerable pilot attention and effort.	3
Oscillations tend to develop when pilot initiates abrupt maneuvers or attempts tight control. Pilot must reduce gain or abandon task to recover.	4
Divergent oscillations tend to develop when pilot initiates abrupt maneuvers or attempts tight control. Pilot must open loop by releasing or freezing the stick.	5
Disturbance or normal control may cause divergent oscillation. Pilot must open loop by releasing or freezing the stick.	6

Figure A-1. Pilot Induced Oscillation Rating Scale

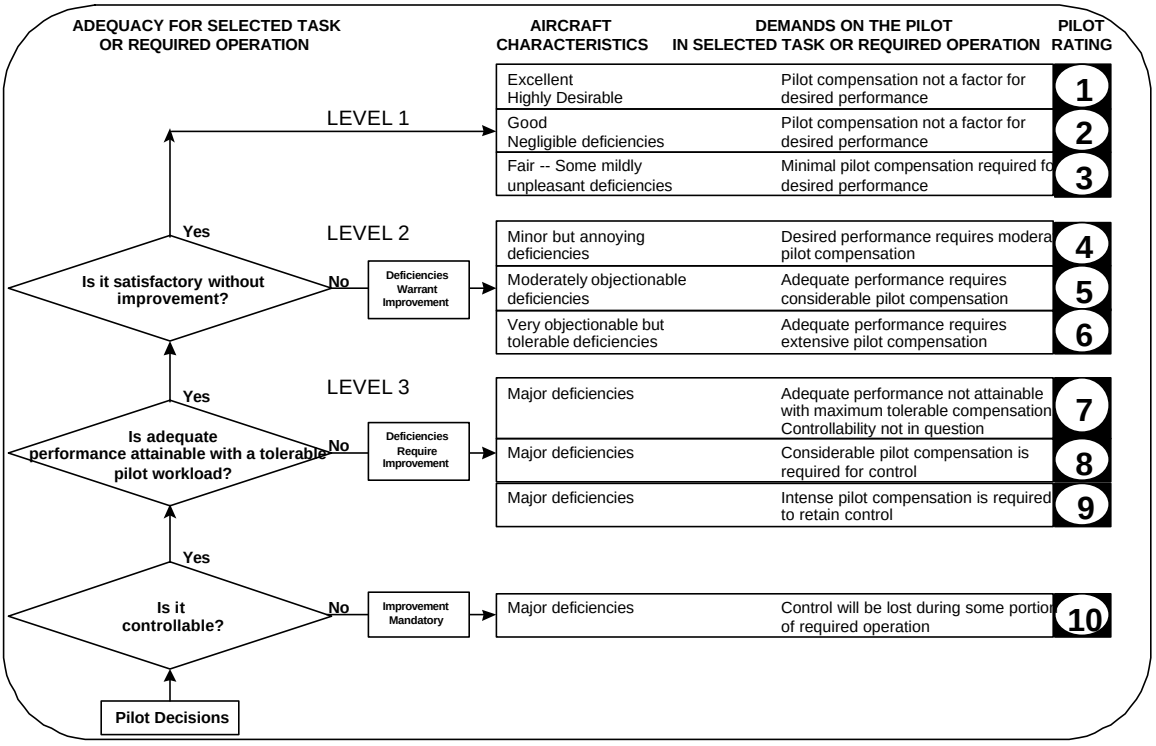

Figure A-2. Cooper-Harper Rating Scale

Appendix B: MATLAB^{Ò} M-files

```
%This M-file will calculate the closed-loop describing function
%for the aircraft model example from AIAA-95-3204-CP
clear all
global w R K magGc magGac phGc phGac dtr qco z
%System input frequency range, amplitude, rate limit
w=logspace(-1,2,100);  qco=1.1;      R=60;

%System numbers
K=13.68;
Gc=tf(5.21*conv([1 -57.36],conv([1 4.26],[1 .55])),conv([1 2*.442*22.85   22.85^2],conv([1 0],[1 1.16])));
Gac=tf(-10.524*conv([1 1.562],conv([1 .038],[1 0])),conv([1 2*.212*.088 .088^2],conv([1 3.75],[1 -
1.44])));
num=K*Gc;
den=zpk([],[],1)+series(Gc,Gac);
pcl=num/den;
dtr=pi/180;

%Find linear response amplitude and phase for initial guess
[magpcl,phi2(1)]=bode(pcl,w(1));
deltao(1)=qco*magpcl;phi2(1);

for z=1:length(w)
[magGc,phGc]=bode(Gc,w(z));
[magGac,phGac]=bode(Gac,w(z));

xo=[deltao(z) phi2(z)]; %initial guess for optimization algorithm

[a,fval(z)]=fminsearch('eqs',xo,optimset('Display','off'));

deltait=a(1);
phi2it=a(2);

[magNit,phNit]=dfunction(w(z),R,deltait);
A=deltait*magGac*magNit/(K*qco);
phi=phi2it+phGac+phNit*180/pi;

%Calculate Open-loop describing function for Nichols plot
NoMag(z)=20*log10(A/sqrt(1-2*A*cos(dtr*phi)+A^2));
NoPh(z)=dtr*phi-atan2(-A*sin(dtr*phi),1-A*cos(dtr*phi));

%Give new initial guess if function cannot converge to zero
%Disply onset frequency where discontinuity starts to occur
if fval(z)>.0001
  deltao(z+1)=24; phi2(z+1)=-237;onset=w(z)
  else
  %Else, use previous solution for next starting point
  deltao(z+1)=a(1); phi2(z+1)=a(2);
end
end
```

```
[mlin,plin]=bode(Gc*Gac,w);
figure(1) %Plot results on Nichols Chart
plot(plin(1,:)-360,20*log10(mlin(1,:)),'-o',NoPh/dtr,NoMag,'-*')
axis([-300,-50,-20,12])

figure(2) %Plot function evaluation vs. frequency to see convergence
semilogx(w,fval)


function f=eqs(x)
global w R dtr magGc magGac phGc phGac K qco z
deltao=x(1); phi2=x(2);

f=(deltao/magGc*cos(dtr*(phi2-phGc))+deltao*magGac*dfuncmag(w(z),R,deltao)...
  *cos(dtr*(phi2+phGac)+dfuncphase(w(z),R,deltao))-K*qco)^2.0...
  +(deltao/magGc*sin(dtr*(phi2-phGc))+deltao*magGac*dfuncmag(w(z),R,deltao)...
  *sin(dtr*(phi2+phGac)+dfuncphase(w(z),R,deltao)))^2.0;

%Function file that determines magnitude and phase of describing function given the input frequency
%rate limit and input amplitude.  Includes cubic spline interpolation coefficients.
function [magN,phN]=dfunction(freq,rate,inamp)
%Describing Function of a rate limiting element
x=freq*inamp/rate;
if x<1, magN=1;phN=0;
elseif x<1.862
      magN=polyval([.2908 -1.4396 1.9232 .223],x);%From cubic spline interpolation
  phN=polyval([.528 -2.6213 3.5056 -1.4171],x);% From cubic spline interpolation
else
  magN=4/x/pi;
  phN=-acos(pi/x/2);
end

%**********************************olop.m**********************
%This M-file is used for application of the Open-loop Onset Point (OLOP) to an aircraft system
%with a rate limiting element in it.  Two simulink models are needed for the analysis.  The first is
%the linear model of the aircraft system with the pilot output as the input and theta as the output
%to include any feedback gains.  The linear model should be named 'namelin.mdl'.  Once the pilot
model
%is chosen the second model is developed called 'nameolop.mdl'.  It has the pilot model in the loop
%and has the output of the rate limiter as its input and the output is the input into the rate limiter.
%**************************************************************************
clear
format short
lin_abcd  %Initialization File to get aircraft model
w=logspace(-2,2,1000);
%Define the rate limiter value and the pilot input amplitude
R=input(' Enter Vector of Rate Limits to evaluate[default = 60]: ');
if(isempty(R))
 R=60;
end

Per=input(' Enter Stick Input Amplitude in percentage (range 0-100) [default = 100% ]: ');
if(isempty(Per))
  Per=100;
end
```

```
Po=Per/100*3.6
if Po<.8 %Takes into account non-linear stik gradient
  Po=2.5*Po;
else Po=2.5*(2.86*Po-1.48);end

tag=input(' Choose desired pilot model (1=Low Gain 2=Med Gain 3=High gain 4=Neal-Smith) [default
Neal-Smith]:');
if(isempty(tag))
 tag=4;
elseif tag==1; xover=-90; %Set crossover angle for gain pilot model
elseif tag==2; xover=-110;
elseif tag==3; xover=-130;
end

Kp=-.05*2.5; Tp1=.06; Tp2=.01; %Gain, lead, and lag time constants for Neal-Smith Pilot Model
%Use LINMOD to find appropriate transfer function for Yc=theta/pilot
[A,B,C,D]=LINMOD('nt33v2Dlin');
Yc=ss(A,B,C(4,:),D(4,:)); %Make sure appropriate row is selected for theta output

%Find pure gain pilot model
Kg=-.7*2.5:.01:-.01;
for i=1:length(Kg)
  [gm,pm,wcg,wcp]=margin(Kg(i)*Yc);
  if tag==4; break, end
  if -180+pm > xover
    xover_angle=-180+pm,
    Pilot_gain=Kg(i)
    break
 end
end

figure(1),ngridneal,nichols(Kg(i)*Yc,w)

%Find Neal-Smith Modified Pilot model
bw=3.5; %Set bandwidth requirement
Yp=Kp*tf([5 1],[1 0])*tf([Tp1 1],[Tp2 1]); set(Yp,'InputDelay',.25);
Ypp=pade(Yp,2);%Need pade approximation for linmod to get OLOP transfer function
figure(2),ngridneal,nichols(Yp*Yc,{.1,3*bw})

%Find closed-loop response amplitude from stick input to RLE input
P_RLE=ss(A,B,C(6,:),D(6,:));
[magP,phP]=bode(P_RLE,w);

for n=1:length(R)
%Calculate Rate Limit Line for frequency plot
[magR,phR]=bode(tf(R(n),[1 0]),w);
%Plot closed-loop amplitude and rate limit line
figure(3),semilogx(w,20*log10(Po*magP(1,:)),w,20*log10(magR(1,:)),'k:')
hold on,axis([.01,10,10,60])
title('Determine Closed-loop Onset Frequency')
%Calculate omega onset for closed-loop system
iter=100;
for i=1:length(w)
    dif(i)=abs(magR(i)-Po*magP(i));
```

```
      if dif(i)<= iter
     iter=dif(i); k=i;
  end
end
w_onset=w(k),Rate=R(n)

%Calculate OLOP on Nichols chart

if tag==4
Pilot=Ypp; %Neal-Smith Pilot Model with Pade approximation for time delay
else
Pilot=tf(Pilot_gain,1); %Simple Gain Pilot Model
end

[AA,BB,CC,DD]=linmod('nt33v2dolop');
OLOP=ss(AA,BB,-CC,-DD);
[magN,phN]=nichols(OLOP,w);
r=150; %Plot range
v1=[-60 -90 -100 -120 -140 -160 -180];v2=[13.5 7.5 5.5 2.5 1.1 0 0];%OLOP stability boundary
%Plot OLOP points for each rate value
if n==1
figure(4),plot(phN(k),20*log10(magN(k)),'o','MarkerFaceColor','k','MarkerSize',7)
elseif n==2
figure(4),plot(phN(k),20*log10(magN(k)),'d','MarkerFaceColor','k','MarkerSize',7)
elseif n==3
figure(4),plot(phN(k),20*log10(magN(k)),'o','MarkerSize',7)
elseif n==4
figure(4),plot(phN(k),20*log10(magN(k)),'p','MarkerFaceColor','k','MarkerSize',7)
elseif n==5
figure(4),plot(phN(k),20*log10(magN(k)),'s','MarkerFaceColor','k','MarkerSize',7)
elseif n==6
figure(4),plot(phN(k),20*log10(magN(k)),'d','MarkerSize',7)
else
figure(4),plot(phN(k),20*log10(magN(k)),'s','MarkerSize',7)
end
hold on
%Plot mag and phase on Nichols chart
plot(phN(1,k-r:r+k),20*log10(magN(1,k-r:r+k)),...
  [-360 0],[0 0],'-k',[-180 -180],[-50 50],'-k')
axis([-200,-60,-10,20]);
plot(v1,v2,'-k','LineWidth',1.5)%Plot OLOP stability boundary
end
```

Appendix C: Flight Log and Mission Data Summary

Table C-1. HAVE OLOP Flight Log

Flight	Mission	Date	FCP	RCP	Duration	Fuel (gal)
1	566	03-Oct-00	Gilbreath	Peer	1.4	1013
2	567	04-Oct-00	Ormsby	Peer	1.4	905
3	568	05-Oct-00	Ippoliti	Peer	1.4	889
4	569	06-Oct-00	Gilbreath	Peer	1.4	828
5	570	06-Oct-00	Ormsby	Peer	1.3	820
6	571	10-Oct-00	Ippoliti	Hutchinson	1.3	880
7	572	10-Oct-00	Gilbreath	Hutchinson	1.2	847
8	573	11-Oct-00	Ormsby	Hutchinson	1.3	823
9	574	11-Oct-00	Ippoliti	Hutchinson	0.8	830
10	575	12-Oct-00	Ormsby	Hutchinson	1.4	581
11	576	12-Oct-00	Gilbreath	Hutchinson	1.1	894
12	577	16-Oct-00	Ippoliti	Hutchinson	1.4	787
				Total	**15.4**	**10097**

The following table contains a summary of the data derived from each test mission (excluding sortie #9 which did not collect any data due to an aircraft malfunction). Included are the PIO rating, Rate Limit Rating, maximum stick amplitude, and pertinent OLOP data which was used to create the Nichols charts for each test run.

Table C-2. Mission Data Summary

Mission	Pilot	Record	VSS Code	A/C Config	Rate Limit	HQ Phase	PIO Rating	Rate Limit Rating	Actual Max Stick (Inches)	OLOP PIO?	OLOP Phase (deg)	OLOP Amp. (dB)	ω_{onset} (rad/sec)
1	Gilbreath	7	66F	A	60	2	5	1	-2.45	Y	-161.5	3.48	5.6
1	Gilbreath	8	66F	A	60	3	3	1	1.5	N	-151.3	-6.2	6.7
1	Gilbreath	9	71F	B	10	2	6	1	-1.71	Y	-161.3	12.56	2.6
1	Gilbreath	10	71F	B	10	3	6	1	-0.92	Y	-160.2	5.28	3.3
1	Gilbreath	12	86F	C	60	2	5	1	2.31	Y	-158	3.51	5.3
1	Gilbreath	13	86F	C	60	3	3	3					
1	Gilbreath	14	91F	D	10	2	6	1	-2.58	Y	-179.8	14.8	1.9
1	Gilbreath	15	91F	D	10	3	6	1	-2.03	Y	-175.7	10.3	2.2
1	Gilbreath	17	61F	A	10	2	5	1	-1.59	Y	-141.5	12.4	4.1
1	Gilbreath	18	61F	A	10	3	4	1	1.02	Y	-145.8	3.33	4.5
1	Gilbreath	20	96F	D	60	2	5	1	2	Y	-171.3	4.52	4.7
1	Gilbreath	21	96F	D	60	3	2	1	1.68	N	-168.2	0.075	5
1	Gilbreath	23	81F	C	10	2	5	1	-2.55	Y	-120.3	14.9	2.5
1	Gilbreath	24	81F	C	10	3	4	1	1.28	Y	-141.7	6.7	3.3
1	Gilbreath	26	76F	B	60	2	4	1	-2.02	Y	-165.5	3.02	4.9
1	Gilbreath	27	76F	B	60	3	2	3					
2	Ormsby	3	66F	A	60	2	2	3					
2	Ormsby	5	66F	A	60	3	3	3					
2	Ormsby	7	71F	B	10	2	6	1	-0.9	Y	-162.8	8.76	3.33
2	Ormsby	8	71F	B	10	3	6	1	-0.59	Y	-160.8	2.69	3.9
2	Ormsby	10	86F	C	60	2	3	3	-2.44	Y	-157	3.94	5.1
2	Ormsby	12	86F	C	60	3	3	2	2.77	N	-158.5	-0.35	4.9
2	Ormsby	13	91F	D	10	2	6	1	1.29	Y	-174.6	11.4	2.7
2	Ormsby	15	91F	D	10	3	6	1	-1.63	Y	-174.1	9.26	2.4
2	Ormsby	18	61F	A	10	2	4	1	2.04	Y	-132.2	14.3	3.9
2	Ormsby	19	61F	A	10	3	4	1	1.19	Y	-143.2	4.51	4.3
2	Ormsby	21	96F	D	60	2	5	1	-2.03	Y	-171.3	4.52	4.7
2	Ormsby	22	96F	D	60	3	3	3					
2	Ormsby	24	81F	C	10	2	5	1	-1.37	Y	-137.2	11.3	3.2
2	Ormsby	25	81F	C	10	3	4	1	0.71	Y	-152.7	2.68	4.2
2	Ormsby	27	76F	B	60	2	4	1	-1.68	Y	-166.4	1.86	5.3
2	Ormsby	29	76F	B	60	3	3	3					
2	Ormsby	32	66F	A	60	2	4	3	-1.11	N	-170.2	-2.43	7.8
2	Ormsby	33	66F	A	60	3	3	3					
2	Ormsby	35	63F	A	30	2	4	1	-1.75	Y	-158.1	5.82	5.1

Table C-2. Mission Data Summary (Continued)

Mission	Pilot	Record	VSS Code	A/C Config	Rate Limit	HQ Phase	PIO Rating	Rate Limit Rating	Actual Max Stick (Inches)	OLOP PIO?	OLOP Phase (deg)	OLOP Amp. (dB)	ω_{onset} (rad/sec)
3	Ippoliti	3	66F	A	60	2	4	2	-2.58	Y	-161.3	3.68	5.6
3	Ippoliti	4	66F	A	60	3	3	no rec					
3	Ippoliti	5	71F	B	10	2	6	no rec					
3	Ippoliti	6	71F	B	10	3	6	1	-1.4	Y	-159.3	7.76	2.8
3	Ippoliti	9	86F	C	60	2	4	1	-2.08	Y	-159.5	2.79	5.5
3	Ippoliti	10	86F	C	60	3	3	1	3.95	Y	-153.8	2.18	4.3
3	Ippoliti	11	91F	D	10	2	6	1	1.06	Y	-173.6	10.3	2.9
3	Ippoliti	12	91F	D	10	3	6	1	-1.26	Y	-172.6	8.01	2.7
3	Ippoliti	13	61F	A	10	2	6	1	-2.13	Y	-130.3	14.6	3.8
3	Ippoliti	14	61F	A	10	3	5	1	0.89	Y	-147.3	2.49	4.6
3	Ippoliti	16	96F	D	60	2	5	1	-1.68	Y	-171.4	3.61	5
3	Ippoliti	17	96F	D	60	3	5	2	-1.76	Y	-168.3	0.32	4.9
3	Ippoliti	18	81F	C	10	2	6	1	1.16	Y	-140.2	10.4	3.4
3	Ippoliti	19	81F	C	10	3	6	1	1.23	Y	-142.7	6.39	3.4
3	Ippoliti	21	76F	B	60	2	5	1	-2.03	Y	-165.5	3.16	4.9
3	Ippoliti	23	76F	B	60	3	6	1	2.35	Y	-161.3	0.16	4.6
3	Ippoliti	27	66F	A	60	2	5	2	-2.5	Y	-161.5	3.48	5.6
3	Ippoliti	28	66F	A	60	3	4	1	3.02	N	-151.3	-1.45	5.3
3	Ippoliti	30	63F	A	30	2	5	1	-2.03	Y	-156.5	6.76	4.9
3	Ippoliti	32	63F	A	30	3	5	1	1.64	N	-150.9	-0.78	5.2
3	Ippoliti	35	64F	A	40	2	5	1	-2.17	Y	-159.2	5.15	5.2
3	Ippoliti	36	64F	A	40	3	4	1	2.01	N	-151.3	-1.45	5.3
4	Gilbreath	2	83F	C	30	2	5	1	-2.03	Y	-149.9	7.01	4.2
4	Gilbreath	4	83F	C	30	3	4	1	1.52	Y	-157.3	0.33	4.7
4	Gilbreath	7	63F	A	30	2	4	1	-2.16	Y	-156.1	7	4.9
4	Gilbreath	9	63F	A	30	3	3	1	1.41	N	-151.5	-1.89	5.4
4	Gilbreath	12	64F	A	40	2	3	1	-2.09	Y	-159.5	4.93	5.3
4	Gilbreath	13	64F	A	40	3	3	1	3	Y	-148.8	1.42	4.8
4	Gilbreath	15	94F	D	40	2	5	1	-1.62	Y	-171.2	5.4	4.4
4	Gilbreath	16	94F	D	40	3	5	1	1.71	Y	-168.9	2.39	4.2
4	Gilbreath	18	73F	B	30	2	5	1	-2.39	Y	-163.1	8.2	3.5
4	Gilbreath	19	73F	B	30	3	5	1	-1.5	Y	-161	1.7	4.1
4	Gilbreath	21	93F	D	30	2	5	1	-2.13	Y	-172.1	8.29	3.5
4	Gilbreath	23	93F	D	30	3	5	1	1.15	Y	-168.7	1.79	4.4
4	Gilbreath	25	74F	B	40	2	5	1	-1.52	Y	-165.1	3.81	4.6
4	Gilbreath	26	74F	B	40	3	5	1	2.01	Y	-161	1.7	4.1
4	Gilbreath	28	84F	C	40	2	4	1	-2.59	Y	-150.3	6.86	4.3
4	Gilbreath	29	84F	C	40	3	3	1	2.45	Y	-154.8	1.68	4.4
4	Gilbreath	31	75F	B	50	2	5	1	-1.8	Y	-165.3	3.42	4.8
4	Gilbreath	34	75F	B	50	3	5	1	-1.26	N	-161.7	-2.71	5.6

Table C-2. Mission Data Summary (Continued)

Mission	Pilot	Record	VSS Code	A/C Config	Rate Limit	HQ Phase	PIO Rating	Rate Limit Rating	Actual Max Stick (Inches)	OLOP PIO?	OLOP Phase (deg)	OLOP Amp. (dB)	ω_{onset} (rad/sec)
5	Ormsby	2	83F	C	30	2	4	1	-1.76	Y	-152.1	6.13	4.5
5	Ormsby	4	83F	C	30	3	3	1	0.97	N	-162.1	-3.1	5.7
5	Ormsby	6	64F	A	40	2	4	1	-2.25	Y	-158.5	5.59	5.1
5	Ormsby	8	64F	A	40	3	3	1	1.05	N	-151.5	-5.87	6.6
5	Ormsby	10	94F	D	40	2	5	1	-1.24	Y	-171.3	4.18	4.8
5	Ormsby	11	94F	D	40	3	4	3					
5	Ormsby	13	73F	B	30	2	5	1	0.98	Y	-165.6	2.89	4.9
5	Ormsby	14	73F	B	30	3	5	1	1.85	Y	-160.7	2.98	3.8
5	Ormsby	16	93F	D	30	2	5	1	-1.01	Y	-171.3	4.52	4.7
5	Ormsby	17	93F	D	30	3	5	1	1.26	Y	-168.8	2.27	4.3
5	Ormsby	19	74F	B	40	2	5	1	-1.33	Y	-165.5	3.02	4.9
5	Ormsby	21	74F	B	40	3	3	2	1.23	N	-161.5	-1.36	5.1
5	Ormsby	23	84F	C	40	2	4	1	-1.92	Y	-154.8	4.95	4.8
5	Ormsby	25	84F	C	40	3	3	2	1.53	N	-160.5	-1.72	5.3
5	Ormsby	27	75F	B	50	2	5	1	-1.57	Y	-165.8	2.63	5
5	Ormsby	28	75F	B	50	3	3	3					
5	Ormsby	30	72F	B	20	2	5	1	0.78	Y	-165	3.95	4.6
5	Ormsby	32	72F	B	20	3	5	1	1.22	Y	-160.7	2.98	3.8
5	Ormsby	34	95F	D	50	2	5	1	-1.33	Y	-171.5	3.38	5.14
5	Ormsby	36	95F	D	50	3	3	2	0.9	N	-167.7	-2.63	6.2
6	Ippoliti	5	83F	C	30	2	4	1	-2.69	Y	-145.2	8.79	3.8
6	Ippoliti	6	83F	C	30	3	3	1	1.54	Y	-157	0.5	4.7
6	Ippoliti	8	94F	D	40	2	5	1	-1.46	Y	-171.2	4.98	4.5
6	Ippoliti	9	94F	D	40	3	5	2	2.32	Y	-169.6	3.95	3.8
6	Ippoliti	11	73F	B	30	2	5	1	-1.26	Y	-164.7	4.34	4.5
6	Ippoliti	12	73F	B	30	3	5	1	-1.62	Y	-160.9	2.13	4
6	Ippoliti	14	93F	D	30	2	5	1	1.37	Y	-171.3	6.13	4.1
6	Ippoliti	16	93F	D	30	2	5	1	0.95	Y	-171.3	4.29	4.8
6	Ippoliti	17	93F	D	30	3	5	1	1.46	Y	-169.1	3	4
6	Ippoliti	19	74F	B	40	2	5	1	1.13	Y	-166.3	1.99	5.3
6	Ippoliti	21	74F	B	40	3	5	1	2.19	Y	-160.9	2.27	4
6	Ippoliti	24	84F	C	40	2	4	1	-1.63	Y	-157.1	3.94	5.1
6	Ippoliti	25	84F	C	40	3	3	1	-1.79	N	-158.7	-0.52	4.9
6	Ippoliti	27	75F	B	50	2	5	1	-1.71	Y	-165.5	3.16	4.9
6	Ippoliti	28	75F	B	50	3	3	2	2.79	Y	-160.8	2.41	4
6	Ippoliti	30	72F	B	20	2	5	1	1.09	Y	-164	5.97	4
6	Ippoliti	31	72F	B	20	3	5	1	1.44	Y	-160.5	3.84	3.6
6	Ippoliti	33	65F	A	50	2	5	1	-2.21	Y	-161	3.88	5.5

Table C-2. Mission Data Summary (Continued)

Mission	Pilot	Record	VSS Code	A/C Config	Rate Limit	HQ Phase	PIO Rating	Rate Limit Rating	Actual Max Stick (Inches)	OLOP PIO?	OLOP Phase (deg)	OLOP Amp. (dB)	ω_{onset} (rad/sec)
7	Gilbreath	4	72F	B	20	2	5	1	-1.04	Y	-164.1	5.69	4.1
7	Gilbreath	7	72F	B	20	3	6	1	1.22	Y	-160.7	2.98	3.8
7	Gilbreath	10	95F	D	50	2	5	1	-1.76	Y	-171.2	4.75	4.6
7	Gilbreath	12	95F	D	50	3	5	1	1.69	Y	-168.4	1.06	4.7
7	Gilbreath	14	62F	A	20	2	4	1	-1.78	Y	-153	8.54	4.6
7	Gilbreath	16	62F	A	20	3	3	1	1.1	N	-150.9	-0.78	5.2
7	Gilbreath	18	85F	C	50	2	3	1	-2.09	Y	-156.7	4.08	5.1
7	Gilbreath	19	85F	C	50	3	2	2	3.32	Y	-153.4	2.35	4.2
7	Gilbreath	21	82F	C	20	2	5	1	-1.57	Y	-147.2	8.05	4
7	Gilbreath	22	82F	C	20	3	4	1	1.16	Y	-155.5	1.35	4.5
7	Gilbreath	24	65F	A	50	2	3	1	1.88	Y	-162.3	2.89	5.8
7	Gilbreath	25	65F	A	50	3	2	1	3.07	N	-150.4	-0.075	5
7	Gilbreath	28	92F	D	20	2	5	1	1.32	Y	-172	7.95	3.6
7	Gilbreath	29	92F	D	20	3	5	1	1.07	Y	-169.4	3.59	3.9
7	Gilbreath	31	86F	C	60	2	3	1	1.89	Y	-160.7	2.22	5.7
7	Gilbreath	34	76F	B	60	2	5	1	-1.67	Y	-166.4	1.86	5.33
7	Gilbreath	35	76F	B	60	3	3	1	2.41	Y	-161.3	0.3	4.6
7	Gilbreath	37	86F	C	60	3	3	2	2.81	N	-158.2	-0.18	4.9
7	Gilbreath	39	63F	A	30	2	4	1	-2.02	Y	-156.5	6.76	4.9
7	Gilbreath	40	63F	A	30	3	3	1	1.38	N	-151.6	-2.1	5.5
8	Ormsby	3	94F	D	40	2	5	1	1.18	Y	-171.4	3.84	4.9
8	Ormsby	4	94F	D	40	3	5	1	1.23	Y	-168.3	0.57	4.9
8	Ormsby	6	66F	A	60	2	4	1	1.8	Y	-164.5	1.24	6.3
8	Ormsby	7	66F	A	60	3	3	3	2.56	N	-151.7	-2.52	5.6
8	Ormsby	10	76F	B	60	2	4	1	-1.87	Y	-165.8	2.63	5
8	Ormsby	11	76F	B	60	3	3	3	1.91	N	-161.5	-0.61	5.1
8	Ormsby	12	76F	B	60	3	3	3	2.54	Y	-161.2	0.72	4.4
8	Ormsby	14	62F	A	20	2	4	1	1.33	Y	-156.9	6.52	4.95
8	Ormsby	15	62F	A	20	3	3	1	1.26	N	-150.2	0.17	5
8	Ormsby	17	65F	A	50	2	5	2	-2.6	Y	-159.5	4.9	5.3
8	Ormsby	18	65F	A	50	3	3	3	0.88	N	-149.6	-8.89	8
8	Ormsby	20	96F	D	60	2	5	1	-2.44	Y	-171.3	5.56	4.31
8	Ormsby	21	96F	D	60	3	3	3	2.3	Y	-168.7	1.79	4.4
8	Ormsby	23	82F	C	20	2	5	1	-1.56	Y	-147.6	7.9	4
8	Ormsby	24	82F	C	20	3	4	1	1.68	Y	-150	3.84	3.9
8	Ormsby	26	75F	B	50	2	4	1	-1.49	Y	-166.1	2.25	5.2
8	Ormsby	27	75F	B	50	3	3	3	2.29	Y	-161.1	1.14	4.3
8	Ormsby	29	85F	C	50	2	5	1	-2.38	Y	-155.1	4.81	4.9
8	Ormsby	30	85F	C	50	3	4	3					
8	Ormsby	32	92F	D	20	2	6	1	-0.68	Y	-171.2	4.64	4.6
8	Ormsby	33	92F	D	20	3	5	1	1.49	Y	-170.3	5.23	3.4

Table C-2. Mission Data Summary (Concluded)

Mission	Pilot	Record	VSS Code	A/C Config	Rate Limit	HQ Phase	PIO Rating	Rate Limit Rating	Actual Max Stick (Inches)	OLOP PIO?	OLOP Phase (deg)	OLOP Amp. (dB)	ω_{onset} (rad/sec)
10	Ormsby	2	63F	A	30	2	4	1	-1.85	Y	-157.7	6.04	5
10	Ormsby	3	63F	A	30	3	3	3	2.8	Y	-146.8	2.76	4.56
10	Ormsby	7	65F	A	50	2	3	1	-2.48	Y	-159.8	4.71	5.33
10	Ormsby	10	66F	A	60	2	3	1	-1.97	Y	-163.6	1.96	6.1
10	Ormsby	13	86F	C	60	2	3	2	-2.11	Y	-159.2	2.93	5.5
10	Ormsby	15	96F	D	60	3	3	3	1.15	N	-167.8	-2.14	5.9
10	Ormsby	17	83F	C	30	2	5	1	-1.84	Y	-151.4	6.42	4.4
10	Ormsby	18	83F	C	30	3	3	3	2.12	Y	-152.7	2.68	4.2
10	Ormsby	23	64F	A	40	2	3	1	-2.23	Y	-158.8	5.37	5.2
10	Ormsby	28	74F	B	40	3	3	3	1.52	N	-161.3	0.022	4.6
11	Gilbreath	3	63F	A	30	2	4	1	-1.72	Y	-158.5	5.59	5.1
11	Gilbreath	4	63F	A	30	3	2	1	1.23	N	-151.8	-2.73	5.6
11	Gilbreath	7	76F	B	60	3	3	1	2.54	Y	-161.2	0.72	4.4
11	Gilbreath	9	85F	C	50	3	4	2	3	Y	-155.2	1.51	4.4
11	Gilbreath	11	86F	C	60	2	3	2	-1.47	Y	-164.7	0.41	6.5
11	Gilbreath	12	86F	C	60	3	2	2	3.03	Y	-157.3	0.33	4.7
11	Gilbreath	14	64F	A	40	2	3	1	-2.03	Y	-159.8	4.71	5.3
11	Gilbreath	15	64F	A	40	3	2	1	2.71	Y	-149.7	0.66	4.9
11	Gilbreath	17	83F	C	30	2	5	1	-1.9	Y	-150.6	6.72	4.3
11	Gilbreath	18	83F	C	30	3	2	1	1.58	Y	-156.7	0.67	4.6
11	Gilbreath	21	66F	A	60	3	2	2	2.67	N	-151.7	-2.31	5.5
11	Gilbreath	23	75F	B	50	3	3	2	2.32	Y	-161.1	1.28	4.3
11	Gilbreath	25	84F	C	40	3	3	2	2.69	Y	-153.4	2.35	4.23
11	Gilbreath	26	83F	C	30	3	4	1	1.96	Y	-153.8	2.18	4.3
12	Ippoliti	3	62F	A	20	2	5	1	-1.65	Y	-154.1	8	4.7
12	Ippoliti	4	62F	A	20	3	4	1	1.56	Y	-148.5	1.68	4.7
12	Ippoliti	5	65F	A	50	3	3	1	2.74	N	-150.9	-0.78	5.2
12	Ippoliti	7	82F	C	20	2	5	1	2.17	Y	-141.6	9.96	3.5
12	Ippoliti	10	82F	C	20	3	5	1	2.22	Y	-144.7	5.76	3.5
12	Ippoliti	12	85F	C	50	2	3	1	-1.53	Y	-161.3	1.94	5.8
12	Ippoliti	13	85F	C	50	3	3	1	3.01	Y	-154.8	1.68	4.4
12	Ippoliti	14	92F	D	20	2	6	1	1.55	Y	-172.4	8.74	3.3
12	Ippoliti	15	92F	D	20	2	5	1	0.77	Y	-171.2	5.21	4.4
12	Ippoliti	16	92F	D	20	3	5	1	1.82	Y	-171	6.26	3.1
12	Ippoliti	18	95F	D	50	2	3	1	-1.31	Y	-171.5	3.26	5.2
12	Ippoliti	19	95F	D	50	3	5	2	3.5	Y	-170.1	5	3.5
12	Ippoliti	20	71F	B	10	2	5	1	-0.72	Y	-163.3	7.49	3.6
12	Ippoliti	21	66F	A	60	3	3	1	1.94	N	-151.9	-4.47	6.1
12	Ippoliti	22	96F	D	60	3	3	1	2.75	Y	-169	2.76	4.1
12	Ippoliti	23	63F	A	30	3	4	1	1.72	N	-150.8	-0.55	5.1
12	Ippoliti	24	64F	A	40	3	3	1	3.08	Y	-148.8	1.42	4.8
12	Ippoliti	25	75F	B	50	3	4	1	2.3	Y	-161.1	1.28	4.3
12	Ippoliti	26	94F	D	40	3	4	1	2.39	Y	-169.7	4.19	3.7
12	Ippoliti	27	63F	A	30	3	4	1	3.2	Y	-145.2	3.62	4.4

Bibliography

[1] Chapa, Michael. Results of Attempts to Prevent Departure and/or Pilot-Induced Oscillations (PIO) Due to Actuator Rate Limiting in Highly-Augmented Fighter Flight Control Systems (HAVE FILTER). AFFTC-TR-98-26, March 1999.

[2] Crassidis, A.L. NT-33A Air Force Test Pilot School Spring '97 Test Management Projects Analysis and Results. Contract No. F33615-93-C-3608, Calspan SRL Corporation, Buffalo NY, 8 Sep 1997.

[3] Department of Defense. Military Standard, Flying Qualities of Piloted Aircraft. MIL-STD 1797A, 30 January 1990.

[4] Dornheim, M.A., "Report Pinpoints Factors Leading to YF-22 Crash," Aviation Week and Space Technology, Vol. 137, No. 19, 1992, pp.53, 54.

[5] Dornheim, M.A., and D. Hughes, "Boeing Corrects Several 777 PIOs," Aviation Week and Space Technology, Vol. 142, No. 19, 1995, p. 32.

[6] Duda, Holger. "Effects of Rate Limiting in Flight Control Systems – A New PIO Criterion," Proceedings of the AIAA Guidance and Control Conference. AIAA-95-3204-CP, Scottsdale AZ, 1-3 August 1994.

[7] Duda, Holger. "Frequency Domain Analysis of Rate Limiting Elements in Flight Control Systems," DLR-FB 94-16, August 1994 (in German).

[8] Duda, Holger, and Lars Forssell. "New Flight Simulator Experiments On PIO Due to Rate Saturation", Proceedings of the AIAA Atmospheric Flight Mechanics Conference and Exhibit. AIAA-98-4336, Boston MA, August 10-12, 1998.

[9] Duda, Holger. "Prediction of Pilot-In-The-Loop Oscillations Due to Rate Saturation," Journal of Guidance, Control, and Dynamics, Vol. 20, No. 3, May-June 1997.

[10] Duus, Gunnar, and Holger Duda. "Analysis of the HAVE LIMITS Database Using the OLOP Criterion", Proceedings of the AIAA Atmospheric Flight Mechanics Conference and Exhibit. AIAA-99-4007, Portland OR, August 9-11, 1999.

[11] Duus, Gunnar. Aerospace Engineer, Institute of Flight Mechanics, DLR, Braunschweig, Germany, Various E-mail Correspondence, June 1999.

[12] Duus, Gunnar. "SCARLET 3 – A Flight Experiment Considering Rate Saturation", AIAA-2000-3987, August 2000.

Bibliography (Continued)

[13] Gilbreath, Gregory P. A Limited Evaluation of a Pilot-Induced-Oscillation Prediction Criterion (HAVE OLOP). AFFTC-TIM-00-07, December 2000.

[14] Graham, Dunstan, and Duane McRuer. Analysis of Nonlinear Control Systems. John Wiley and Sons, Inc., New York, 1961.

[15] Kish, B.A., W.B. Mosle III, A.S. Remaly, J.S. Seo, J.F. Kromberg, and R. Cabiati, "A Limited Flight Test Investigation of Pilot-Induced Oscillation Due to Rate Limiting," Proceedings of the AIAA Guidance, Navigation, and Control Conference, AIAA-97-3703, 1332-1341, New Orleans LA, 11-13 August 1997.

[16] Klyde, David H., Duane T. McRuer, and Thomas T. Myers. Unified Pilot-Induced Oscillation Theory, Volume I: PIO Analysis With Linear and Nonlinear Effective Vehicle Characteristics, Including Rate Limiting, Final Report. Contract F33615-94-C-3613. Flight Dynamics Directorate, Wright Laboratory, Wright-Patterson AFB OH, December 1995.

[17] Kreyszig, Erwin. Advanced Engineering Mathematics. John Wiley and Sons, Inc., New York, 1993.

[18] Kullberg, E., and Per-Olov Elgerona. "SAAB Experience with PIO," Flight Vehicle Integration Panel Workshop on Pilot Induced Oscillations, AGARD-AR-335, February 1995.

[19] MATLAB® and Simulink®. Versions 5.3 and 3.0. Computer Software. The Math Works Inc., Natick MA, 1999.

[20] McRuer, Duane T. "Pilot-Induced Oscillations and Human Dynamic Behavior," NASA CR-4683, NASA Dryden Research Center, Edwards AFB CA, July 1995.

[21] Mitchell, David G., Bimal L. Aponso, and Roger H. Hoh. Minimum Flying Qualities, Volume I: Piloted Simulation Evaluation of Multiple Axis Flying Qualities, WRDC-TR-89-3125, Vol. I, January 1990.

[22] Mitchell, David G., Klyde, David H. "A Critical Examination of PIO Prediction Criteria" , AIAA-98-4335, 1998

[23] Neal, T.P., and Rogers E. Smith, An In-Flight Investigation to Develop Control System Design Criteria for Fighter Airplanes. AFFDL-TR-70-74, December 1970.

[24] Ohmit, Eric E. Aerospace Engineer, Calspan Corporation, Various E-mail Correspondence, June 1999.

Bibliography (Concluded)

[25] Peters, Patrick J. The Effects of Rate Limiting and Stick Dynamics On Longitudinal Pilot-Induced Oscillations. MS Thesis, AFIT/GAE/ENY/97M-02. School of Engineering, Air Force Institute of Technology (AU), Wright-Patterson AFB OH, March 1997.

[26] Schifferle, Paul T., Paul R. Deppe, and Randall E. Bailey, "Large Aircraft Rate Limit Flight Test Program", Proceedings of the AIAA Atmospheric Flight Mechanics Conference and Exhibit. AIAA-99-3963, Portland OR, August 9-11, 1999.

[27] Smith, Ralph H. A Theory for Longitudinal Short-Period Pilot Induced Oscillations. AFFDL-TR-77-57, Air Force Flight Dynamics Laboratory, Wright-Patterson AFB OH, June 1977.

Vita

Captain Gregory P. Gilbreath was born in Houston, Texas. He graduated from South Lakes High School, Reston, Virginia, in 1987. He went on to earn a Bachelor of Science Degree in Aerospace Engineering from Virginia Polytechnic Institute and State University. He graduated *cum laude* in May 1991 and was commissioned into the USAF.

After graduation he worked for a short time at the NASA Space Station Headquarters in Reston, Virginia. He entered Undergraduate Pilot Training at Vance AFB, Oklahoma, in January 1992. He received his wings a year later and went to Davis-Monthan AFB to learn to fly the A-10. Capt Gilbreath served three operational tours in the A-10 with the 354th Fighter squadron, McChord AFB, the 70th Fighter Squadron, Moody AFB, and the 25th Fighter Squadron, Osan AB. He was selected for the joint AFIT/TPS program in March 1998 while serving as an instructor/evaluator pilot in the 25th FS. After graduation from TPS/AFIT he was assigned to the 40th Flight Test Squadron, Eglin AFB.

REPORT DOCUMENTATION PAGE

Form Approved
OMB No. 074-0188

1. REPORT DATE *(DD-MM-YYYY)*	2. REPORT TYPE	3. DATES COVERED *(From – To)*
01-03-2001	Master's Thesis	Jun 1999 – Feb 2001

4. TITLE AND SUBTITLE

PREDICTION OF PILOT-INDUCED OSCILLATIONS (PIO) DUE TO ACTUATOR RATE LIMITING USING THE OPEN-LOOP ONSET POINT (OLOP) CRITERION

5a. CONTRACT NUMBER

5b. GRANT NUMBER

5c. PROGRAM ELEMENT NUMBER

6. AUTHOR(S)

Gilbreath, Gregory P., Captain, USAF

5d. PROJECT NUMBER

5e. TASK NUMBER

5f. WORK UNIT NUMBER

7. PERFORMING ORGANIZATION NAMES(S) AND ADDRESS(S)

Air Force Institute of Technology
Graduate School of Engineering and Management (AFIT/EN)
2950 P Street, Building 640
WPAFB OH 45433-7765

8. PERFORMING ORGANIZATION REPORT NUMBER

AFIT/GAE/ENY/01M-02

9. SPONSORING/MONITORING AGENCY NAME(S) AND ADDRESS(ES)

USAF Test Pilot School
Attn: Lt Col Thomas A. Buter
220 S. Wolfe Ave
Edwards AFB CA 93524 DSN 527-3000

10. SPONSOR/MONITOR'S ACRONYM(S)

11. SPONSOR/MONITOR'S REPORT NUMBER(S)

12. DISTRIBUTION/AVAILABILITY STATEMENT

APPROVED FOR PUBLIC RELEASE; DISTRIBUTION UNLIMITED.

13. SUPPLEMENTARY NOTES

14. ABSTRACT

Rate limiting has been a causal or contributing factor for Pilot Induced Oscillations (PIO). As part of the joint Air Force Institute of Technology/Test Pilot School (AFIT/TPS) program, an examination of the Open-Loop Onset Point (OLOP) criterion, developed by DLR German Aerospace, was conducted to see if it could predict PIO due to rate limiting and to evaluate its' potential as a design tool.

The criterion was applied to three previous flight test programs involving rate limiting. Findings from this analysis led to the HAVE OLOP flight test which was flown on the NF-16D Variable Stability In-flight Simulator Test Aircraft (VISTA). HAVE OLOP evaluated four longitudinal configurations with rate limiting elements inside the feedback loop .

OLOP was found to over-predict PIO in some cases when using maximum stick amplitude as DLR suggests. When using actual stick amplitudes, correlation between OLOP predictions and PIO ratings was good. A new metric called stick ratio was developed to help explore the full range of stick amplitudes when using OLOP.

OLOP could be a useful design tool, but because of the strong influence of stick amplitude, engineering judgement would have to be exercised. Recommendations on its use as a design tool are presented.

15. SUBJECT TERMS

pilot-induced oscillation, PIO, rate limiting, Test Pilot School, TPS, open-loop onset point, OLOP, HAVE OLOP, NF-16D, VISTA

16. SECURITY CLASSIFICATION OF:			17. LIMITATION OF ABSTRACT	18. NUMBER OF PAGES	19a. NAME OF RESPONSIBLE PERSON
REPORT	ABSTRACT	c. THIS PAGE			Dr. Bradley S. Liebst, ENY
U	U	U	UU	169	19b. TELEPHONE NUMBER *(Include area code)* 937-255-3636 x4636

Standard Form 298 (Rev. 8-98)
Prescribed by ANSI Std. Z39-18

Form Approved
OMB No. 074-0188